

ANALYSIS OF MEMBRANES SUBJECTED TO AN
UNDERWATER EXPLOSION

By

LAWRENCE EDWARD EHLERS

Bachelor of Science
Kansas State University
Manhattan, Kansas
1957

Master of Science
Kansas State University
Manhattan, Kansas
1960

Submitted to the faculty of the Graduate College
of the Oklahoma State University
in partial fulfillment of the requirements
for the Degree of
DOCTOR OF PHILOSOPHY
August, 1969

NOV 5 1969

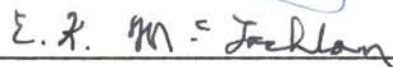
ANALYSIS OF MEMBRANES SUBJECTED TO AN
UNDERWATER EXPLOSION

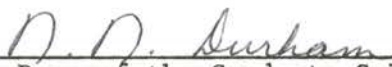
Thesis Approved:



Thesis Adviser







Dean of the Graduate College

729922

PREFACE

Because of industrial demands and technological developments, the use of explosives as a source of power for the rapid forming of metal parts has greatly increased. A great many experimental studies have been made using explosives for the forming of metal parts, but only basic analytical studies have been completed. In this dissertation, a simple analytical technique is developed for describing the entire deformation process caused by a nearby underwater explosion. Several parametric studies are made using the technique developed.

The author wishes to express his sincere appreciation to the following individuals and organizations:

To Dr. Donald E. Boyd, who served as my major adviser and graduate committee chairman, for his invaluable encouragement, interest, friendship, and guidance during my graduate study at Oklahoma State University.

To my graduate committee, composed of Doctors A. E. Salama, R. L. Janes, and E. K. McLachlan, who rendered guidance and council.

To the Ford Foundation, for their financial support.

To the School of Civil Engineering, for its financial support and to Professor J. V. Parcher, for his friendship and advice.

To Dr. Carl Kurt, Dr. R. Munshi, Mr. Jack Vetter, and Mr. Eldon Hardy for their friendship.

To Professor William B. LeMar, Mr. Phillip G. Smith, Mr. Eldon Hardy, and Mrs. Mary Ann Kelsey for their very valuable assistance in

the preparation of the manuscript.

And finally, to my wife, Judy, and children, Pamela and Douglas, for their confidence, encouragement, and patient understanding, which greatly helped the author to complete this dissertation.

TABLE OF CONTENTS

Chapter	Page
I. INTRODUCTION	1
1.1 Statement and Need of the Problem	1
1.2 Historical Review	2
1.3 Approach of This Study	9
II. FORMULATION OF THE GOVERNING EQUATIONS	11
2.1 General	11
2.2 Chain of Events After Detonation	11
2.3 Shock Wave Pressure	12
2.4 Boundary Interactions	17
2.5 Equation of Motion	21
2.6 Kinematic Equation	24
2.7 Constitutive Equations	24
2.8 Cavitation Occurring-Afterflow Theory	29
2.9 Influence of the Water Surface	36
2.10 Migration of the Gas Bubble	38
III. NUMERICAL SOLUTION OF THE GOVERNING EQUATIONS	43
3.1 Introduction	43
3.2 Boundary and Initial Conditions	43
3.3 Numerical Solution for Displacement	45
3.4 Pressure at the Membrane Center	46
3.5 Formulation for the Gas Bubble Expansion	47
3.6 Reloading Velocity	50
3.7 Numerical Solution of the Equation of Motion After Reloading	51
3.8 Numerical Solution With Cavitation	51
3.9 Numerical Solution Without Cavitation	52
IV. NUMERICAL RESULTS	55
4.1 General	55
4.2 Influence of the Ambient Pressure on the Damage	56
4.3 Influence of the Hydrostatic Head on the Center Deformation	56
4.4 Influence of Stand-off Distance on the Center Deformation	66
4.5 Influence of Charge Weight on Center Deformation	71
4.6 Influence of the Center Velocity on the Center Deformation	71

Chapter	Page
4.7 Actual Pressure on the Membrane Center.	76
4.8 Summary of Results.	82
V. CONCLUSIONS AND RECOMMENDATIONS	84
5.1 General	84
5.2 Conclusions From This Study	84
5.3 Recommendations for Future Studies.	85
A SELECTED BIBLIOGRAPHY.	86
APPENDIX A - THE ACTUAL INCIDENT PRESSURE ON THE MEMBRANE FROM AN UNDERWATER EXPLOSION BASED ON DIFFRACTION THEORY .	88
APPENDIX B - THE RELOADING VELOCITY FOR A MEMBRANE SUBJECTED TO AN UNDERWATER EXPLOSION	100
APPENDIX C - FLOW CHARTS	104

LIST OF FIGURES

Figure	Page
1. Loading on Membrane	5
2. Illustration of Loading Cycle	13
3. A Typical Experimental Set-up	14
4. p-t Variation in Water.	16
5. Membrane Geometry at Times t and τ	18
6. Loading on Membrane	22
7. Membrane Deformation During One Time Interval	25
8. Spheroidal Coordinate System.	34
9. Point Sources of Charge e	39
10. Deformed Membrane	48
11. Influence of the Ambient Pressure on the Damage at a Stand-off Distance of One Foot.	57
12. Influence of the Ambient Pressure on the Damage at a Stand-off Distance of One-half Foot	58
13. Influence of the Head on the Center Deformation for a Steel Membrane and One Foot Stand-off Distance.	59
14. Influence of the Head on the Center Deformation for a Brass Membrane and One Foot Stand-off Distance.	60
15. Influence of the Head on the Center Deformation for a Steel Membrane and One-half Foot Stand-off Distance	61
16. Influence of the Head on the Center Deformation for a Brass Membrane and One-half Foot Stand-off Distance	62
17. Effect of Depth on Damage	63
18. Influence of Stand-off Distance on Center Deformation for a Charge Weight of 6.25 Grams	67

Figure	Page
19. Influence of Stand-off Distance on Center Deformation for a Charge Weight of 9.0 Grams.	68
20. Influence of Stand-off Distance on Center Deformation for a Charge Weight of 12.0 Grams	69
21. Influence of Stand-off Distance on Center Deformation for a Charge Weight of 15.0 Grams	70
22. Influence of Charge Weight on Center Deformation With Cavitation	72
23. Influence of Charge Weight on Center Deformation Without Cavitation.	73
24. Center Velocity-Center Deformation History for a One-half Foot Stand-off Distance.	74
25. Center Velocity-Center Deformation History for a One Foot Stand-off Distance	75
26. Center Velocity-Center Deformation History for a Four Foot Stand-off Distance.	77
27. Center Velocity-Center Deformation History for a Seven Foot Stand-off Distance	78
28. Pressure-Time History for a Charge Weight of 6.25 Grams Plaster Gelatine.	79
29. Pressure-Time History for a Charge Weight of 7.0 Pounds TNT . . .	81
30. Membrane Geometry at Times t and τ	92

NOMENCLATURE

A_c	Acceleration of membrane center
a	Membrane radius
c_o	Speed of sound in conducting medium
D	Stand-off distance
dA'	Differential area
$\frac{dz_c}{dt}, \dot{z}_c$	Velocity of membrane center
$\frac{d^2z_c}{dt^2}, \ddot{z}_c$	Acceleration of membrane center
E	Energy
e	Point source
H	Membrane thickness
h	Depth of water above charge
K	Explosive parameter
P_h	Hydrostatic pressure
P_m	Peak pressure
p	Applied pressure
P_g	Pressure in gas bubble
P_i	Local shock wave pressure
P_o	Initial pressure in gas bubble
Q	$R_o^3 u/\beta$
R	Radius of gas bubble
\dot{R}	Velocity of gas bubble surface

\ddot{R}	Acceleration of gas bubble surface
R_1	Radius of curvature
R_0	Initial radius of gas bubble
r	Radial polar coordinate
\bar{r}	Distance from origin to membrane center
\bar{r}'	Distance from origin to disturbance
r_0, r_1, r_2	Radial coordinates
r_j	Radial coordinate of jth element
S	Displacement of gas bubble
S_c	Displacement of water at cavitation front
Subscript j	jth element of membrane surface
s	Distance from dA' to membrane center
s_j	Distance from jth element to membrane center
t	Time
U, U_1, U_2	Gas bubble velocities
u	A time-dependent parameter
u_n	Velocity component
V	Potential function
V_c	Velocity of membrane center
V_d	Potential function
V_s	$V - V_d$
v_0	Velocity of water at cavitation front
W	Charge weight
Z_c	Displacement of membrane center
z	Deflection of membrane
α	Energy correction factor

β	$R_o \sqrt{\rho_o / 2p_o}$
γ	Explosive parameter
Δl_j	Width of jth element
δ_f	Final membrane deformation
δ_o	Deflection at the end of the second stage
δt	Time increment
δz_c	Center deformation during one time interval
$\delta \gamma_{oct}$	Incremental octahedral shear strain
$\delta \bar{\epsilon}$	Incremental effective strain
$\delta \epsilon_1, \delta \epsilon_2, \delta \epsilon_3$	Incremental linear principal strains
$\delta \epsilon_\phi, \delta \epsilon_r$	Incremental change in strains
θ	Time constant
θ_d	a/c_o
ξ, ζ, ψ	Spheroidal coordinates
ρ	Density of membrane material
ρ_o	Density of conducting medium
$\bar{\sigma}$	Effective stress
σ_1	Principal stress
σ_2	Principal stress
σ_y	Yield stress of the membrane material
τ	An earlier time
τ_{oct}	Octahedral-shearing stress
ϕ	Potential function

CHAPTER I

INTRODUCTION

1.1 Statement and Need of the Problem

A simple analytical method is developed for predicting the deformation of a clamped circular membrane subjected to large transient pressures resulting from a nearby explosion. The motion of the membrane depends on the pressure and the pressure depends on the motion of the membrane, and the theory of this coupling effect is examined in the present study. An important objective of this study is to develop a method of studying the several parameters influencing the damage to the membrane caused by an adjacent underwater explosion.

In recent years the aircraft and missile industries have been using explosives for forming metals into various shapes. This method has been found to be quite efficient when the forming of very large shell structures is required, because conventional forming techniques would result in the use of massive and expensive equipment.

The office of United States Naval Research has conducted many studies on the damage to naval vessels from underwater explosions. The results of these studies have been used for two purposes: first, as a source of information in designing ships; and second, as a source of information in the positioning of mines. The need for protection against nuclear bomb attacks has prompted the need for predicting the response of a structure to impulsive loading from sudden high energy

releases.

Boyd (1) suggested that a method is needed for finding the actual pressure felt by a membrane from an adjacent underwater explosion.

Cole (2) provided much insight into the problem although an accurate description of the actual loading of the membrane has not been found.

A great many experimental studies have been made using explosives for the forming of metal parts, but only basic analytical studies have been completed. Johnson (5) conducted extensive experiments to determine the influence of several parameters on the deformation of circular membranes. Since a general method of studying these parameters analytically has not been found, Johnson's work suggests that an analytical parametric study is needed in these areas.

Therefore, a simple technique is needed for describing the entire deformation process. The deformation process begins when the shock wave reaches the membrane and ends when the membrane comes permanently to rest. With this technique, the history of the membrane motion can be studied, quantitative results from the parametric studies can be observed, and the actual pressure loading history of the membrane can be described. These statements point out the need for this study.

1.2 Historical Review

Because of industrial demands and technological developments, the use of explosives as a source of power for rapid forming of metal parts has greatly increased. Research by American and English investigators has contributed greatly to the understanding of all phases of the explosive process. This research has been published in three volumes as a reference (17, 18, 19).

In the past two decades, the high-energy rate forming of metal parts and the impulsive loading of structures by bomb explosions has been of interest to the United States Defense Department and the aerospace industry. The use of explosives for high-energy rate forming of metals continues today and is of increasing interest. The flexible elastic membrane was treated by Rayleigh (7), who assumed that the tension was great enough that it could be taken as constant. The displacements were sufficiently small that they could be assumed normal to the original plane. The assumptions linearize the mathematical model and the method yields a set of linear ordinary differential equations for the unknown coefficient functions. The resulting equations can be solved by ordinary methods, and the solution is applicable to a rigid perfectly plastic membrane without spring-back and undergoing small deformations.

Timoshenko (15) applied the same techniques as Rayleigh to both circular and rectangular membranes. He assumed the deflection to be time-dependent and the deflection surface to be described by trigonometric series. These assumptions when applied yield the frequency of the fundamental mode. The results of applying the above approach to membranes of several shapes are tabulated in reference 15.

Timoshenko (16) formulated the equations of equilibrium for shells of revolution (loaded symmetrically about their axes) using a spherical coordinate system. Assuming no bending resistance and considering the portion of the shell above a parallel circle, an equilibrium equation results which gives directly the stresses in the shell along a parallel circle. This approach gives the necessary equation of motion for a dynamically loaded perfectly plastic infinitesimal element above a

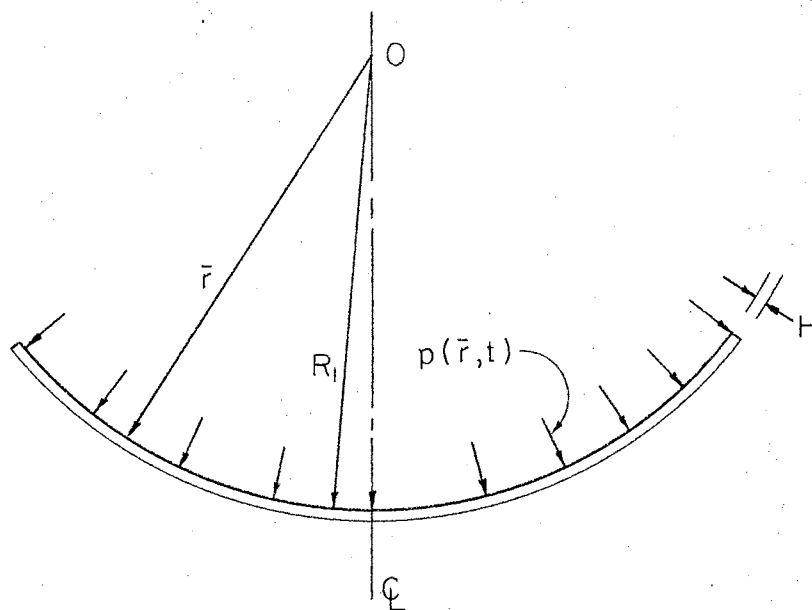
parallel circle (see Figure 1). Newton's second law is applied to the element from the membrane rather than the equilibrium equation.

Boyd (1) analyzed the motion of membranes using the deformation theory of plasticity and impulsive loading. The starting momentum supplied by the impulse was dissipated in plastic deformation with unloading neglected. The equations of motion for the dynamically loaded membrane were formulated by imposing the conditions of a "stationary action integral" ($\delta A=0$) with the energy terms of "A" written as a function of the stresses and strains.

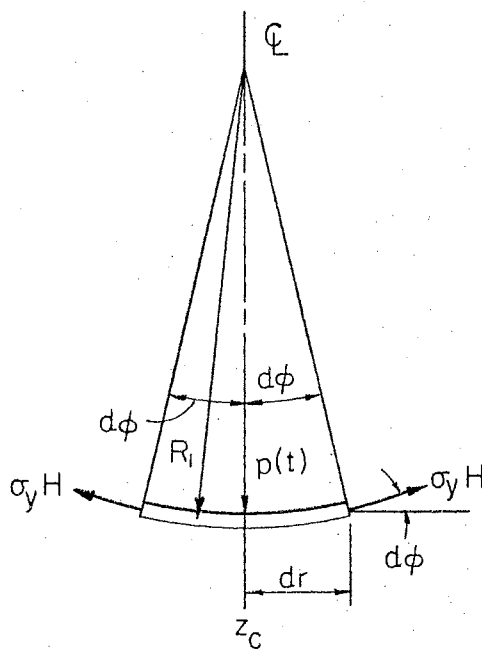
These equations were solved numerically on a digital computer using finite differences and a predictor-corrector technique. The results compared favorably with earlier, more complex analytical studies and with some experimental findings. Boyd suggested in the above study that a means of describing analytically the actual pressure felt by the membrane from the energy-transferring medium (water) should be provided.

Lamb (6) presented a general discussion of the transmission of sound waves and showed that the effect of a disturbance at a point can be represented by analyzing a point source. Then the pressure at a distant point due to a system of point sources can be found by integrating over the entire region. This point source representation provides the basis for the "diffraction theory" of sound waves. Rayleigh (8) showed that this diffraction theory is applicable to the case of disturbances originating from a plane surface. He found the effects at a point due to the disturbances (the movement of the surface) by integrating over the entire surface.

Cole (2) applied the diffraction theory of sound to the problem of blast loading of membranes in order to account for the coupling effect.



(a) BODY OF REVOLUTION



(b) CENTER ELEMENT OF BODY OF REVOLUTION

Figure 1. Loading on Membrane

between the membrane motion and the pressure in the incident wave. The important boundary condition of the problem is that the particle velocity in the medium (water) must be the same as the normal velocity component of the surface at the same point. A physical concept which describes the mathematical analysis of the problem is diffracted spherical waves originating at all points on the moving surface of the membrane. When these superimposed waves from the point sources are combined with the incident pressure wave, the boundary conditions and hydrodynamic equations are satisfied. This linear superposition of effects from the point sources on the membrane surface is possible only when the hydrodynamic equations are linear and, therefore, applies only to waves of acoustic intensity.

Kirkwood and Richardson (19) assumed linear acoustical theory (an incompressible inviscid fluid) to develop an expression for the maximum membrane deflection from a nearby explosion. The coupling effect is included in the development. The theory also assumed that cavitation does not occur and the development gives the criterion for determining the occurrence of cavitation behind a free plate. Kirkwood and Richardson considered a circular diaphragm clamped at its edges and acted on by an exponential pressure-time explosion wave. They assumed a parabolic shape for the diaphragm at all times and applied a Laplace transform technique to find the diaphragm deformation. The solution compared closely with experimental data. Since the baffle was small (theory assumes a large baffle), the theoretical results were used with a factor of one-half multiplied into the expression for the maximum deflection.

Fye and Eldridge (19) conducted extensive experimental studies and

compared their results with theoretical developments by Kirkwood and Richardson (19). Since Fye and Eldridge used diaphragms the same size as Kirkwood and Richardson, the factor of one-half was used. The comparison was quite good.

Kennard (19) extensively studied the phenomenon associated with the underwater explosion and the diaphragm deformation. His quantitative discussion contributed greatly to the general knowledge of explosively loaded diaphragms. He started with the most common case and then treated a number of topics including: the various characteristic times that are involved; cavitation at the interface; the transition to non-compressive action; the effect of the baffle; formulas for the swing time and the deflection of the diaphragm; the factors determining damage; and the departure from Hooke's law of the water.

Rinehart (9) surveyed the entire field of explosive working including the diffraction theory. The equations given by Rinehart for the pressure based on the diffraction theory can be applied only during certain phases of the damage process.

Temperly (19) studied the damage process of a membrane when cavitation occurs. He found that the damage process consists of three phases of motion. The first phase includes the membrane motion up to the occurrence of cavitation. This motion is essentially that of a free plate acted upon by a pressure wave. The pressure wave is modified by the motion of the plate. This phase has been described by many authors and can be found in Rinehart (9). The second phase includes the motion of the plate after cavitation and until the time when the cavitation cavity is filled. The kinetic energy of the plate at the end of the first phase of motion and the kinetic energy of "bubbly"

water layers impinging on the plate is dissipated in plastic deformation. The plate may be considerably decelerated or come to complete rest during the second phase of motion. Temperly describes the third phase as possibly a reloading due to the filling of the remaining void space in front of the plate. These void spaces are filled with water that has never cavitiated; this water may have a high velocity which causes additional deformation.

Schauer (11) divided the damage process into four parts: the shock wave loading phase; the first phase of deformation; the reloading phase; and the second phase of deformation.

The shock wave loading phase is the period of time up to the occurrence of cavitation. During this very short time period, the plate is considered to be free and a very high velocity is attained. The actual pressure acting on the plate during this time interval is the shock wave pressure modified by the motion of the plate. The plate reaches a relative maximum velocity at the onset of cavitation, after which the plate is moving with zero pressure forces acting on it.

During the first phase of deformation, the only forces acting on the plate are the stress forces in the plate. Since the deformations are large, they are plastic. The kinetic energy of the plate at the end of the first phase is continuously dissipated in plastic deformation. The end of this phase is reached when the target (plate) comes to rest or when reloading occurs.

The reloading phase is caused by the gas bubble remaining after complete detonation of the explosive. The gas bubble expands, which causes the surrounding water to rush radially outward, gradually filling the void left by cavitation. When this large mass of water overtakes

the plate, the plate is almost instantaneously accelerated to the velocity of the onrushing water.

The second phase of deformation is the time required for the plastic forces in the target to bring it to rest. The deformation is found by equating the kinetic energy of the target (and the effective mass of water following it) to the plastic work done on the target. The plastic work done during this phase does not include the plastic work done during the first two phases of the deformation process. Schauer's (11) developments compare favorably with experimental data of the Navy. This method seems to work well for targets at greater depths in the water and for greater stand-off distances. However, the method is only applicable to problems in which cavitation occurs.

1.3 Approach of This Study

As stated earlier, the development of a simple technique for analytically describing the entire deformation history of a membrane subjected to an underwater explosion is the objective of this study.

The pressure-producing shock wave which strikes the membrane is caused by an explosion in the conducting medium (water). When detonation of the explosive charge is complete, a shock wave from the explosion radiates outward through the conducting medium. The pressure in the shock wave at some fixed distance from the explosion center can be described by an exponentially decaying function (5).

The coupling effect, as described earlier, is usually treated by the "diffraction theory". The diffraction theory as presented by Cole (2) and Kennard (19) can be described by the physical concept of diffracted spherical waves originating at points on the membrane surface.

These spherical waves combine with the incident shock wave to satisfy the condition that the normal velocity component of the fluid particles must be the same as the normal velocity component of the membrane surface.

The equation which describes the motion of the membrane is found by considering a small element at the center and applying Newton's Second Law of Motion. By assuming a rigid, perfectly plastic material and neglecting bending, a single differential equation is found for the motion of the membrane. The necessary kinematic equation is based on the assumption that there will be very small deformations during any very short time period.

The actual pressure at the membrane center is given by the "diffraction theory" and the pressure in the incident shock wave is described by an exponentially decaying function. The actual pressure used with the equation of motion of the center membrane element, assuming a parabolic shape for the membrane at all times, and applying the deformation theory of plasticity, gives the necessary tools to begin a numerical solution. In the deformation theory of plasticity, the total finite deformation is the sum of the accumulated small displacements. The use of a time-incremental numerical process and a predictor method with the aid of the IBM 360 computer provides an efficient method of finding the final deformation, the loading history, and the complete deformation history.

CHAPTER II

FORMULATION OF THE GOVERNING EQUATIONS

2.1 General

This chapter contains the mathematical formulation of the governing equations for the problem. Pressure from the shock wave is given by an exponentially decaying function. The coupling effect between the shock wave pressure and the motion of the membrane is determined from the diffraction theory. The equation of motion of the center element is derived by applying Newton's Second Law of Motion. Combining these equations with the constitutive and kinematic equations gives the equations necessary to describe completely all phases of the deformation process.

2.2 Chain of Events After Detonation

Detonation is a process by which the decomposition of an explosive, with accompanying formation of gas and heat, takes place in a very short time. The decomposition front moves through the explosive at several thousand feet per second, leaving gas at a high temperature and pressure in its wake (9). For example, plaster gelatine detonates at approximately 20,000 feet per second with a calorific value of about 1400 calories per gram of explosive detonated (5). (This explosive is about 40% more powerful than TNT.)

When the detonation front reaches the boundary of the explosive,

detonation is complete and the shock wave is emitted into the surrounding medium. Figure 2a shows the location of the charge relative to the membrane.

During the second stage, the shock wave propagates through the medium (usually water) until it reaches the circular membrane. Figure 2b shows the shock wave just as it reaches the membrane.

Next, the shock wave strikes the circular membranes and sets it into motion. At the same time, the shock wave is reflected and this reflected wave propagates back into the medium. Figure 2c shows the partially deflected membrane and the reflected wave.

Finally, the shock wave is completely reflected and the circular membrane is at rest (Figure 2d). The kinetic energy of the membrane and that of the water following it is dissipated in the plastic deformation of the membrane.

A typical experimental setup is shown in Figure 3.

2.3 Shock Wave Pressure

The shock wave generated by the explosion propagates through the conducting medium with a velocity equal to the speed of sound. Since the front is an expanding spherical wave, the maximum pressure is approximately inversely proportional to the distance from the original position of the explosive charge. Cole (2) gives the following expression for the peak pressure:

$$P_m(R) = K \left(\frac{W^{1/3}}{R} \right)^\gamma, \quad (2-1)$$

where

R = distance from charge,

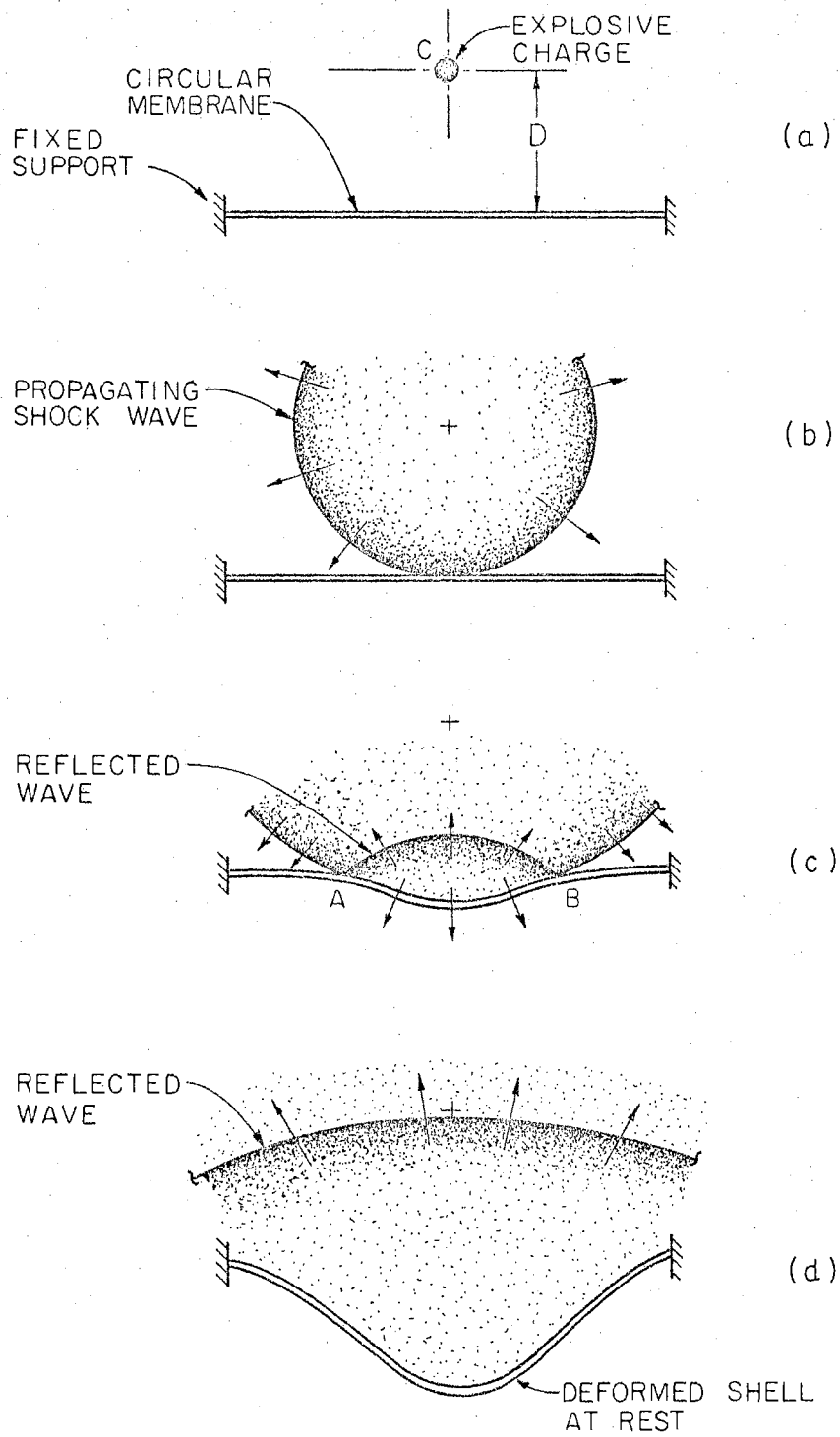


Figure 2. Illustration of Loading Cycle.

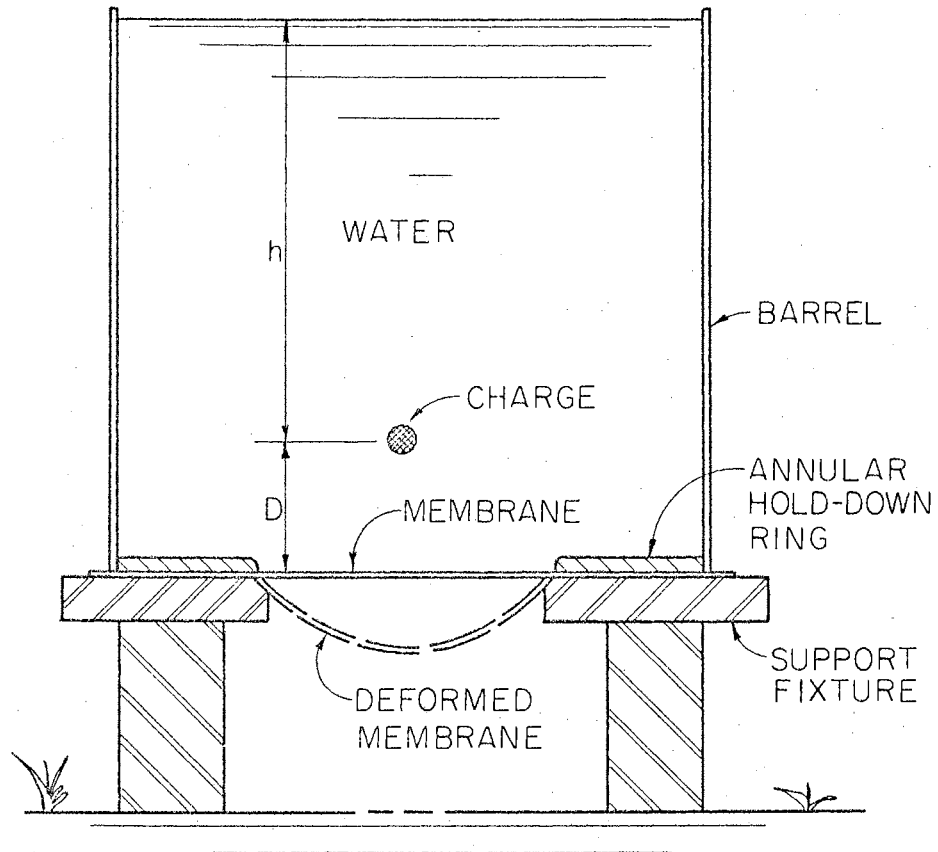


Figure 3. A Typical Experimental Set-up

- W = charge weight,
 P_m = peak pressure,
 K = parameter depending on the explosive, and
 γ = parameter depending on the explosive.

When the shock wave arrives at some given point on the membrane, there is an almost instantaneous rise in pressure at that point to the peak value. After the arrival of the shock wave, the pressure decays exponentially with time. This phenomenon is shown pictorially in Figure 4. The following equations apply:

$$p_i(R,t) = 0 \text{ when } t < t_a, \text{ and} \quad (2-2)$$

$$p_i(R,t) = P_m(R) \exp^{-(t-t_a)/\theta} \text{ when } t \geq t_a, \quad (2-3)$$

where

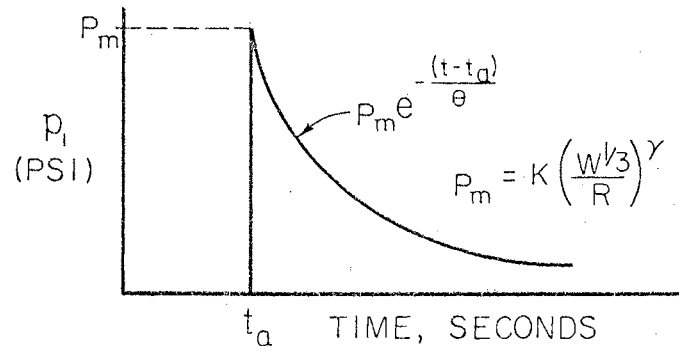
- t = time after detonation,
 t_a = the time of arrival of the shock wave at a given distance R ,
 R = distance from the center of charge,
 p_i = the local pressure, and
 θ = the time constant which gives the time for the pressure to decay to $1/e$ of its peak value.

If time is measured from the arrival time of the shock wave at the membrane, equations (2-2) and (2-3) become

$$p_i(R,t) = 0 \text{ when } t < 0 \text{ and} \quad (2-4)$$

$$p_i(R,t) = P_m(R) \exp^{-t/\theta} \text{ when } t \geq 0. \quad (2-5)$$

These equations, the time of arrival, and the propagation rate through the medium are based on the assumption of an incompressible acoustic medium. The values of K and γ depend on the explosive. For TNT, typical values are (19)



p-t VARIATION IN WATER

Figure 4. p-t Variation in Water

$$K = 20,400 \text{ psi,}$$

$$\gamma = 1.4, \text{ and}$$

$$\theta = 73.5 W^{0.29} R^{0.14} \text{ microseconds.}$$

2.4 Boundary Interactions

When a plane wave of acoustical intensity strikes a plane rigid boundary, continuity of pressure and particle velocity requires that the pressure in the reflected wave and the particle velocity in the reflected wave must be the same as their counterparts in the incident shock wave. From these considerations it can be shown (2) that the pressure acting on the rigid boundary must be twice that of the incident wave.

If the boundary is not rigid, the pressure in the incident wave and the motion of the boundary are coupled so that the actual pressure on the boundary is reduced. The following equation accounts for the effect of the target velocity on the applied pressure (2).¹

$$p(R, t) = 2p_i(R, t) - \frac{\rho_o}{2\pi} \iint_A \frac{1}{s} \left(\frac{\partial u_n}{\partial \tau} \right)_{\tau} dA', \quad (2-6)$$

where (see Figure 5)

p_i = the pressure in the incident wave,

ρ_o = the mass density of the conducting medium,

dA' = a differential area at some point on the surface,

u_n = a velocity component (at an earlier time τ) normal to the surface at dA' and directed away from the water,

s = the distance from dA' to the point where the pressure

¹See Appendix A for a complete development.

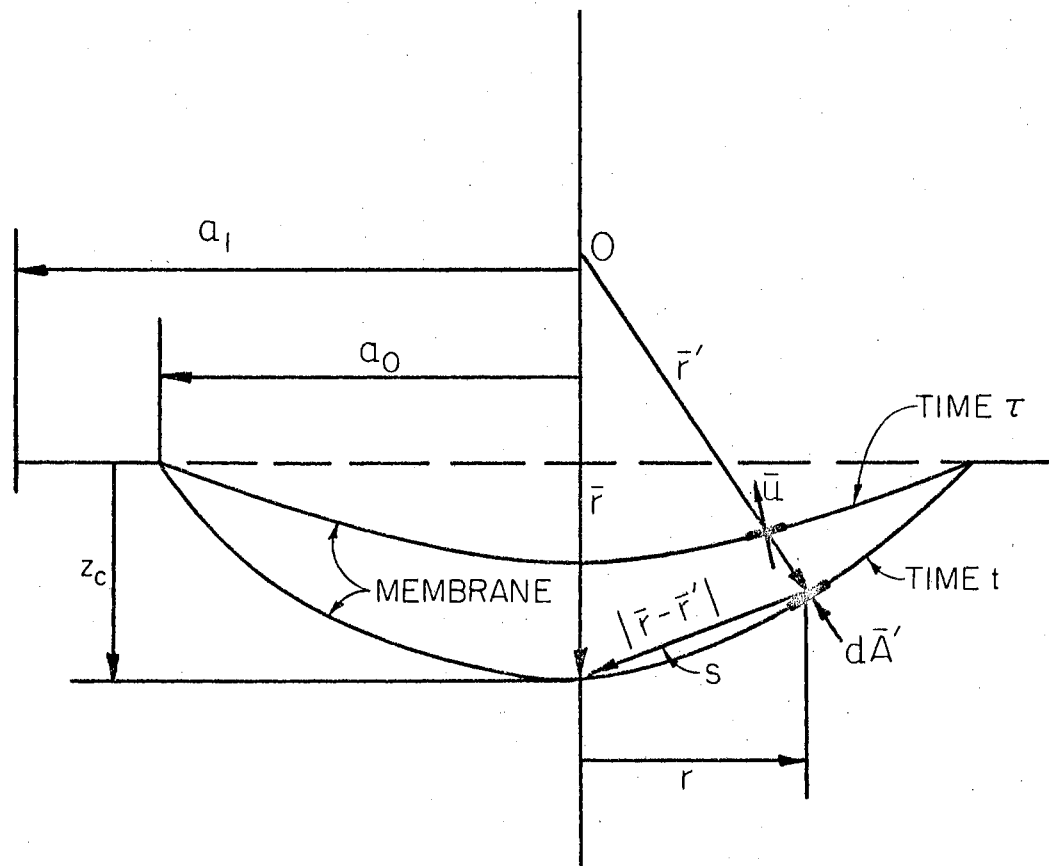


Figure 5. Membrane Geometry at Times t and τ

p is to be found,

$$\tau = (t - s/c_0),$$

c_0 = the speed of sound in the medium;

t = the time beginning with the impact of the incident shock wave on the membrane surface, and

s/c_0 = the time required for a wave of acoustical intensity to travel a distance s .

Equation (2-6) is valid for all points on the membrane surface if the following conditions are met:

- a) cavitation does not occur;
- b) the conducting medium is incompressible;
- c) the conducting medium is inviscid;
- d) the particle velocities are small;
- e) the membrane is mounted in a rigid infinite baffle;
- f) the membrane is backed by air or a vacuum.

The assumption that the plate deflection is always paraboloidal (which is fairly typical) leads to a simpler form for equation (2-6).

The paraboloidal form is

$$z(r,t) = z_c(t) \left(1 - \frac{r^2}{a^2} \right) \text{ when } t \geq 0 \text{ and} \quad (2-7)$$

$$z(r,t) = 0 \text{ when } t < 0,$$

where

$z(r,t)$ = the time-dependent deflection of the membrane,

$z_c(t)$ = the time-dependent deflection of the membrane center,

$\frac{dz_c}{dt}$ = the velocity of the membrane center,

$\frac{d^2 z_c}{dt^2}$ = the acceleration of the membrane center,

r = the radial polar coordinate, and

a = the radius of the membrane.

Equation (2-6) becomes

$$p(t) = 2p_i(t) - \frac{\rho_o}{2\pi} \iint_A \frac{1}{s} \left(\frac{d^2 z_c}{dt^2} \right)_{\tau} \left(1 - \frac{r^2}{a^2} \right) dA' . \quad (2-8)$$

The special case of small deflection, using the following simplifications

$$s = r \text{ and}$$

$$dA' = 2\pi r dr ,$$

gives

$$p(t) = 2p_i(t) - \rho_o \iint_A \left(\frac{d^2 z_c}{dt^2} \right)_{\tau} \left(1 - \frac{r^2}{a^2} \right) dr . \quad (2-9)$$

Under these conditions, changing the variable of integration and integrating by parts gives the following equation:²

$$p(t) = 2p_i(t) - \rho_o c_o \left[\frac{dz_c}{dt} + \frac{2}{\theta_d} z_c(t - \theta_d) \right. \quad (2-10)$$

$$\left. - \frac{2}{\theta_d} \int_{t - \theta_d}^t z_c(\tau) d\tau \right],$$

where θ_d is equal to a/c_o .

²See Appendix A for complete treatment.

In the earlier stages of motion (that is, $t \ll \theta_d$) the pressure at the center of the membrane is

$$p(t) = 2p_i(t) - \rho_o c_o \frac{dz_c}{dt} . \quad (2-11)$$

For $t \gg \theta_d$, equation (2-9) reduces to

$$p(t) = 2p_i(t) - \frac{2}{3} \rho_o a \frac{d^2 z_c}{dt^2} . \quad (2-12)$$

The last term on the right side of equation (2-12) represents the pressure on the membrane due to the deceleration of the mass of water following the membrane.

In this study, the paraboloidal form for the membrane shape is used. Numerical integration of the following equation gives the pressure at the membrane center at any time t .

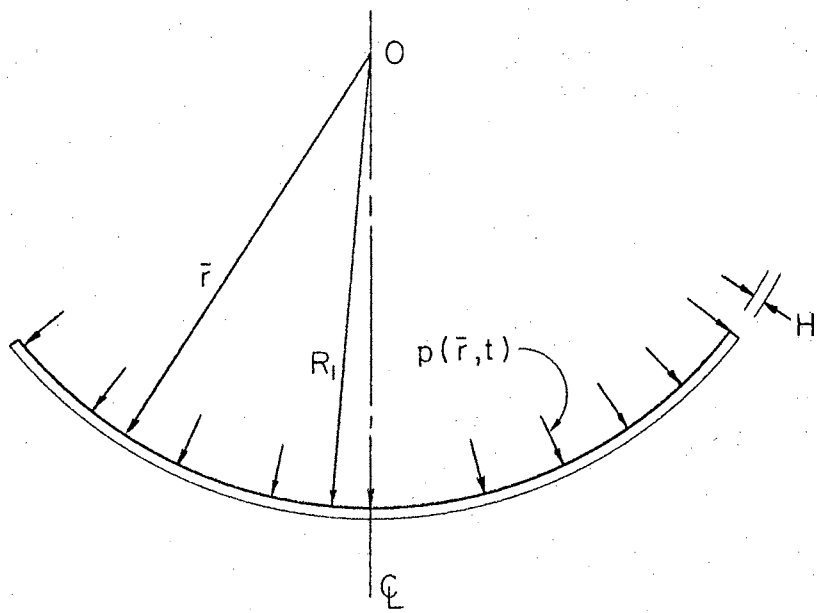
$$p(t) = 2p_i(t) - \rho_o \int_0^a \frac{1}{s} \left(\frac{d^2 z_c}{dt^2} \right) \left(1 - \frac{r^2}{a^2} \right) r dr . \quad (2-13)$$

2.5 Equation of Motion

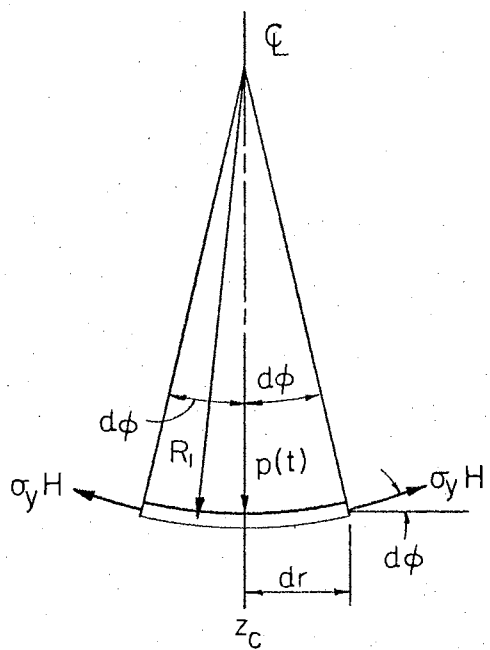
The equation of motion of a small element below a parallel circle of a body of revolution is found by applying Newton's Second Law of Motion. The element to be considered and the body of revolution from which the element is taken are shown in Figure 6.

Newton's Second Law of Motion applied to the element shown in Figure 6 is

$$\sum F_z = m \frac{d^2 z_c}{dt^2} . \quad (2-14)$$



(a) BODY OF REVOLUTION



(b) CENTER ELEMENT OF BODY OF REVOLUTION

Figure 6. Loading on Membrane

where

$$\begin{aligned}\sum F_z &= p(t) dA - 2\sigma_y H\pi(dr)(d\phi), \\ dA &= \pi(dr)^2, \text{ and} \\ dr &= R_1 d\phi.\end{aligned}\tag{2-15}$$

Thus equation (2-15) becomes

$$\sum F_z = p(t)\pi R_1^2(d\phi)^2 - 2\sigma_y H\pi R_1(d\phi)^2.\tag{2-16}$$

Finally substituting

$$m = \rho\pi(dr)^2H$$

and combining equations (2-14) and (2-16) gives

$$\begin{aligned}p(t)\pi R_1^2(d\phi)^2 - 2\sigma_y H\pi R_1(d\phi)^2 \\ = \rho\pi R_1^2(d\phi)^2 H \frac{d^2 z_c}{dt^2}.\end{aligned}\tag{2-17}$$

Equation (2-17) reduces to

$$\frac{d^2 z_c}{dt^2} = \frac{p(t)}{\rho H} - \frac{2\sigma_y}{\rho R_1}.\tag{2-18}$$

This is the equation of motion of the center membrane element where

$$\frac{d^2 z_c}{dt^2} = \text{the acceleration of the center element,}$$

ρ = the mass density of the membrane material,

σ_y = the yield stress of the membrane material,

H = the thickness of the membrane,

$p(t)$ = the pressure acting on the membrane center, and

R_1 = the radius of curvature.

Due to the restriction that the membrane deflection is given by equation (2-7), the motion of the center element determines the motion of the entire shell.

2.6 Kinematic Equation

Although the total deformation of the membrane is finite, the deformation during any increment of time is small. Consider the sketch shown in Figure 7 and the change in strain during one time interval can be easily seen. The change in strain is defined as the increase in length of a line element during a time increment, divided by the line element length at the beginning of the time interval. The kinematic equation (see Figure 7) is

$$\delta\epsilon_{\phi} = \frac{A'B' - AB}{AB}, \quad (2-19)$$

where

$$A'B' = 2(R_1 + \delta z_c)d\phi \quad \text{and} \quad (2-20)$$

$$AB = 2R_1d\phi. \quad (2-21)$$

Then

$$\delta\epsilon_{\phi} = \frac{2(R_1 + \delta z_c)d\phi - 2R_1d\phi}{2R_1d\phi} \quad (2-22)$$

or

$$\delta\epsilon_{\phi} = \frac{\delta z_c}{R_1}. \quad (2-23)$$

$\delta\epsilon_{\phi}$ is the change in strain along a great circle of the membrane.

2.7 Constitutive Equations

Since the initial impulse of the shock wave is large, a high membrane velocity results. Hence, the stresses move almost immediately

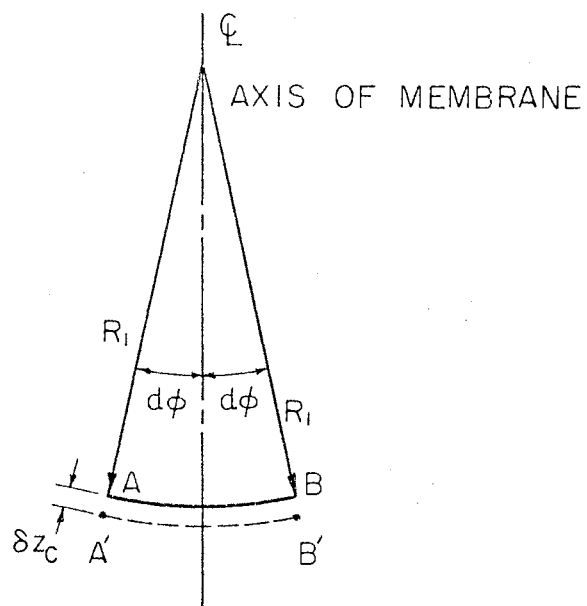


Figure 7. Membrane Deformation
During One Time
Interval

into the plastic range, and the strains will also be in the plastic range. Considering a biaxial state of stress, the "energy-of-distortion condition" that was introduced by von Mises (3) and modified by Hencky (3), gives the criterion for yielding the following equation:

$$\tau_{\text{oct}} = \frac{\sqrt{2}}{3} \sigma_y, \quad (2-24)$$

where

$$\tau_{\text{oct}} = \frac{\sqrt{2}}{3} \sqrt{\sigma_1^2 + \sigma_2^2 - \sigma_1 \sigma_2}, \quad (2-25)$$

τ_{oct} = octahedral-shearing stress,

σ_1 = a principal stress,

σ_2 = a principal stress, and

σ_y = yield stress of material.

Saint-Venant's theory (3) is considered to be the most suitable description of the plastic-flow phenomenon. For a state of biaxial stress, Saint-Venant's theory may be stated as follows:

$$2\sigma_1 - \sigma_2 = \frac{6\lambda}{\delta t} \delta\epsilon_1, \quad \text{and} \quad (2-26)$$

$$2\sigma_2 - \sigma_1 = \frac{6\lambda}{\delta t} \delta\epsilon_2. \quad (2-27)$$

It can also be shown (3) that the octahedral-shearing stress and the incremental octahedral-shearing strain are related as follows:

$$\tau_{\text{oct}} = \frac{\lambda \delta\gamma_{\text{oct}}}{\delta t}, \quad (2-28)$$

where

$$\delta\gamma_{\text{oct}} = \frac{2}{3} \sqrt{(\delta\epsilon_1 - \delta\epsilon_2)^2 + (\delta\epsilon_2 - \delta\epsilon_3)^2 + (\delta\epsilon_3 - \delta\epsilon_1)^2}, \quad (2-29)$$

$\delta\epsilon_1$, $\delta\epsilon_2$, and $\delta\epsilon_3$ = incremental linear principal strains, and

λ = a scalar factor which is a function σ_y and

the strain rate.

For an incompressible material, the following relationship holds:

$$\delta\epsilon_1 + \delta\epsilon_2 + \delta\epsilon_3 = 0. \quad (2-30)$$

If equation (2-28) is substituted into equations (2-26) and (2-27), the following results are obtained:

$$2\sigma_1 - \sigma_2 = \frac{6\tau_{\text{oct}}}{\delta\gamma_{\text{oct}}} \delta\epsilon_1, \quad \text{and} \quad (2-31)$$

$$2\sigma_2 - \sigma_1 = \frac{6\tau_{\text{oct}}}{\delta\gamma_{\text{oct}}} \delta\epsilon_2. \quad (2-32)$$

Substituting equation (2-30) into equation (2-29) gives

$$\delta\gamma_{\text{oct}} = \frac{2\sqrt{6}}{3} \sqrt{\delta\epsilon_1^2 + \delta\epsilon_1 \delta\epsilon_2 + \delta\epsilon_2^2}. \quad (2-33)$$

The incremental effective strain and effective stress are defined as follows:

$$\delta\bar{\epsilon} = \frac{\sqrt{2}\sqrt{6}}{3} \sqrt{\delta\epsilon_1^2 + \delta\epsilon_1 \delta\epsilon_2 + \delta\epsilon_2^2}, \quad \text{and} \quad (2-34)$$

$$\bar{\sigma} = \sqrt{\sigma_1^2 - \sigma_1 \sigma_2 + \sigma_2^2}. \quad (2-35)$$

It follows that the incremental octahedral strain and octahedral stress are related to the incremental effective strain as follows:

$$\delta\gamma_{\text{oct}} = \sqrt{2} \delta\bar{\epsilon}, \quad \text{and} \quad (2-36)$$

$$\tau_{\text{oct}} = \frac{\sqrt{2}}{3} \bar{\sigma}. \quad (2-37)$$

Substitution of equation (2-36) and (2-37) into (2-31) and (2-32) yields

$$\sigma_1 - \frac{\sigma_2}{2} = \frac{\bar{\sigma}}{\delta\bar{\epsilon}} \delta\epsilon_1 \quad \text{and} \quad (2-38)$$

$$\sigma_2 - \frac{\sigma_1}{2} = \frac{\bar{\sigma}}{\delta\bar{\epsilon}} \delta\epsilon_2. \quad (2-39)$$

The constitutive equations are

$$\delta \varepsilon_1 = \sigma_1 - \frac{\sigma_2}{2} \frac{\delta \bar{\varepsilon}}{\bar{\sigma}} \quad \text{and} \quad (2-40)$$

$$\delta \varepsilon_2 = \sigma_2 - \frac{\sigma_1}{2} \frac{\delta \bar{\varepsilon}}{\bar{\sigma}}. \quad (2-41)$$

For a perfectly plastic material, the principal stresses are equal, that is

$$\sigma_1 = \sigma_2. \quad (2-42)$$

Substituting equation (2-42) into the constitutive equations (2-40 and 2-41) shows that

$$\delta \varepsilon_1 = \delta \varepsilon_2. \quad (2-43)$$

For an incompressible material, the following is true (3)

$$\delta \varepsilon_3 = -\delta \varepsilon_1 - \delta \varepsilon_2 \quad (2-44)$$

or

$$\delta \varepsilon_3 = -2\delta \varepsilon_1. \quad (2-45)$$

For the case of a membrane acted upon by an impulsive pressure

$$\sigma_3 = 0,$$

and

$$\sigma_1 = \sigma_2 = \sigma_y, \quad (2-46)$$

$$\delta \varepsilon_1 = \delta \varepsilon_\phi, \quad \text{and} \quad (2-47)$$

$$\delta \varepsilon_3 = \delta \varepsilon_r, \quad (2-48)$$

so that

$$\delta \varepsilon_r = -2\delta \varepsilon_\phi, \quad (2-49)$$

and from equation (2-23)

$$\delta \epsilon_r = -2 \frac{\delta z_c}{R_1} \quad (2-50)$$

where $\delta \epsilon_r$ is the strain increment normal to the membrane. Using the definition of the strain increment, the thickness of the membrane at any time t is found to be

$$H(t) = [H(t - \delta t)] [1 + \delta \epsilon_r] \quad (2-51)$$

2.8 Cavitation Occurring-Afterflow Theory

When the pressure on the face of the moving membrane drops to the vapor pressure of water, cavitation occurs. Physically, the water begins to vaporize and the membrane separates from the water, creating a void space.

The afterflow theory for the reloading of an airbacked membrane subjected to an underwater explosion is best developed by analyzing the response of the plate (11). This response is divided into four stages. Stage one includes the period of time up to the occurrence of cavitation. The equation of motion of the membrane, along with the modified pressure given by the diffraction theory, is sufficient to determine the actual pressure on the membrane center and the history of the membrane motion.

During the second stage the pressure acting on the membrane is zero and the membrane moves with only plastic forces acting on it. This phase is characterized by a decreasing velocity of the membrane center. The equation of motion is applicable during this stage and the applied pressure is equal to zero. This stage terminates when reloading starts, which happens when the membrane is brought to rest (or nearly so) by the plastic forces acting within the membrane.

Many efforts have been made to explain the reloading phase with the diffraction theory; however, as pointed out in Section 2.4, the diffraction theory is not satisfactory when cavitation occurs (11). The diffraction theory assumes the continuous transmission of the diffracted spherical waves. This transmission is not possible when the void space caused by cavitation is present. The approach to be used when cavitation is present is to assume the water surrounding the gas bubble to be incompressible, and then to examine the outward flow of water as the gas bubble, remaining after detonation, expands (11).

When detonation of the explosive is complete, a shock wave is emitted into the surrounding medium. This shock wave causes the initial motion of the membrane. After the shock wave is emitted, the gas bubble begins to expand because of the high pressure inside the gas-filled cavity. For an incompressible medium, such as water, and neglecting the friction, Bernoulli's equation describes the motion of the water surrounding the gas bubble.

Close to the bubble surface where the influence of the far boundaries can be neglected, a simple potential function adequately gives the velocity field (6). The potential function

$$\phi = \frac{\dot{R}R^2}{r} \quad (2-52)$$

when substituted into Bernoulli's equation, gives

$$p - P_h = \frac{\rho_o}{r} \left[\frac{\partial}{\partial t} (\dot{R}R^2) \right] - \frac{\rho_o}{2} \left(\frac{\dot{R}R^2}{r^2} \right)^2, \quad (2-53)$$

where

p = the pressure in the water at any position r ,

P_h = the hydrostatic pressure at the bubble surface if the water

is undisturbed.

- R = radius of the gas bubble,
 \dot{R} = velocity of bubble surface,
 r = distance from membrane center, and
 ρ_o = mass density of water.

If the pressure on the gas bubble surface (at $r=R$) is p_g , the equation for the bubble expansion is

$$p_g - P_h = \rho_o \ddot{R}R + \frac{3}{2} \rho_o \dot{R}^2 . \quad (2-54)$$

Letting (6)

$$p_g = \left(\frac{R_o}{R} \right)^4 p_o , \quad (2-55)$$

where R_o is the initial radius of the gas bubble, equation (2-54) becomes

$$\left(\frac{R_o}{R} \right)^4 p_o - P_h = \rho_o \ddot{R}R + \frac{3}{2} \rho_o \dot{R}^2 . \quad (2-56)$$

The following are the necessary boundary conditions:

$$R = R_o \text{ for } t=0 , \text{ and}$$

$$\dot{R} = 0 \text{ for } t=0 .$$

Then the solution to equation (2-56) with $P_h=0$ can be written in the following form (11):

$$R = R_o (1 + u^2) , \quad (2-57)$$

where

$$t = 2\beta \left(u + \frac{2}{3} u^3 + \frac{1}{5} u^5 \right) , \quad (2-58)$$

$$\beta = R_o \sqrt{\rho_o / 2p_o} ,$$

p_0 = the pressure in the bubble immediately after complete detonation,

\ddot{R} = acceleration of gas bubble surface, and

u = a time-dependent parameter.

The expanding gas bubble forces the water surrounding it to rush radially outward. The solution of equation (2-56) gives the radially outward motion of the water immediately surrounding the gas bubble.

As the gas bubble expands, the outward moving water fills the cavity caused by cavitation. When the cavity is filled, the reloading of the membrane takes place. During reloading, the membrane is accelerated rapidly, almost instantaneously, to the velocity of the outward-rushing water. This is based on the assumption that the mass of water is much larger than the mass of the membrane. Therefore, initially the membrane is forced to move with a velocity equal to that of the water. This approximation has proved satisfactory in several cases (11). After reloading, the kinetic energy of water and membrane is absorbed in plastic deformation of the membrane.

During reloading, the reloading velocity is described using the assumptions that the water is incompressible and the circular membrane is mounted in an infinite rigid baffle. The gas globe is represented by a point source of strength $4\pi Q$. A solution for the plane above the membrane is then found in the form of a potential function which satisfies the Laplace equation. This potential function (V) describes the motion of the water near the membrane and the baffle, while the potential function ϕ (equation 2-52) is used for the water motion immediately surrounding the gas bubble.

The boundary conditions are $V=0$ on the cavitation boundary and

$\partial V/\partial n$ on the baffle surface. Spheroidal coordinates (ξ, ζ, ψ) are suited to this problem³ and are shown in Figure 8. The transformation from cylindrical coordinates is given by (14)

$$\begin{aligned} z &= a\zeta\xi, \\ x &= a\sqrt{(1+\zeta^2)(1-\xi^2)}, \text{ and} \\ \psi &= \psi \end{aligned} \quad (2-59)$$

Laplace's equation in spheroidal coordinates with axial symmetry is (14)

$$\frac{\partial}{\partial \xi} \left[(1-\xi^2) \frac{\partial V}{\partial \xi} \right] + \frac{\partial}{\partial \zeta} \left[(1+\zeta^2) \frac{\partial V}{\partial \zeta} \right] = 0 \quad (2-60)$$

with the boundary conditions becoming

$$V=0 \text{ for } \zeta=0 \text{ and}$$

$$\partial V/\partial \xi=0 \text{ for } \xi=0,$$

and a source of strength $4\pi Q$ at

$$\xi=1 \text{ and } \zeta=\zeta_0=D/a,$$

where

$$a = \text{membrane radius,}$$

$$Q = \frac{R_o^3 u}{\beta}, \text{ and}$$

$$D = \text{distance from charge to membrane.}$$

The potential function which satisfies Laplace's equation and the boundary condition is (12)

³See Appendix B for a more complete development by Schauer (12).

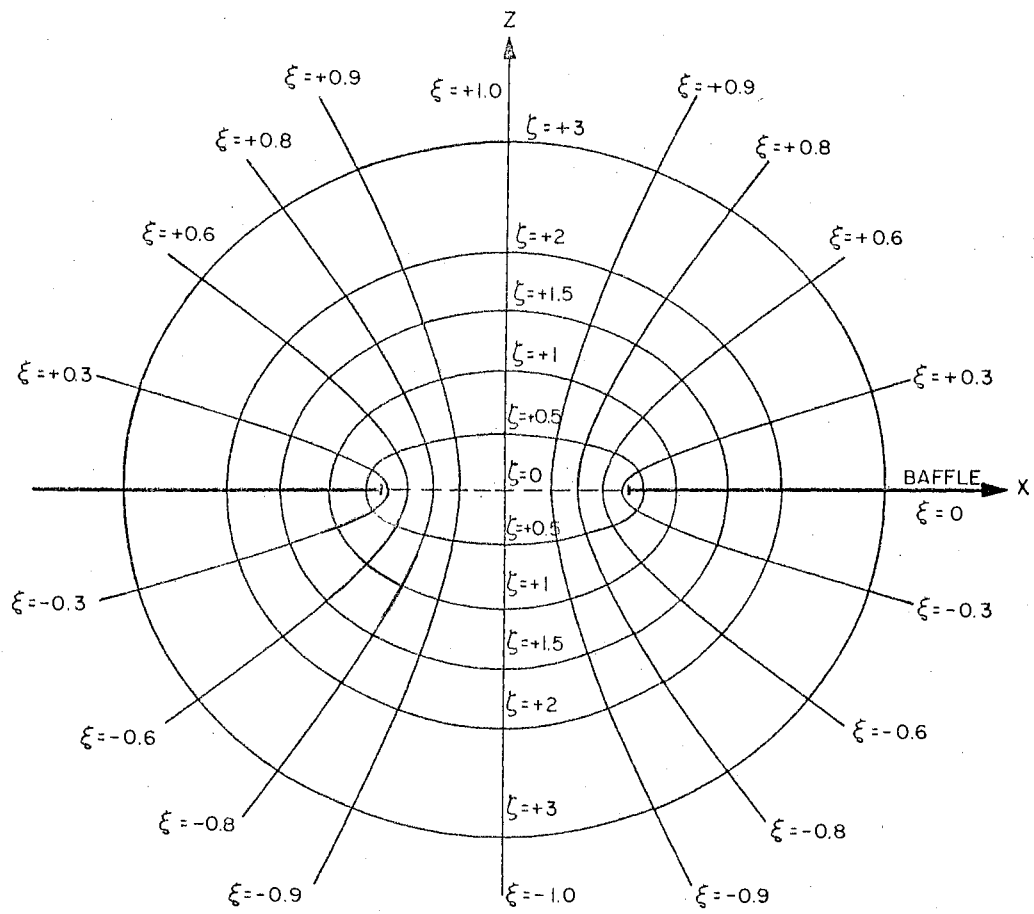


Figure 8. Spheroidal Coordinate System

$$V = \sum_{n=0}^{\infty} \left[2iQ \frac{(4n+1)}{a} Q_{2n}(i\zeta_0) P_{2n}(\xi) \right] \quad (2-61)$$

$$\left[P_{2n}(i\zeta) + \frac{2}{i\pi} Q_{2n}(i\zeta) \right],$$

where i is equal to $\sqrt{-1}$.

P_{2n} and Q_{2n} are Legendre functions of the first and second kind, respectively. The velocity on the cavitation surface is

$$v = \frac{1}{a\xi} \frac{\partial V}{\partial(i\xi)} \Big|_{\zeta=0} \quad (2-62)$$

At the center ($\xi=1$, $\zeta=0$), the velocity is

$$v_0 = \sum_{n=0}^{\infty} i^{(2n+1)} \frac{4(4n+1)}{\pi a^2} Q \frac{2^{2n} (n!)^2}{(2n)!} Q_{2n}(i\zeta_0). \quad (2-63)$$

For large values of ζ this converges to (12)

$$v_0 = \frac{4Q}{\pi a D} \quad (2-64)$$

Since the velocity (v_0) at the center of the cavitation surface is a function of time, the displacement of the water at the same position is (11)

$$s_c = \int_0^t v_0 dt \quad (2-65)$$

or

$$s_c = \frac{4R_0^3}{\pi a D} (u^2 + u^4 + u^6/3). \quad (2-66)$$

Reloading occurs when the displacement (5) of the water is sufficient to close the cavitation void and the reloading velocity is v_0 .

The last stage of the deformation process is the dissipation of the reloading energy into plastic deformation. If an equivalent mass

of water is associated with the water velocity v_o , the final deformation of the membrane is given by (11).

$$\delta_f^2 = 0.90 \frac{R_o^3 p_o a}{D \sigma_y H} \left(\frac{a \delta_o}{D^2} \right)^{1/3} + \delta_o^2, \quad (2-67)$$

where

δ_o = the deflection at the end of the second stage,

δ_f = the final deformation of the membrane center,

σ_y = yield stress of the material,

H = thickness of the membrane, and

a = the membrane radius.

In this study, the diffraction theory is applied to account for the effect of the water following the membrane. The equations are found in Section 2.4.

2.9 Influence of the Water Surface

Schauer (13) determined the influence of the free water surface on reloading by calculating the difference in kinetic energies of the water before and after reloading. The ratio of the difference in energies (evaluated at the depth of a particular membrane) to the difference in energies (at an infinite depth) is called the energy reduction factor alpha (α).

To determine the kinetic energy of the water after reloading, the free cavitation surface is replaced by a rigid surface and a potential function (V_d) is found for this condition. It has been shown (13) that the difference in energies at a depth h below the water surface is

$$E = -2\pi \sigma_y Q (V_s) \zeta_o, \quad (2-68)$$

where

$$V_s = V - V_d \quad \text{and}$$

$$\zeta_0 = D/a .$$

Therefore

$$\alpha = \frac{E \text{ at depth } h}{E \text{ at depth } \infty} . \quad (2-69)$$

From this

$$\alpha = \frac{(V_s)_{\zeta_0} \text{ at depth } h}{(V_s)_{\zeta_0} \text{ at depth } \infty} . \quad (2-70)$$

Finally,

$$\alpha = \left(1 - \frac{\zeta_0}{\zeta_2} \right) \frac{\frac{\pi}{2} (\zeta_1 - \zeta_0)}{\frac{\pi}{2} \zeta_1 - 1} \text{ for } \zeta_1 > \zeta_0 \quad \text{and} \quad (2-71)$$

$$\alpha = 0 \text{ for } \zeta_1 < \zeta_0 , \quad (2-72)$$

where

$$\zeta_1 = \sqrt{\left(\frac{2h}{a}\right)^2 - 1} ,$$

$$\zeta_2 = \frac{D}{a} \sqrt{1 + \left(\frac{2h}{D}\right)^2} ,$$

$$\zeta_0 = D/a ,$$

D = the distance from the charge to the membrane,

a = the plate radius, and

h = the depth of water above the charge.

Since α is the energy reduction factor, the square root of α will be used as the reloading velocity reduction factor.

2.10 Migration of the Gas Bubble

Bryant (18) gave a simplified theory for the effect that the surfaces have on the motion of a gas bubble from an underwater explosion. Quantitative expressions for the motion of the gas bubble are obtained by representing the gas bubble as originating from a point source. The influence of the surfaces is found from application of the method of images to satisfy the boundary conditions. The boundary conditions are: (1) the pressure must be zero at the free surface (which is approximated by letting the potential function be zero along the free surface), and (2) the velocity component of water must be parallel to the membrane and baffle (see Figure 9). These boundary conditions take the following form:

$$\phi = 0 \text{ at the free surface, and}$$

$$\frac{\partial \phi}{\partial n} = 0 \text{ at the membrane and baffle.}$$

The charge is represented by a point source e at O (see Figure 9) with a strength

$$e = 4\pi R^2 \dot{R}, \quad (2-73)$$

where

$$R = \text{the radius of the gas bubble, and}$$

$$\dot{R} = \text{the velocity of the gas bubble surface.}$$

Since e is a positive source, the motion of the water surrounding the bubble is radially outward. If a positive source of strength e is placed at O_1 (see Figure 9), a distance D below the membrane, the second boundary condition is satisfied. The source at O_1 also causes an outward flow which, when combined with the outward flow from the source at O , produces only tangential flow at the baffle.

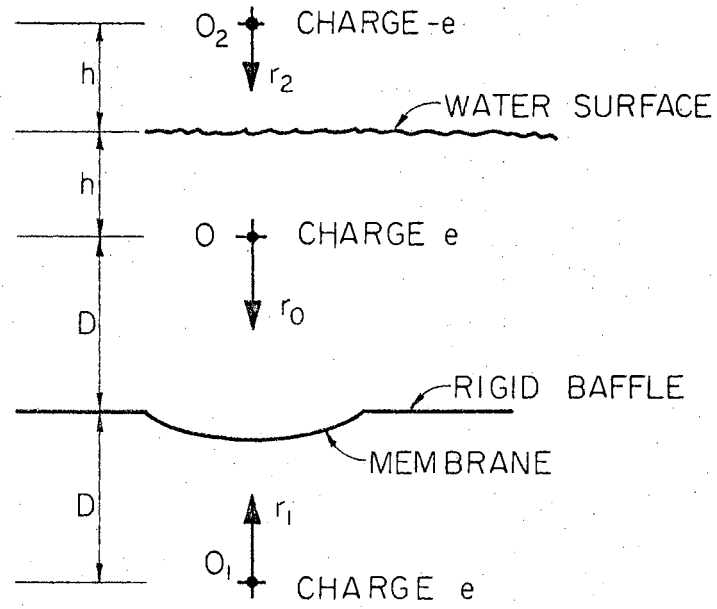


Figure 9. Point Sources of Charge e

The first boundary condition is satisfied by placing a negative source $(-e)$ a distance (h) above the water surface. Since the potential functions representing the sources at O and O_2 are opposite in sign, their sum is zero at any point on the free surface. This arrangement of images only approximately satisfies the boundary conditions. Images in pairs would have to be added at greater distances to improve the boundary conditions. These images would have the same strength as the images at O_1 and O_2 .

Figure 9 shows the arrangement of the images, each with its own coordinate system. The potential functions for the sources are

$$\phi_0 = -\frac{R^2 \dot{R}}{r_0} \text{ at } O ,$$

$$\phi_1 = -\frac{R^2 \dot{R}}{r_1} \text{ at } O_1 , \text{ and}$$

$$\phi_2 = \frac{R^2 \dot{R}}{r_2} \text{ at } O_2 ,$$

where

r_0 = the radial coordinate from the origin O ,

r_1 = the radial coordinate from the origin O_1 , and

r_2 = the radial coordinate from the origin O_2 .

Since the effect of the baffle and membrane on the gas bubble at O is given by the point source at O_1 , the movement of the gas bubble can now be found. The image source at O_1 will cause the water in the vicinity of O to have a velocity as follows:

$$U_1 = \left. \frac{\partial \phi_1}{\partial r_1} \right|_{r_1 = 2D} \quad (2-74)$$

In addition, a pressure gradient is developed due to the image at O_1 around O_1 . The gradient is (18)

$$\frac{\partial p}{\partial r_1} = \rho \frac{\partial}{\partial t} \left[\frac{\partial \phi}{\partial r_1} \right] \Big|_{r_1} = 2D . \quad (2-75)$$

Since the pressure gradient is positive at points between O_1 and O , the pressure at O is greater than the pressure at O_1 . Therefore the movement of the gas bubble at O is toward O_1 and the baffle. G. I. Taylor (18) shows that the velocity of a gas globe due to a pressure gradient is

$$U_2 = \frac{2}{R^3} \int_0^t \left[\frac{1}{\rho} \left(\frac{\partial p}{\partial r_1} \right) \Big|_{r_1} = 2D \right] R^3 dt \quad (2-76)$$

or upon substitution of equation (2-75)

$$U_2 = \frac{2}{R^3} \int_0^t \left[\frac{\partial}{\partial t} \left(\frac{\partial \phi_1}{\partial r_1} \right) \Big|_{r_1} = 2D \right] dt . \quad (2-77)$$

The total velocity for the gas bubble is

$$U = U_1 + U_2 \quad (2-78)$$

or

$$U = \frac{\partial \phi_1}{\partial r_1} \Big|_{r_1} = 2D + \int_0^t \left[\frac{\partial}{\partial t} \left(\frac{\partial \phi_1}{\partial r_1} \right) \Big|_{r_1} = 2D \right] dt . \quad (2-79)$$

This equation (2-79) upon substitution for ϕ , and integrating by parts becomes

$$U = \frac{3}{4} \frac{R^2 \dot{R}}{D^2} - \frac{3}{2D^2 R^3} \int_0^t R^4 \dot{R}^2 dt , \quad (2-80)$$

where

U = the velocity of the gas bubble at 0 away from the baffle,

R = the radius of the gas bubble,

\dot{R} = the velocity of the gas bubble surface, and

D = the distance of the charge from the membrane.

If the signs in the expression for U are reversed, the velocity of the gas bubble toward the baffle and membrane is

$$U = -\frac{3}{4} \frac{R^2 \dot{R}}{D^2} + \frac{3}{2D^2 R^3} \int_0^t R^4 \dot{R}^2 dt . \quad (2-81)$$

Similarly the effect of the free surface on the gas bubble is represented by the image source at O_2 . The motion of the gas bubble at 0 toward the baffle and membrane, due to the free water surface, is

$$U = -\frac{3}{4} \frac{R^2 \dot{R}}{h^2} + \frac{3}{2h^2 R^3} \int_0^t R^4 \dot{R}^2 dt . \quad (2-82)$$

The total velocity of the gas bubble at 0, resulting from the point sources at O_1 and O_2 , is

$$U = \left[\frac{1}{D^2} + \frac{1}{h^2} \right] \left[-\frac{3R^2 \dot{R}}{4} + \frac{3}{2R^3} \int_0^t R^4 \dot{R}^2 dt \right] , \quad (2-83)$$

where h is the depth of the charge below the water surface. Finally, the displacement of the gas bubble at 0 is

$$S = \int_0^t U dt . \quad (2-84)$$

CHAPTER III

NUMERICAL SOLUTION OF THE GOVERNING EQUATIONS

3.1 Introduction

If the equation of motion for the problem is examined, it is found that an analytical solution is not obtainable by ordinary methods. This paradox becomes apparent when the expression for pressure is substituted into the equation for the motion of the membrane. The governing equation of motion depends on conditions at earlier times of the deformation process and on the shape of the membrane at time t . Thus, the equation of motion is nonlinear which suggests a numerical solution. The numerical process used in this study is an incremental predictor technique; that is, the conditions at time t are used to predict the conditions at time $t + \delta t$. The description of the method is detailed in the following sections.

3.2 Boundary and Initial Conditions

The boundary conditions for the membrane are quite simple because of the assumption of zero bending resistance in the membrane. The boundary conditions based on this assumption become one of zero deformation at the clamped edge of the membrane. In equation form, the boundary condition is

$$z(a,t) = 0 .$$

The initial conditions are: (1) the membrane is at rest at the instant the shock wave strikes it, and (2) the deformation is zero. In equation form, these initial conditions are

$$\begin{aligned} z(r,0) &= 0 \quad \text{and} \\ \dot{z}(r,0) &= 0 \quad , \end{aligned}$$

where z and \dot{z} are the displacement and velocity of the membrane respectively.

The initial acceleration of the center membrane element is found from the equation of motion (2-18). The acceleration is

$$\ddot{z}_c = \frac{p(t)}{\rho H} \quad (3-1)$$

and

$$p(t) = 2P_m \quad \text{for } t = 0 \quad .$$

The coupling effect is initially zero because the membrane is at rest.

The velocity and displacement at the end of the first time interval are found by solving the equation of motion. During the first time period of the membrane motion, the pressure, including the coupling, is very nearly

$$p(t) = 2P_m e^{-t/\theta} - \rho_o c_o \dot{z}_c \quad (3-2)$$

When this is substituted into the equation of motion (2-18), the equation of motion becomes

$$\ddot{z}_c = \frac{(2P_m e^{-t/\theta} - \rho_o c_o \dot{z}_c)}{\rho H} - \frac{2\sigma_y}{R_1} \quad , \quad (3-3)$$

where

$$R_1 = \frac{a^2}{2z_c} \quad .$$

When rearranged, equation (3-3) becomes

$$\ddot{z}_c + \frac{\rho_o c_o \dot{z}_c}{\rho H} + \frac{4\sigma y_c}{a^2} = \frac{2P_m e^{-t/\theta}}{\rho H}, \quad (3-4)$$

for which an analytical solution is easily obtained.

3.3 Numerical Solution for Displacement

If the acceleration of the center membrane element is assumed to be constant during a very small time interval, the velocity and displacement at the end of the time interval are

$$V_c(t + \delta t) = V_c(t) + A_c(t) \cdot (\delta t) \quad \text{and} \quad (3-5)$$

$$Z_c(t + \delta t) = Z_c(t) + V_c(t) \cdot (\delta t) + A_c(t) \cdot (\delta t)^2/2,$$

where

δt = the length of the time interval,

Z_c = the displacement of the membrane center,

V_c = the velocity of the membrane center, and

A_c = the acceleration of the membrane center.

The equation of motion (2-18) is used to calculate the acceleration in each new position of the membrane and is

$$A_c(t) = \frac{p(t)}{\rho H} - \frac{2\sigma y}{\rho R_1}, \quad (3-6)$$

where R_1 is the radius of curvature and is given as follows:

$$R_1 = \frac{a^2}{2Z_c(t)}.$$

It is obvious that this incremental predictor process can be repeated continually until the deformation process is completed. The

calculated value at each time gives the history of the motion of a membrane after being subjected to a nearby underwater explosion. For solution on a digital computer these equations are rewritten as follows:

$$V_c(k+1) = V_c(k) + A_c(k) \cdot (\delta t) ,$$

$$Z_c(k+1) = Z_c(k) + V_c(k) \cdot (\delta t) + A_c(k) \cdot (\delta t)^2 / 2 ,$$

$$A_c(k) = \frac{p(k)}{\rho H(k)} - \frac{2\sigma_y}{\rho R_1(k)} ,$$

$$R_1(k) = \frac{a^2}{2Z_c(k)} ,$$

$$H(k) = [H(k-1)] [1 + \delta\epsilon_r] , \text{ and}$$

$$\delta\epsilon_r = - \frac{2[Z_c(k) - Z_c(k-1)]}{R_1(k-1)} .$$

This process can be continually repeated to the end of the deformation process if the pressure can be calculated at the beginning of each time interval.

3.4 Pressure at the Membrane Center

In the preceding equations, the pressure at the membrane center is the one unknown term. The pressure from the incident shock wave is coupled to the motion of the membrane as long as cavitation does not occur. The coupling effect is described by the diffraction theory. The actual pressure felt by the membrane has been given in equation (2-13), which is rewritten as:

$$p(t) = 2p_i(t) - \rho_o \int_0^a \frac{1}{s} (\ddot{z}_c)_r (1 - r^2/a^2) r dr . \quad (3-7)$$

For use on the digital computer, equation (3-7) is written as follows:

$$p(k) = 2p_i(k) - \rho_o \sum_{j=1}^n (A_c)_\tau \frac{(1-r_j^2/a^2)(r_j)(\Delta l_j)}{s_j}, \quad (3-8)$$

where the above summation includes the entire area. This equation gives the pressure for each deflection position of the membrane. The terms in the equation are (see Figure 10):

$$p_i = P_m e^{-t/\theta},$$

$(\ddot{z}_c)_\tau = (A_c)_\tau$ = the acceleration membrane center at an earlier time τ ,

$$\tau = t - s_j/c_o,$$

r_j = radial coordinate of j^{th} element,

s_j = the distance from j^{th} element to the membrane center,

$$s_j = \left[\{ (z_c(k) - z(k))^2 + r_j^2 \}^{1/2},$$

$$z(k) = z_c(k) (1 - r_j^2/a^2),$$

$$\Delta l_j = (\Delta r^2 + \Delta z^2)^{1/2}, \text{ and}$$

$$\Delta l_j = \Delta r \left[1 + \frac{4z_c^2(k)}{a^4} r_j^2 \right]^{1/2}.$$

3.5 Formulation for the Gas Bubble Expansion

The equation (2-54) governing the expansion of the gas bubble (when there is cavitation) is written as follows:

$$\ddot{R}_k = \frac{R_o^4 \rho_o}{R_k^5 \rho_o} - \frac{P_h}{\rho_o R_k} - \frac{3\dot{R}_k^2}{2\rho_o R_k}. \quad (3-9)$$

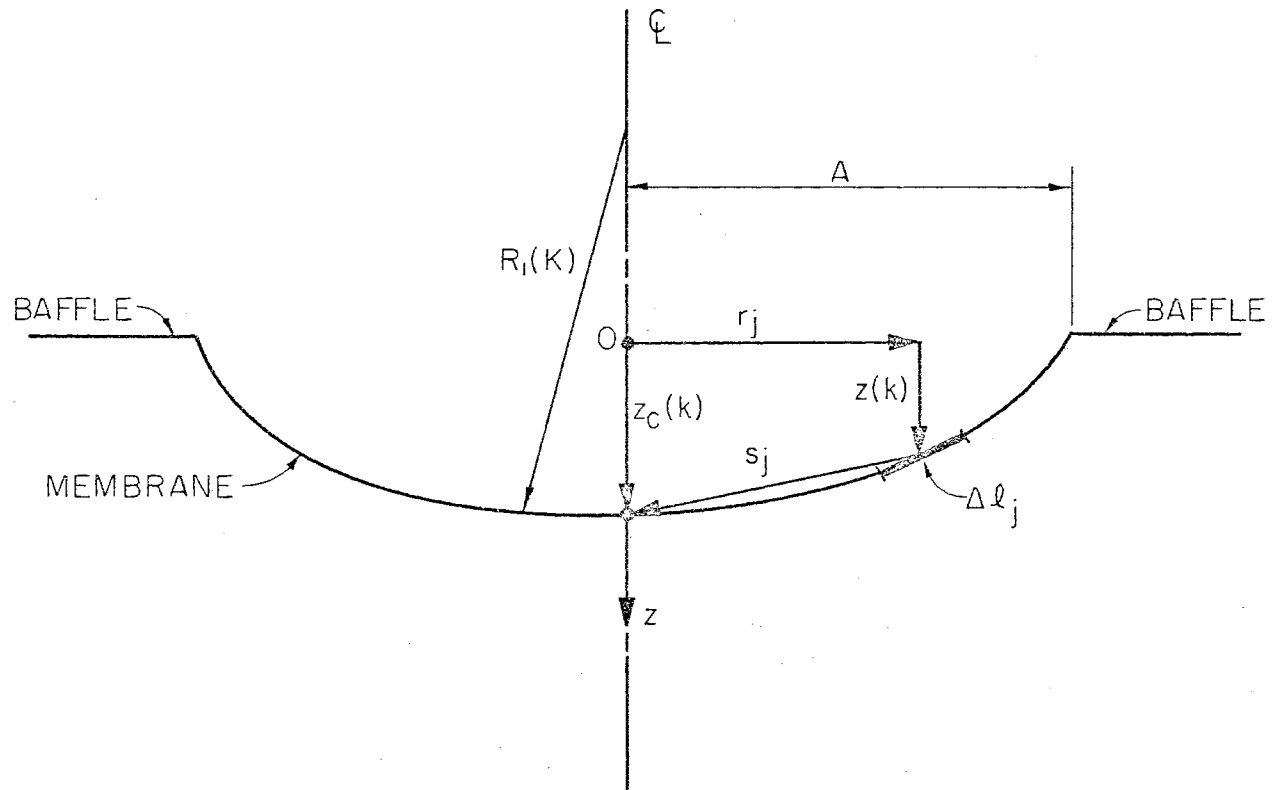


Figure 10. Deformed Membrane

The initial conditions for the bubble expansion are

$$R = R_0 \text{ at } t = 0 \text{ and}$$

$$\dot{R} = 0 \text{ at } t = 0 .$$

If the acceleration (\ddot{R}) is assumed constant during a small time interval, the velocity of the bubble surface is

$$\dot{R}_{k+1} = \dot{R}_k + \ddot{R}_k \cdot \delta t \quad (3-10)$$

and the bubble radius is

$$R_{k+1} = R_k + \dot{R}_k \cdot \delta t + \frac{\ddot{R}_k \cdot (\delta t)^2}{2} . \quad (3-11)$$

While the gas bubble is expanding, it is also moving toward the membrane. This motion has been given in equation (2-83) as

$$U_{k+1} = \left[\frac{1}{D_k^2} + \frac{1}{h_k^2} \right] \left[-\frac{3}{4} R^2 \dot{R} \Big|_k^{k+1} + \frac{3}{2} R_k \dot{R}_k^2 \delta t \right] + U_k , \quad (3-12)$$

where

$$U_{k+1} = \text{the bubble velocity at } t + \delta t \text{ and}$$

$$U_k = \text{the bubble velocity at } t .$$

The displacement is found by integrating the expression for U with respect to time. The terms on the right of equation (3-12) are considered constant during the time interval. The displacement of the gas bubble from its original position is

$$S_{k+1} = S_k + \left[\frac{1}{D_k^2} + \frac{1}{h_k^2} \right] \left[\left(-\frac{3}{4} \dot{R} R^2 \Big|_k^{k+1} \right) \delta t + \frac{3}{2} R_k \dot{R}_k^2 \frac{(\delta t)^2}{2} \right] + U_k \delta t . \quad (3-13)$$

Finally the stand-off distance (D) (see Figure 3) and the head (h) at any time (t) are

$$D(k+1) = D_0 - S(k+1) \quad \text{and}$$

$$h(k+1) = h_0 + S(k+1) ,$$

where

D_0 = the original distance of the charge from the membrane, and

h_0 = the original depth of the water over the charge.

3.6 Reloading Velocity

The preceding section and this section apply only when cavitation occurs. Due to the coupling effect, the pressure acting on the membrane drops rapidly from the initial value of the pressure in the incident shock wave. When the pressure drops to the vapor pressure of the medium, cavitation occurs. After cavitation occurs the pressure on the membrane is zero and the membrane begins to decelerate.

Reloading of the membrane occurs when the membrane comes to rest or when the water forced outward by the expanding gas bubble overtakes the membrane.

Since the mass of water rushing toward the membrane is large, the membrane is accelerated almost instantaneously to the velocity of the water. The reloading velocity is (equation 2-64)

$$v_0 = \frac{1.27Q}{aD} , \quad (3-14)$$

where

$$Q = \frac{R_0^3 u}{\beta} = \dot{R} R^2 .$$

From the integration of the reloading velocity v_o with respect to time, the displacement of the water at the cavitation front is

$$S_c(k) = \{v_o(k-1)\}\{\delta t\} + S_c(k-1) . \quad (3-15)$$

3.7 Numerical Solution of the Equation of Motion After Reloading

After reloading of the membrane takes place, the kinetic energy of the membrane and the mass of water following it is dissipated in plastic deformation of the membrane. The equation of motion is applicable as written in Section 3.3 and the velocity and displacement expressions are also given in Section 3.3.

The equation for the pressure (equation 3-8) is applied as follows:

$$p(k) = 2p_i(k) - \rho_o A_c(k) \sum_{j=1}^n \frac{(1-r_j^2/a^2)(r_j)(\Delta \ell_j)}{s_j} . \quad (3-16)$$

The acceleration term has been removed from within the summation because the acceleration is changing very slowly with time (2). This in effect is assuming that the acceleration of the center element of the shell at an earlier time τ is nearly the same as at the time t . With this assumption, the equation of motion becomes

$$\left[pH(k) + \rho_o \sum_{j=1}^n \frac{(1-r_j^2/a^2)(r_j)(\Delta \ell_j)}{s_j} \right] A_c(k) = 2p_i(k) - \frac{2\sigma_y H(k)}{R_1(k)} . \quad (3-17)$$

The incremental predictor process is applied until the membrane comes to rest.

3.8 Numerical Solution with Cavitation

The initial conditions are applied and starting values for the

membrane are calculated (see Section 3.2). Then the equation of motion is applied with the pressure as given by the diffraction theory until cavitation occurs (see Sections 3.3 and 3.4). The equations for velocity and displacement are found in Section 3.3. After cavitation and until reloading occurs the motion is described by the equations in Section 3.3 except that the pressure is zero. When the outward rushing water overtakes the membrane (the cavitation cavity is closed), reloading occurs. The reloading velocity is calculated and described in Section 3.6. Knowledge of the bubble expansion is necessary to calculate the reloading velocity. The bubble expansion is described in Section 3.5. After reloading, the membrane and mass of water has kinetic energy which is dissipated in plastic deformation. This phase of motion is given in Section 3.7.

3.9 Numerical Solution Without Cavitation

The primary difference in the deformation process without cavitation is the absence of the reloading phase. When cavitation does not occur, the pressure drops rapidly to some minimum positive value and increases to an almost constant value. During the last part of the deformation process when the pressure is almost constant, the acceleration of the membrane center is negative and nearly constant. When the membrane is brought to rest by the plastic forces in the shell, the pressure drops from a positive value to zero. This positive pressure results when the membrane decelerates the mass of water following it.

The sections of this paper used for calculations of the above described phenomena are given below. The initial conditions, boundary conditions and the velocity and displacement at the end of the first

time interval are found in Section 3.2. The acceleration at the beginning of each time interval is found by the method outlined in Section 3.3. Since the diffraction theory is applicable, the method of obtaining the actual pressure on the membrane center is given in Section 3.4. During the latter part of the membrane deformation process, the acceleration is changing very slowly. Therefore, the pressure acting on the membrane center is given by equation (3-16) and the acceleration of the membrane center is calculated using equation (3-17).

Instead of using the equations for the velocity and displacement given in Section 3.3, the following relationships are used. The equation for the displacement is found by passing a quadratic parabola through three points equidistant from each other (10). The parabola is

$$y = Ax^2 + Bx + C \quad (3-18)$$

Evaluating the dependent variable at three points, the center point taken as the origin, gives three equations to use in solving for the constants A, B, and C. In addition, the second derivative of y is equal to 2A. The solution for y at the forward point is found to be

$$y(k+1) = [y''(k)] h^2 + 2y(k) - y(k-1) \quad (3-19)$$

In terms of the variables of this problem, equation 3-19 becomes

$$z_c(k+1) = 2z_c(k) - z_c(k-1) + [A_c(k)] [(\delta t)^2] \quad (3-20)$$

The equation for the velocity is based on the Runge-Fox (10) method for linear equations. The velocity and displacement functions are expanded in Taylor's series. The higher order terms (third derivatives and higher) are neglected in the expansions and the resulting simultaneous equations are solved for the velocity at the forward point. By this method, the velocity is

$$v_c(k+1) = \frac{2}{\delta t} [z_c(k+1) - z_c(k)] - v_c(k) \quad (3-21)$$

Equations (3-20) and (3-21), along with the method of obtaining the acceleration outlined in the first part of the section, give the entire history of the deformation process. These equations (3-20 and 3-21) have a smoothing effect on the numerical process and help to control its numerical stability.

CHAPTER IV

NUMERICAL RESULTS

4.1 General

The numerical calculations were made on a Model 360 IBM computer. A block flow diagram is shown in Appendix C. The initial conditions, boundary conditions, and governing equations are all incorporated in the program. This program provides a simple method of studying the several parameters influencing the damage to the membrane caused by an adjacent underwater explosion. The program which is based on the preceding theory is introduced to the computer by means of IBM cards. The varying parameters are fed into the computer from the data cards as needed.

An extensive study of the parameters influencing the damage to a membrane subjected to a transient pressure from an underwater explosion is presented in this chapter. The parametric areas investigated are:

- a) the influence of the ambient pressure on the damage,
 - b) the influence of the hydrostatic head on the damage,
 - c) the influence of the stand-off distance on the damage,
 - d) the influence of charge weight on the damage,
 - e) the influence of the center velocity on the center deflection,
- and
- f) the actual pressure on the membrane.

In all cases, a circular membrane is the configuration used.

4.2 Influence of the Ambient Pressure on the Damage

After the shock wave from the explosion is transmitted to the surrounding medium, the gas bubble begins to expand. The rate at which it expands influences the reloading velocity of the water after cavitation. The reloading velocity of the water is directly related to the damage of the membrane.

If the ambient pressure (the pressure at the same depth as the charge in undisturbed surroundings) is neglected, the bubble expands faster; therefore, greater damage to the membrane results from the explosion. If the ambient pressure is neglected, the maximum increase in deformation is 1.7 percent (see Figure 11) for a one foot stand-off distance and a steel membrane. The maximum increase in deformation is only 0.9 percent (see Figure 12) for a stand-off distance of 0.5 feet and a steel membrane.

4.3 Influence of the Hydrostatic Head on the Center Deformation

Figures 13, 14, 15, 16, and 17 show the influence of the hydrostatic head on the center deformation of the membrane. Except at certain heads where Johnson found the damage to be maximized, the results of this study and the calculations using Schauer's (11) equation (2-67) show the same trends as the experimental findings of Johnson (5). The author of this dissertation incorporates into this study and into Schauer's equation (2-67) the theory for the influence of the hydrostatic head on the damage as developed by Schauer (13). The author's study shows that at greater hydrostatic heads their influence can be neglected. The experimental work of Johnson (5) and Fye and Eldridge (19) show the same effects at greater hydrostatic heads as found in this

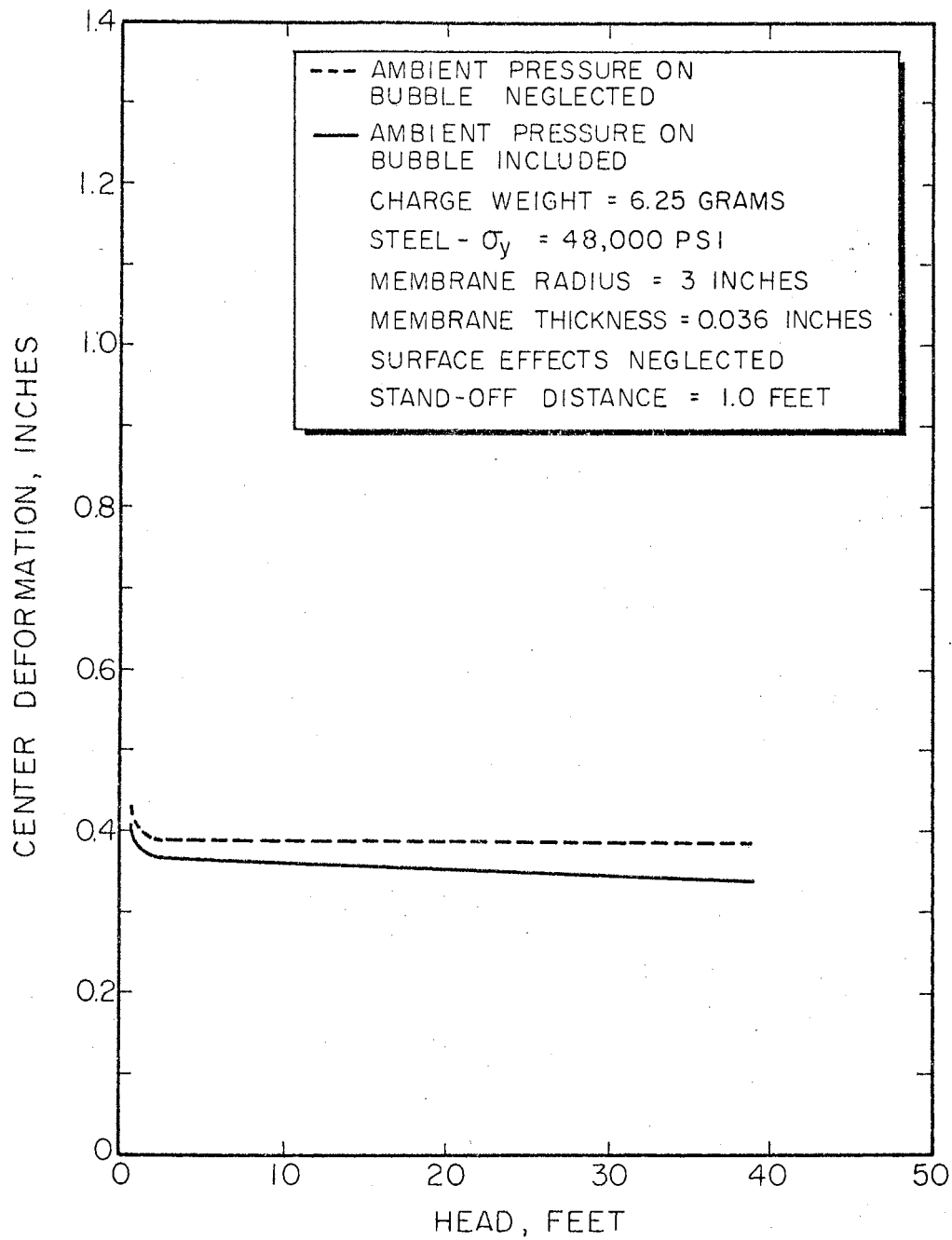


Figure 11. Influence of the Ambient Pressure on the Damage at a Stand-off Distance of One Foot

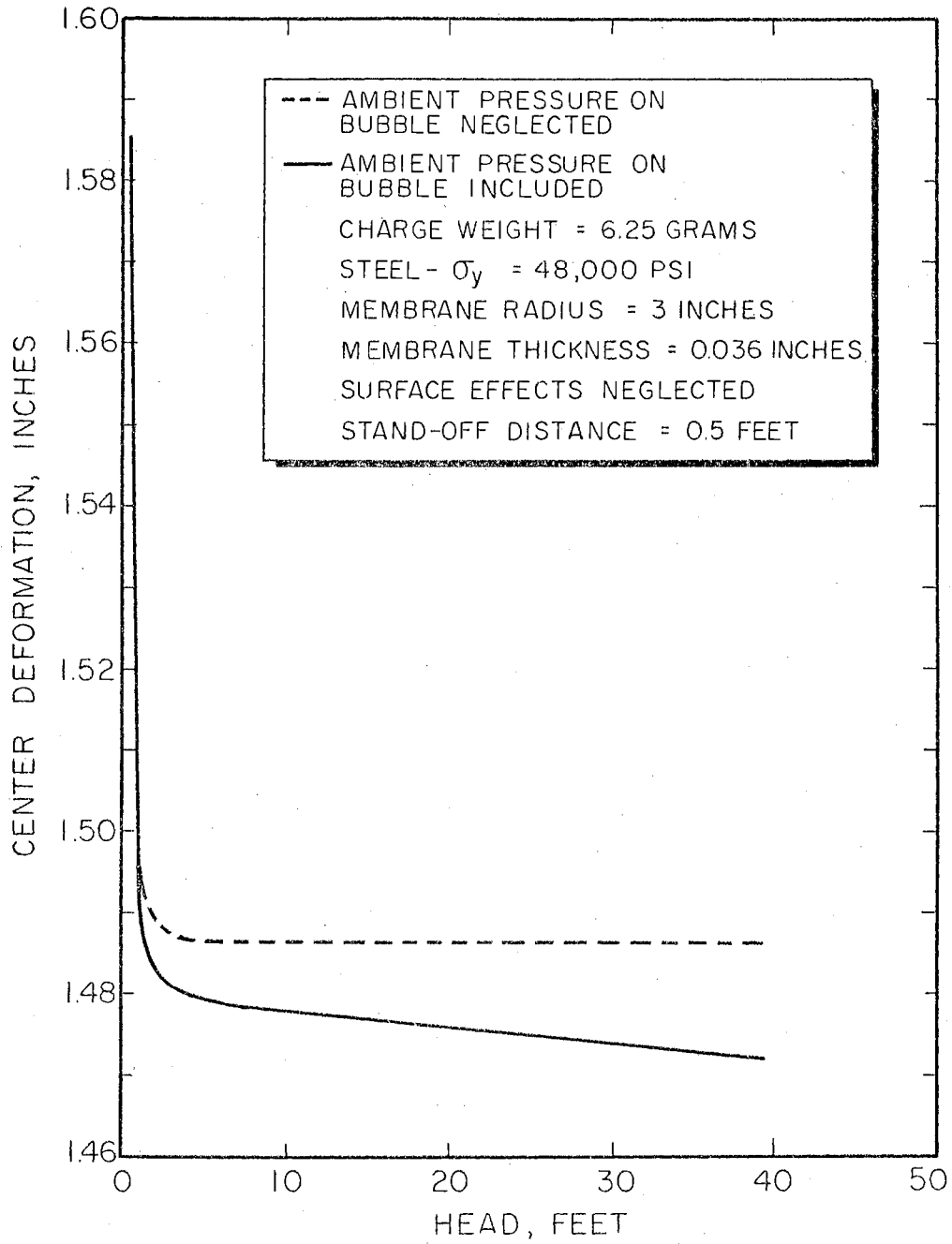


Figure 12. Influence of the Ambient Pressure on the Damage at a Stand-off Distance of One-half Foot.

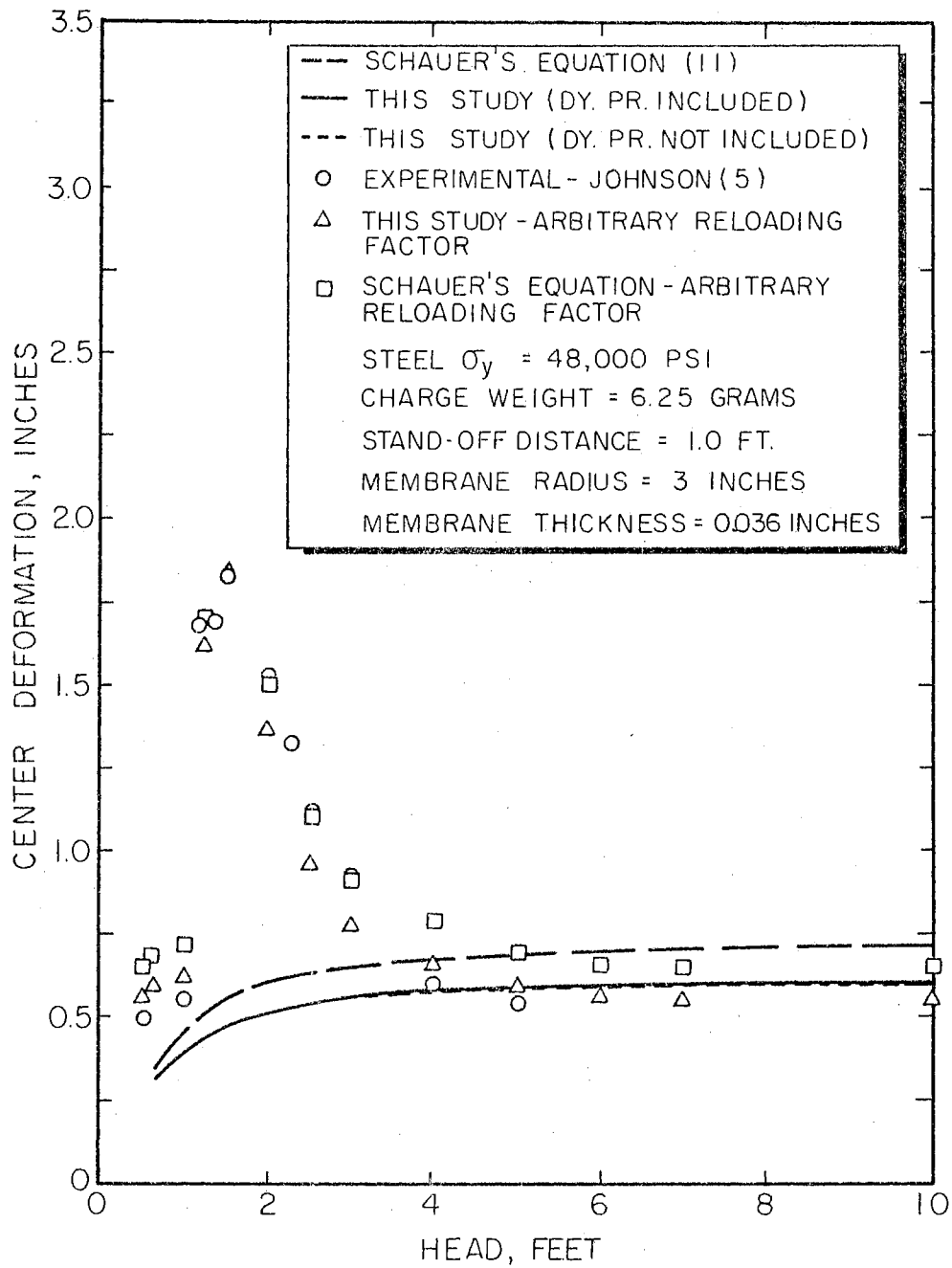


Figure 13. Influence of the Head on the Center Deformation for a Steel Membrane and One Foot Stand-off Distance

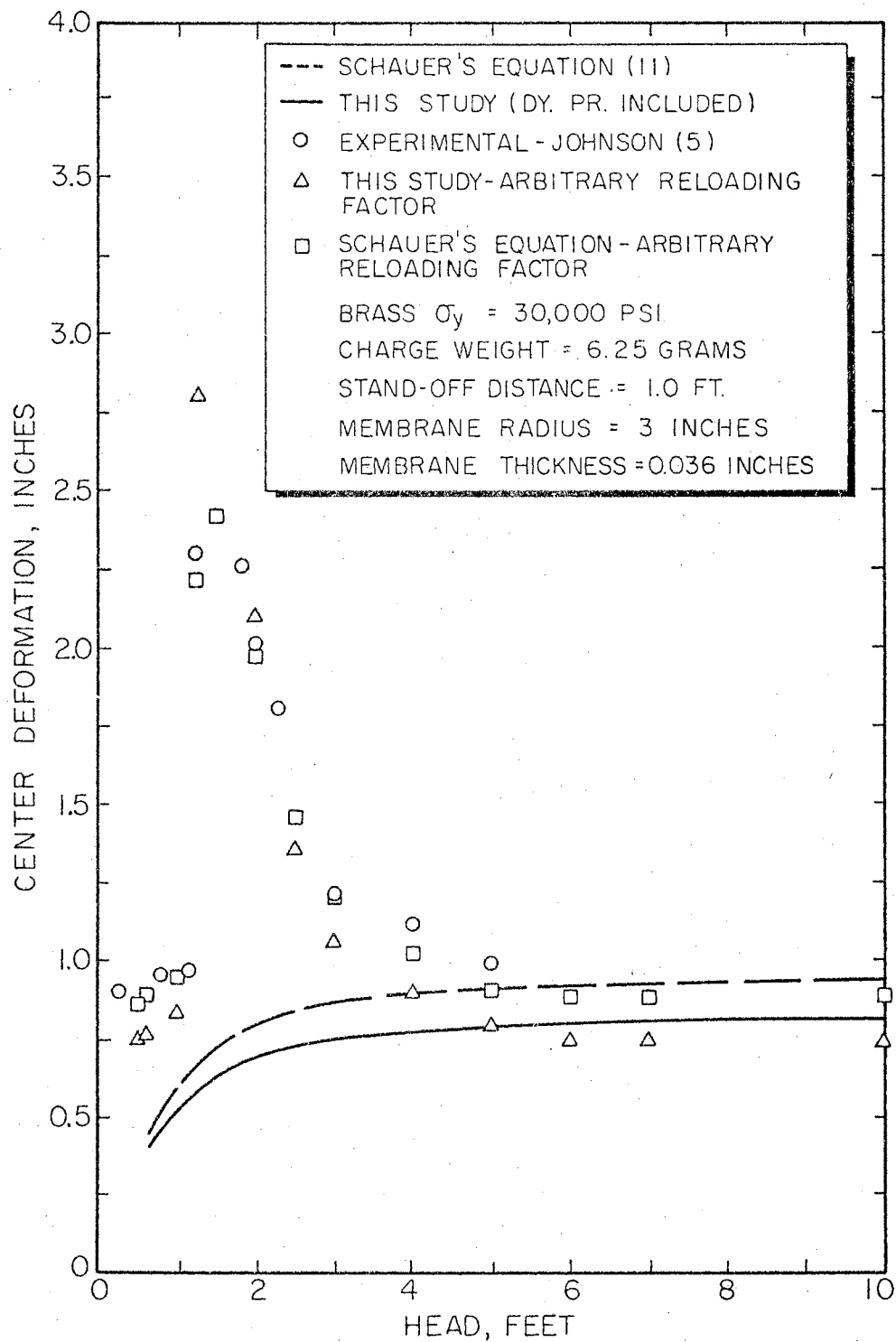


Figure 14. Influence of the Head on the Center Deformation for a Brass Membrane and One Foot Stand-off Distance

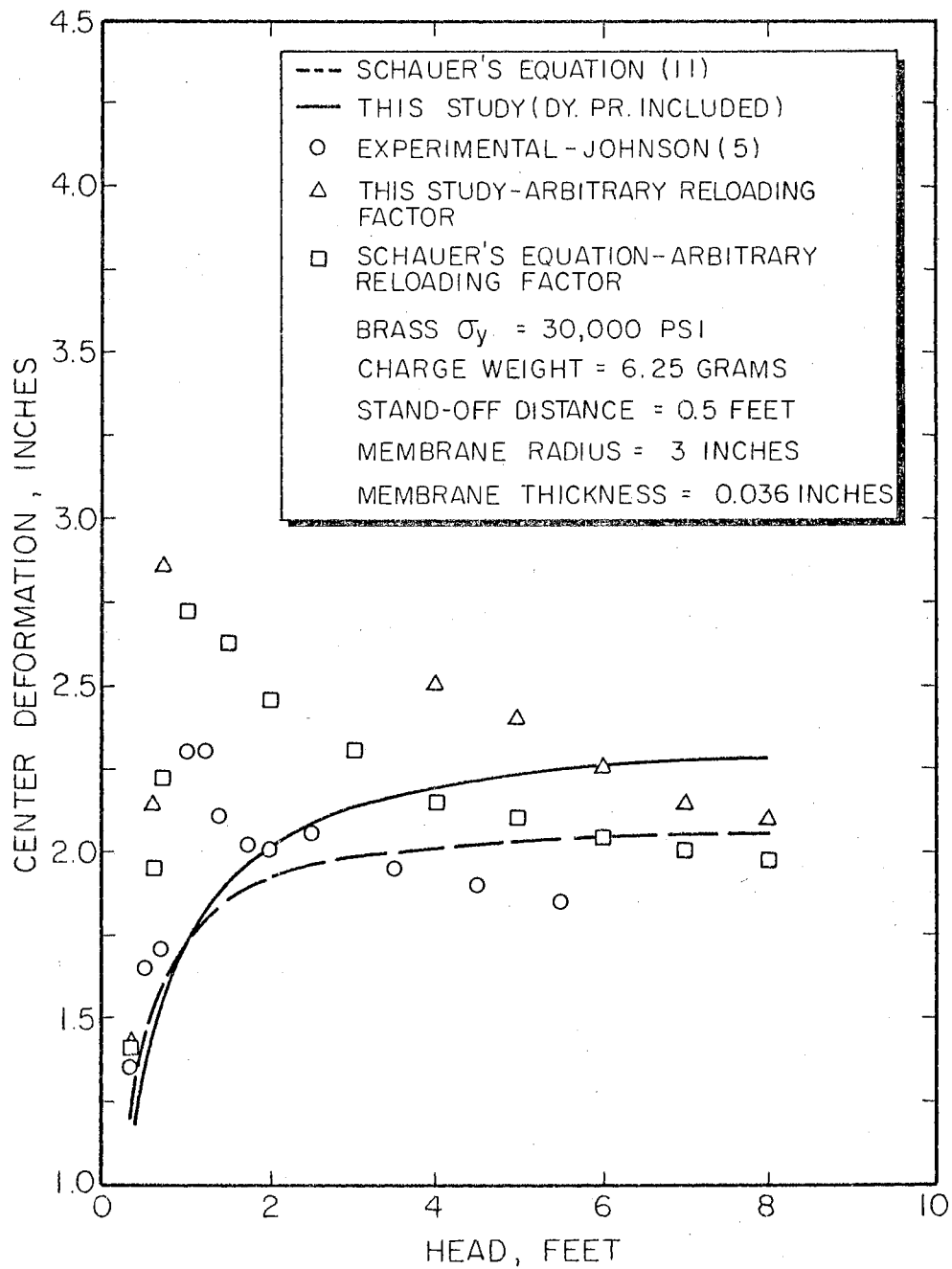


Figure 16. Influence of the Head on the Center Deformation for a Brass Membrane and One-half Foot Stand-off Distance

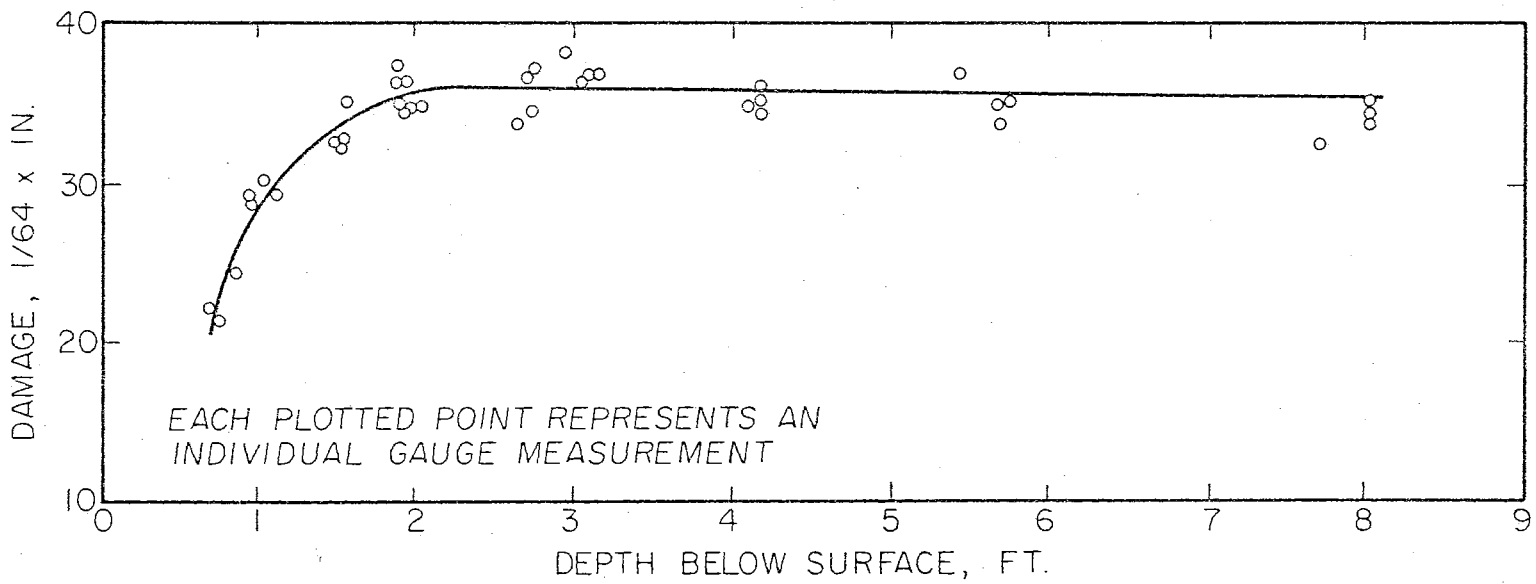


Figure 17. Effect of Depth on Damage (19)

study. For a summary of the above experimental work see Figures 13 through 17.

The experimental work of Johnson (5) shows that the damage is maximized at certain hydrostatic heads. At these heads, with the same charge weight, the damage to a steel membrane at a one foot stand-off distance is greater than the damage to another steel membrane at a six inch stand-off distance.

When the author of this dissertation first encountered this maximizing of deformation, it was thought that this phenomena was due to a second shock wave emitted by the gas bubble at the end of its first period. This, however, proved to be wrong. The time to the end of the first period of the gas bubble far exceeds the total time required for the entire deformation process to take place.

Next, the migration of the gas bubble was investigated and incorporated into this study. It was found that this migration of the gas bubble did not cause the maximizing effect. However, the migration of the bubble was found to contribute up to an eight percent increase in deformation for small hydrostatic heads and stand-off distances when compared to large values of this parameter (see Figure 12). To date a theory which adequately accounts for this maximizing of deformation has not been found. This maximizing effect is taken into account by introducing an arbitrary factor for the reloading velocity. These factors were found by computing the ratio of the plastic work done on a membrane with the maximizing effect to the plastic work done on membranes without the maximizing effect. The values for the plastic work done on the membranes are found in Johnson's (5) paper and are determined from experimental findings.

The arbitrary factors gave reasonable results, as shown in Figures 13 and 14, and indicate quantitatively the trends as shown in Figure 16. The use of the arbitrary factors when applied to the situation shown in Figure 15 does not seem to apply, perhaps because of the difference in the material properties of the membrane.

Fye and Eldridge (19) experimentally studied the influence of the parameter of depth to the charge on the damage to metal diaphragms. Figure 17, which is reproduced from page 547 of their paper, shows the same trends as are analytically found in this study. They did not find this maximizing of the damage, therefore, this phenomena found by Johnson (5) must occur for only certain conditions.

One additional observation can be made when the results from this study and the results from Schauer's equation (2-67) are compared. Since this study is based primarily on the theory presented by Schauer (11), it would seem that the results of the author's study and the results of applying Schauer's equation should be the same or at least the same relatively. However, upon examining Figures 13, 14, 15, and 16, this is not found to be true. There exists a different cross-over deformation value for each of the situations shown in Figures 13 through 16. At this cross-over value, this study and Schauer's equation give the same results. When the deformation damage is below the cross-over value for a particular membrane stand-off distance combination, this study gives deformation values smaller than the results from Schauer's equation. The damage calculated from Schauer's equation is smaller than the results of this study when the deformation values are larger than the cross-over value.

If the assumptions made in this study and the assumptions made by

Schauer (11) are examined, an explanation can be offered for the observation discussed above. After reloading of the membrane occurs, Schauer assumes a fixed mass of water following the membrane. The diffraction theory, which assumes an ideal fluid, is applied in this study to give the effect of the water following the membrane. For the smaller deformations, the effective mass assumed by Schauer is too large. Also, Schauer neglected certain terms in deriving his equation. These differences in assumptions could account for the larger calculated deformation from Schauer's equation. Viscous effects, which are neglected in the diffraction theory, become important for larger deformations. These viscous effects would tend to decelerate the water following the membrane, thus aiding in bringing the mass of water to rest sooner. Neglecting these viscous effects could account for this study giving larger deformations than Schauer's equation when the deformations are larger.

Neglecting the dynamic pressure of the water on the membrane during the latter part of the cavitation phase gives calculated values for the deformation only slightly smaller than when the dynamic pressure is included. This can be seen in Figures 13 and 15.

4.4 Influence of Stand-off Distance on the Center Deformation

Figures 18, 19, 20, and 21 show the results of this parametric study along with the experimental findings of Johnson (5). The analytical results of this study and the experimental findings of Johnson show the same trends and compare well as shown in Figures 18 and 19. Some scattering of experimental findings by Johnson is noted; however, this is due to the maximizing of the damage discussed earlier. Other

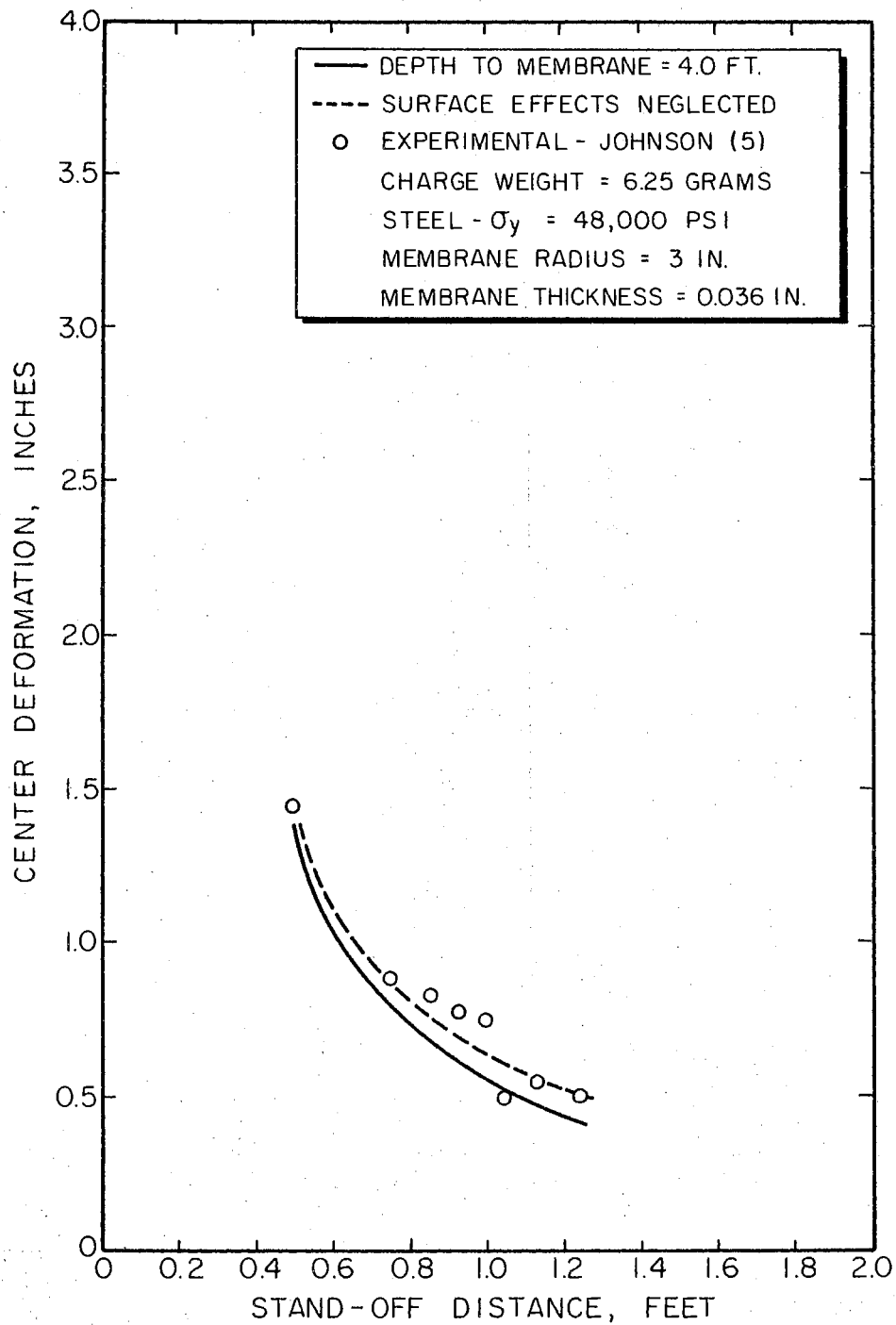


Figure 18. Influence of Stand-off Distance on Center Deformation for a Charge Weight of 6.25 Grams

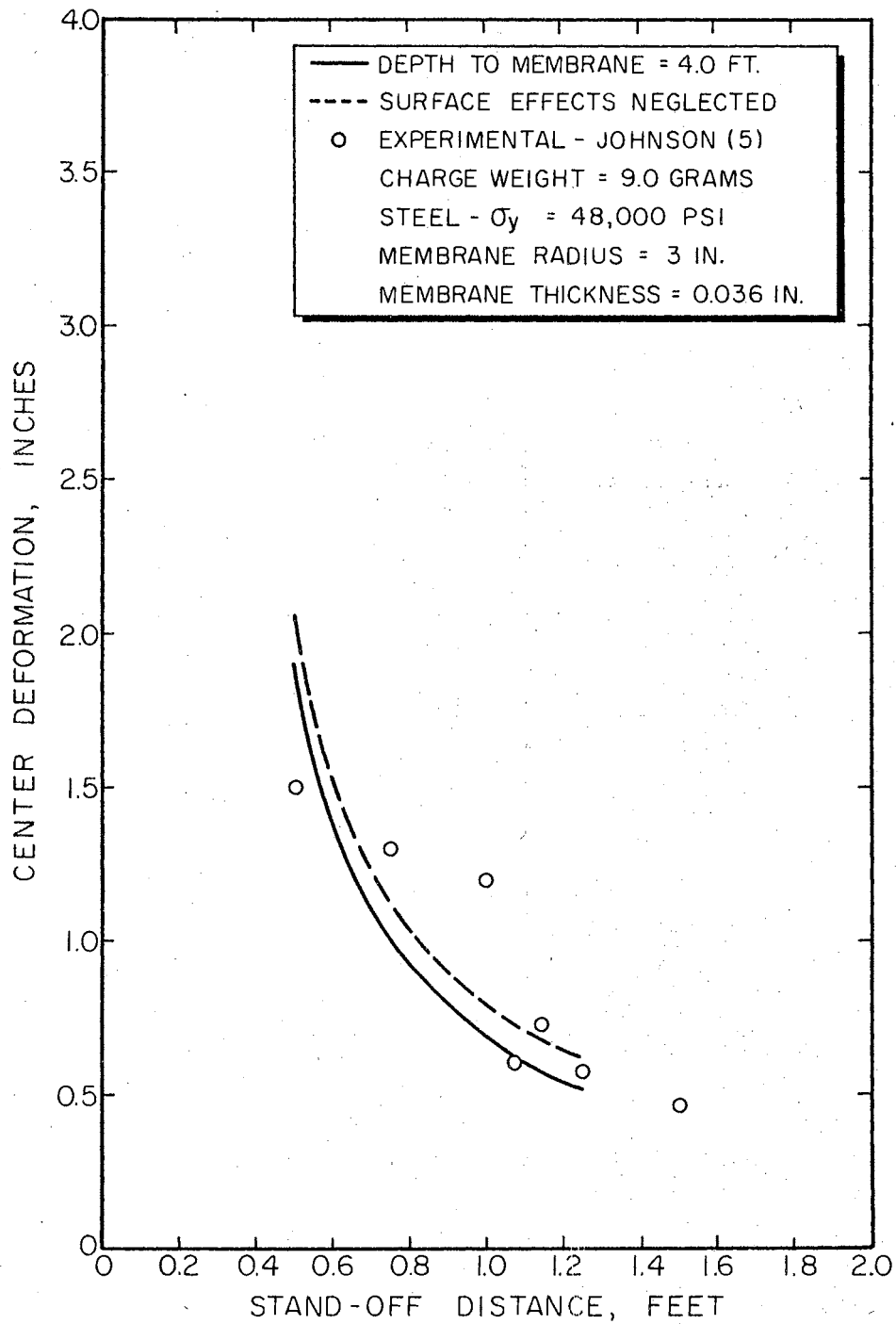


Figure 19. Influence of Stand-off Distance on Center Deformation for a Charge Weight of 9.0 Grams

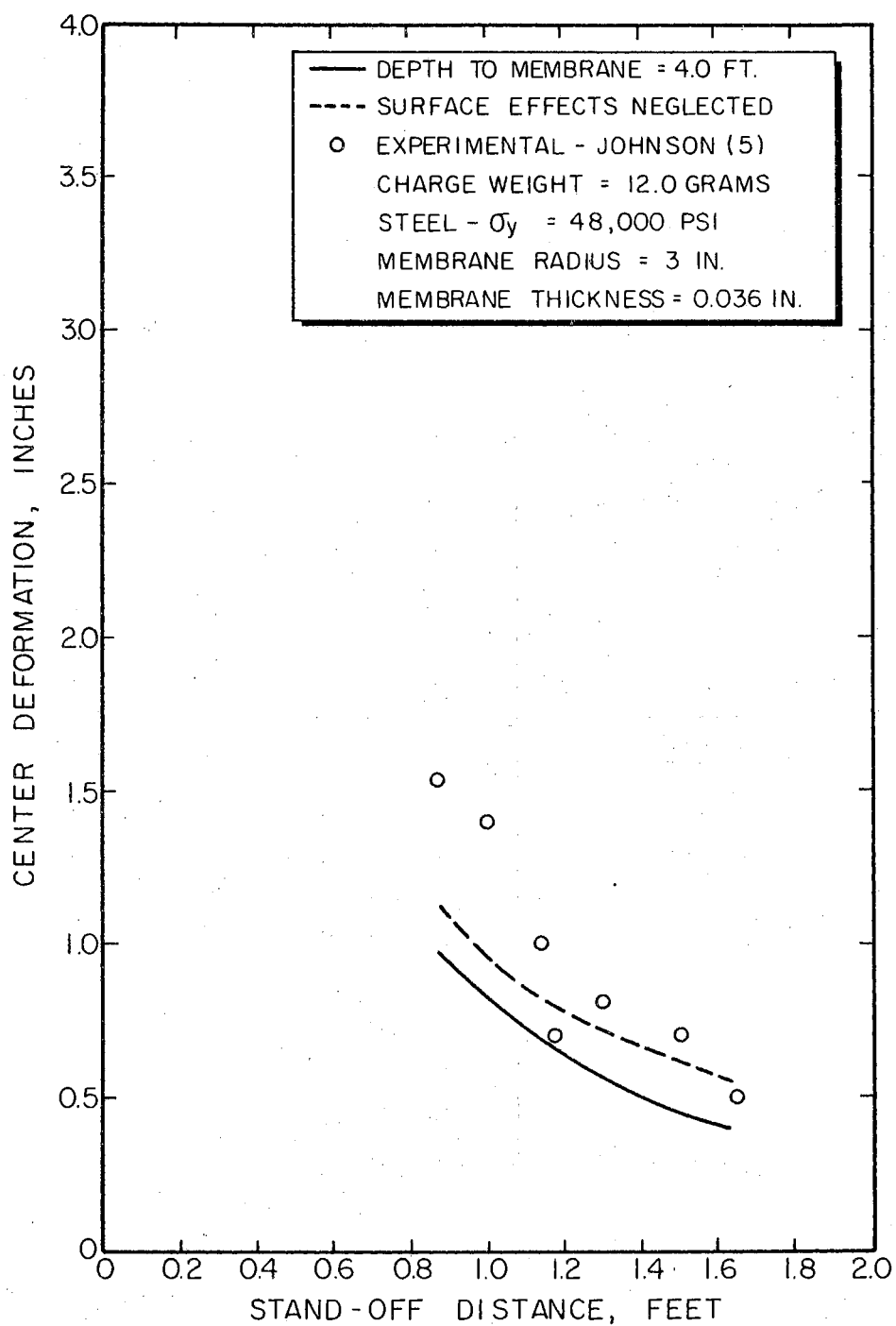


Figure 20. Influence of Stand-off Distance on Center Deformation for a Charge Weight of 12.0 Grams.

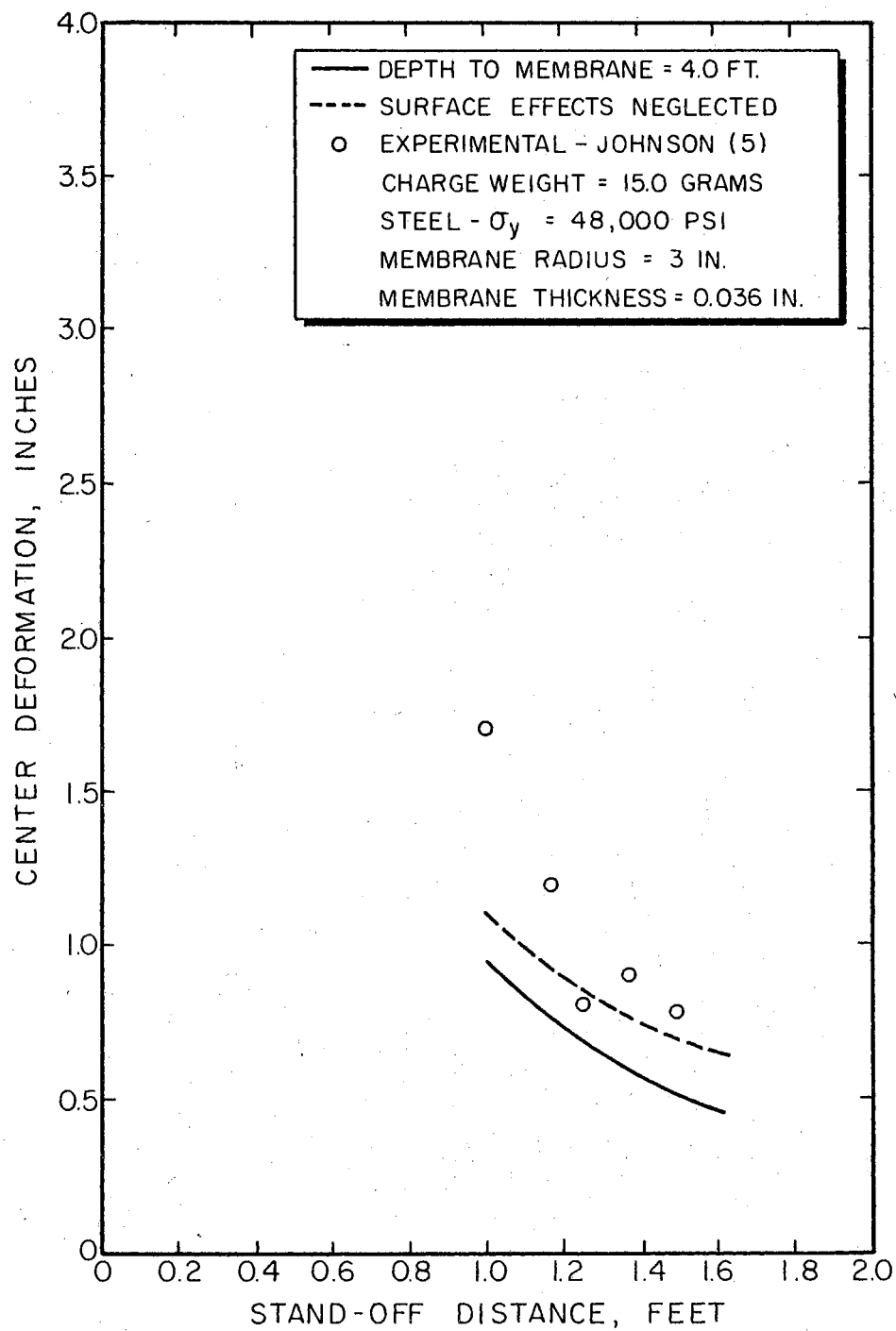


Figure 21. Influence of Stand-off Distance on Center Deformation for a Charge Weight of 15.0 Grams

experimenters, such as Hudson and Johnson (19), have found the same general trends as this study.

4.5 Influence of Charge Weight on Center Deformation

For greater charge weights, greater deformation is expected and this is found to be true in Figures 22 and 23. Figure 22 shows that the results of this study do not agree very well with Johnson's (5) experimental studies, however, the general trends are the same. This may be partially due to inadequate information on the properties of the explosive and of the metal membranes.

Figure 23 shows that the results of this study and the experimental data of Fye and Eldridge (19) agree quite well. Cavitation did not occur for the results presented in Figure 23. When the deformations calculated in this study exceed 0.9 inches, they diverge from Kirkwood's (17) theoretical curve (see Figure 23). The observation made about greater deformations in Section 4.3 also seems to apply here; that is, the neglecting of viscous effects, as assumed in the diffraction theory, may lead to excessive calculated deformations as in this study. Since experimental data is not available in this range, a definite conclusion cannot be reached.

4.6 Influence of the Center Velocity on the Center Deformation

The results of this study with cavitation occurring are shown in Figure 24 and 25. First, examination of the curves shows that the initial part of the motion up to the time when reloading takes place is independent of the hydrostatic head. Second, cavitation occurs very early in the motion of the membrane. Cavitation occurred at a time

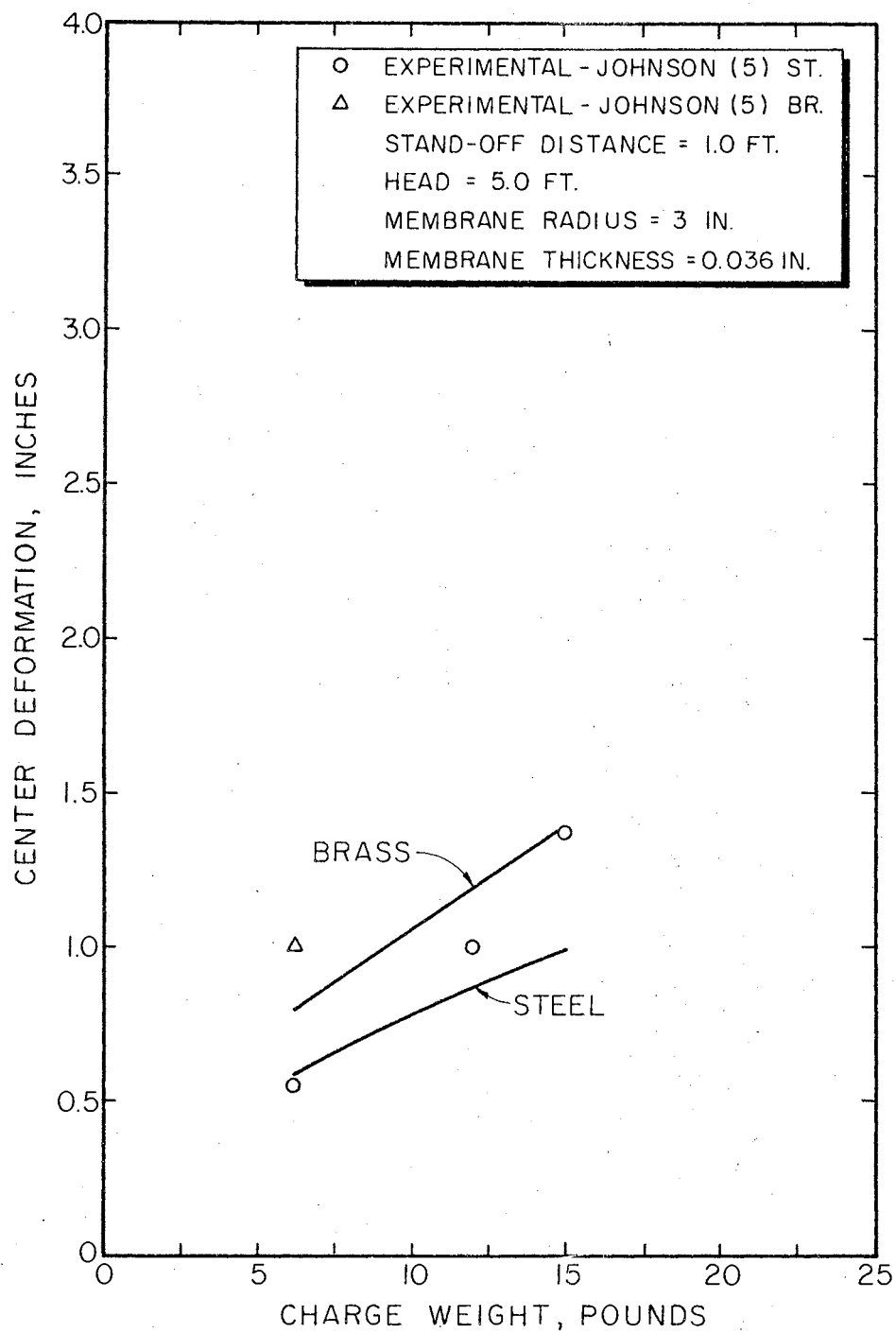


Figure 22. Influence of Charge Weight on Center Deformation With Cavitation

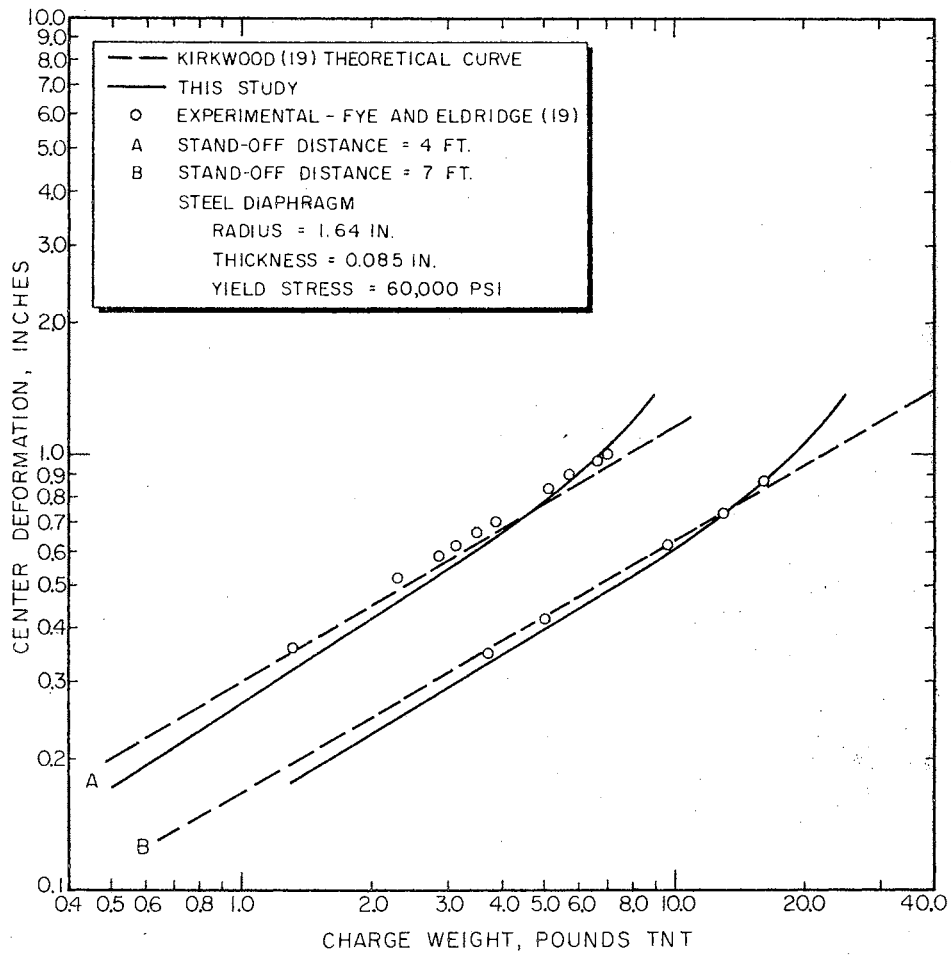


Figure 23. Influence of Charge Weight on Center Deformation Without Cavitation

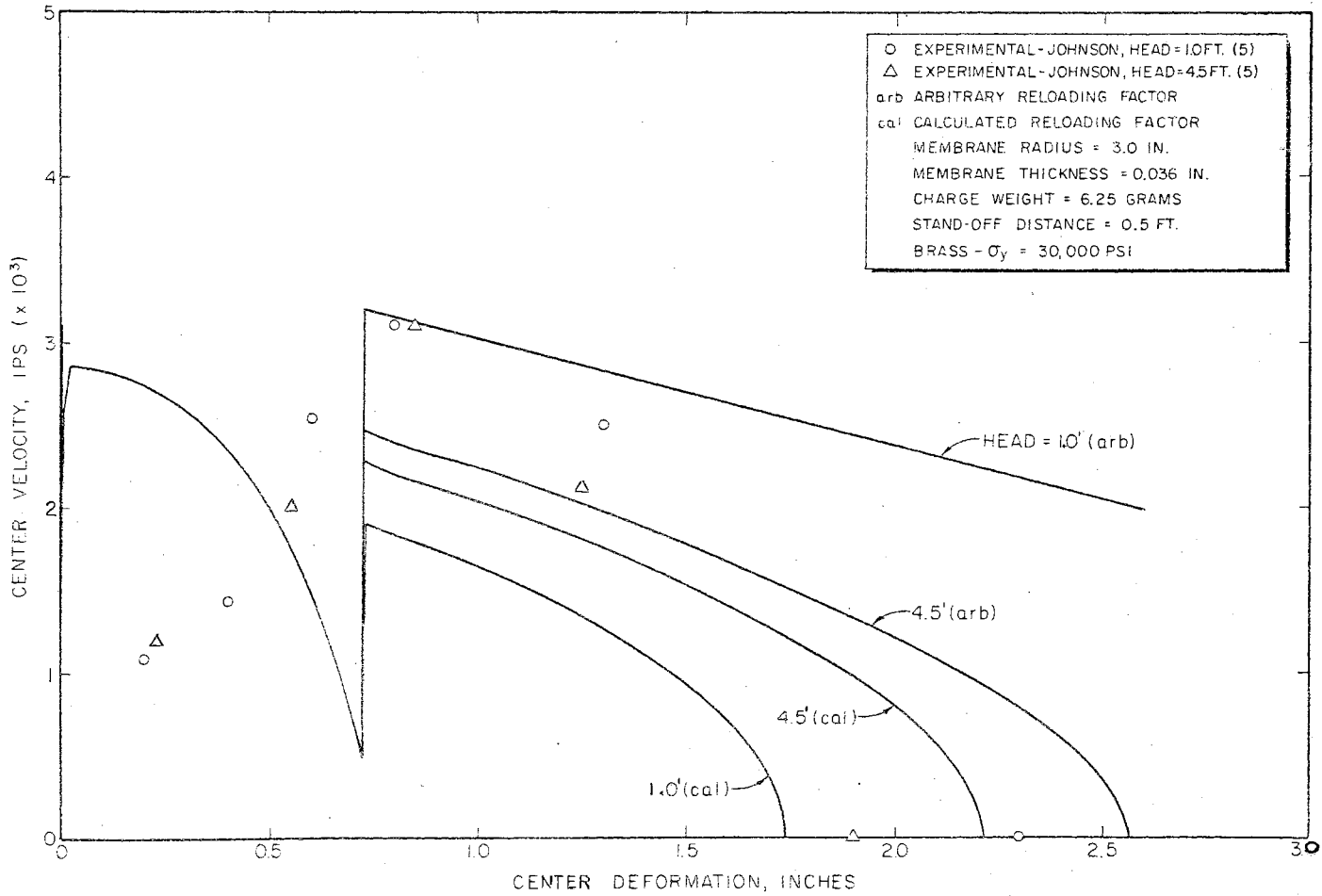


Figure 24. Center Velocity-Center Deformation History for a One-half Foot Stand-off Distance

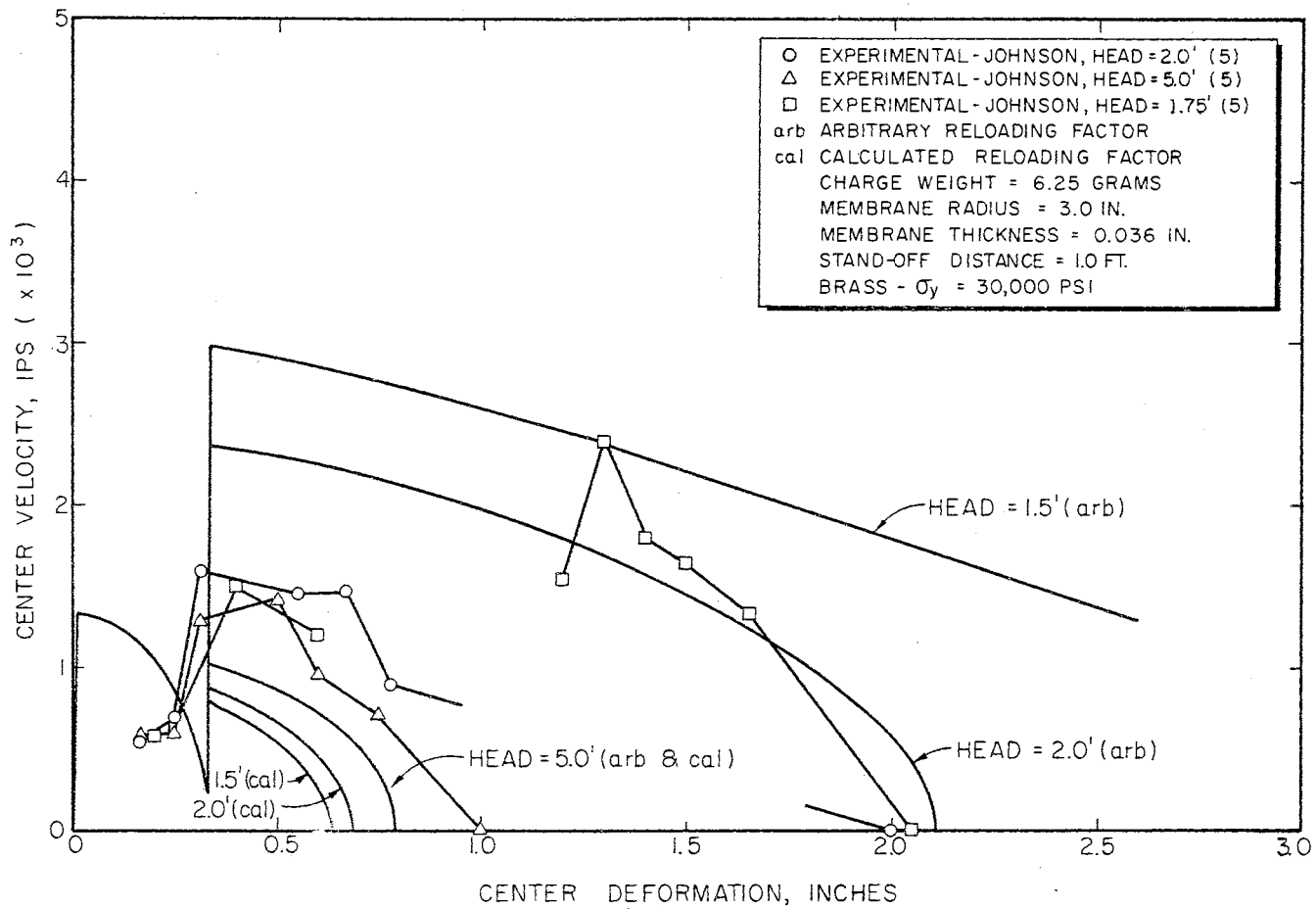


Figure 25. Center Velocity-Center Deformation History for a One Foot Stand-off Distance

when the velocity of the membrane reached its first maximum. The experimental data shows the first portion of the motion to be the same for all hydrostatic heads, however, the experimental data does not compare well with this study. The reason for this may be in the method of obtaining the experimental data. The experimental data were obtained as follows: pins were set at intervals below the membrane, and the time for the membrane to travel from one pin to the next was measured. Then the average velocity was calculated and plotted at the mean pin depth. This experimental setup would be insensitive to the initial high accelerations and to the sudden changes as in reloading.

After reloading, the velocity deformation curves are different for each hydrostatic head. The results of this study and the experimental data are difficult to compare; however, several observations can be made. The assumption of no friction in the fluid is again apparent when it is observed that the membrane does not come to rest quickly enough for cases with a high reloading velocity. Also, from examination of the experimental data, the hydrostatic pressure must have some influence on the mass of water following the membrane.

Figures 26 and 27 show results for which cavitation did not occur. The results for this situation fit a definite pattern, that is, for greater charge weights a higher maximum velocity at a greater deformation is found, and in turn the final deflection is greater.

4.7 Actual Pressure on the Membrane Center

Figure 28 shows the actual pressure acting on a membrane for explosive loading when cavitation occurs. First, the pressure drops very quickly from twice the peak shock wave pressure zero. It drops in fact

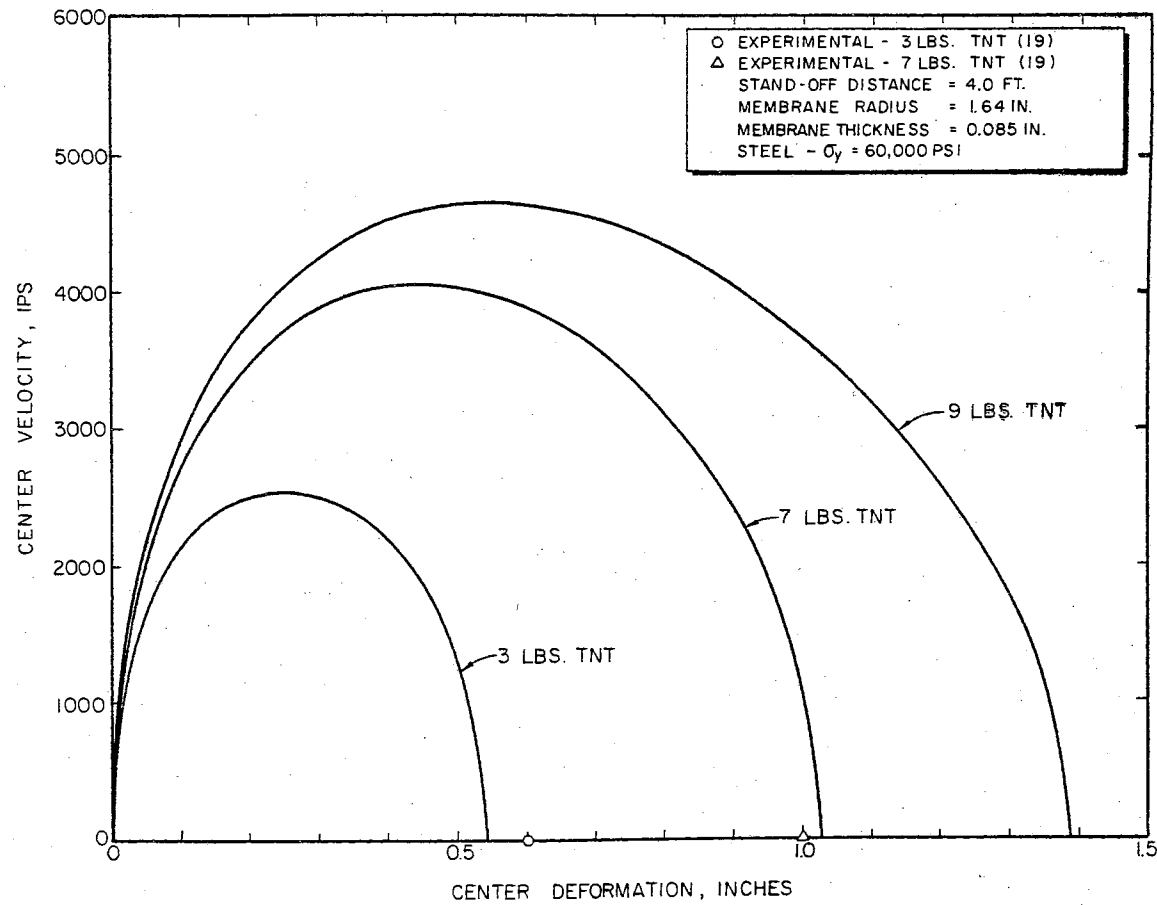


Figure 26. Center Velocity-Center Deformation History for a Four Foot Stand-off Distance

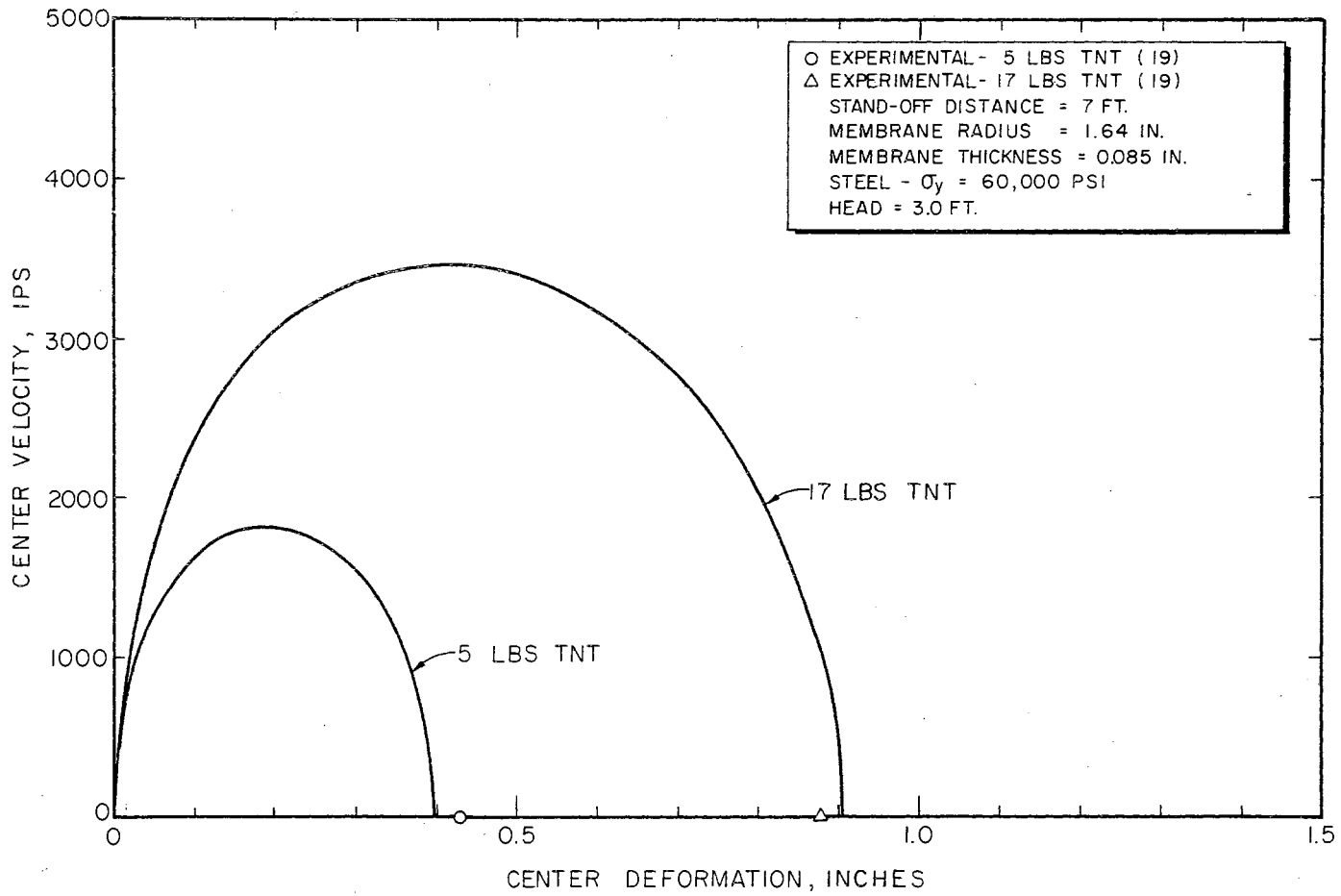


Figure 27. Center Velocity-Center Deformation History for a Seven Foot Stand-off Distance

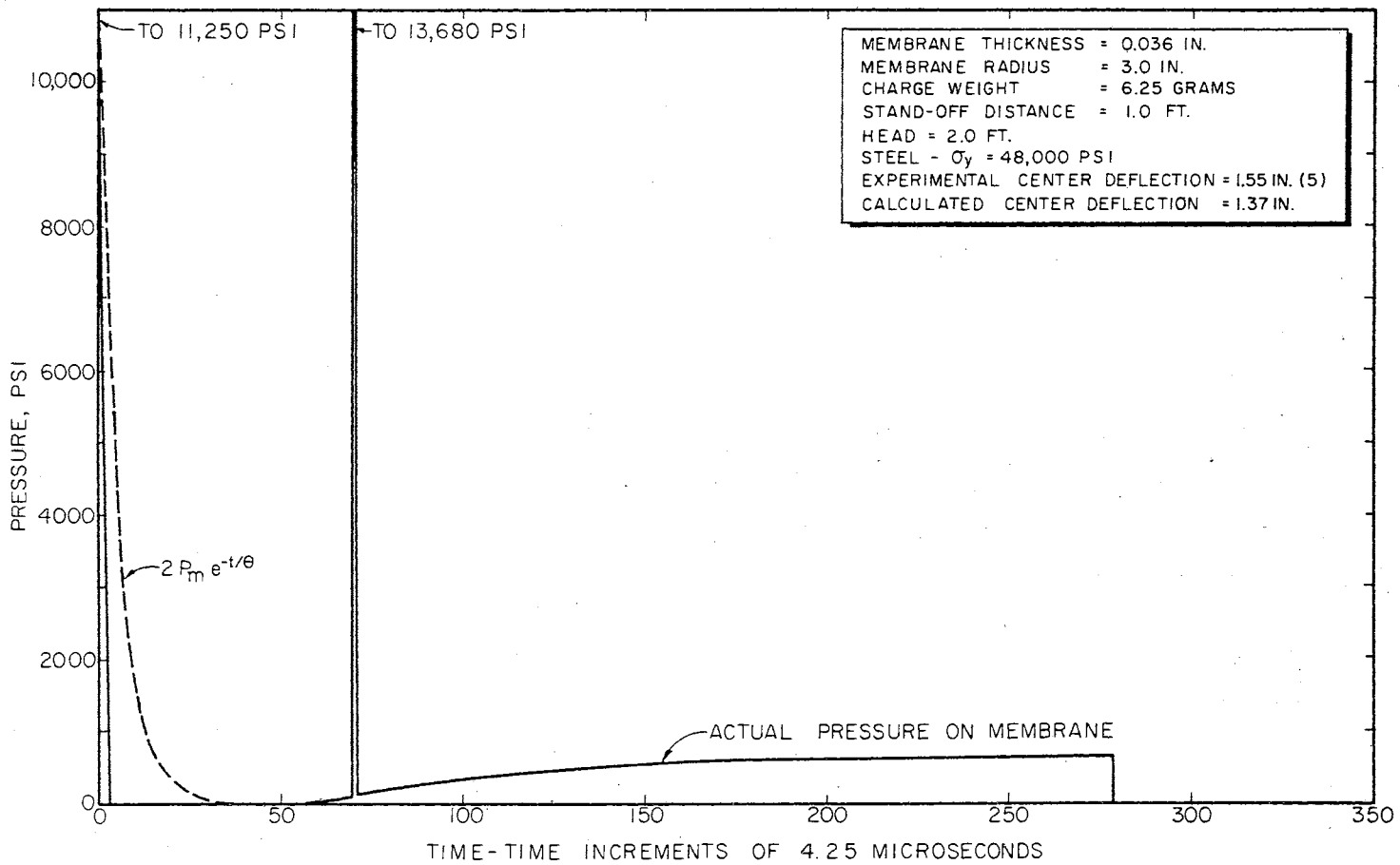


Figure 28. Pressure-Time History for a Charge Weight of 6.25 Grams Plaster Gelatine

much faster than the exponentially decaying pressure of the shock wave. The time when cavitation occurs was found for the case shown in Figure 28 to be 10.4 microseconds. Cole (1) on page 407 gives an equation for predicting the time to cavitation. Using this equation, the time was calculated to be 9.2 microseconds. One of the assumptions made by Cole in deriving his equation is that the plate moves freely and since the author of this study did not make this assumption, the comparison is good. Also, for the assumptions made in this paper, the time to cavitation from the author's study should be larger.

The pressure remains at zero for a period of time and slowly builds up until reloading takes place. This build up of pressure is due to the dynamic pressure of the water which is beginning to overtake the membrane just before reloading. When the large mass of water, which overtakes the membrane, accelerates the target to the water velocity instantaneously, a large pressure spike results.

After reloading, the pressure acting on the membrane results from the mass of water behind the membrane being decelerated. Schauer (11) has experimentally found a pressure-time curve which is similar to the curves shown in Figure 28.

In Figure 29, the pressure did not drop to zero, therefore, cavitation did not occur for the explosive loading shown. The actual pressure drops rapidly from the peak shock wave pressure to a minimum. The pressure then increases to another maximum and finally becomes almost constant. The final portion of the pressure curve is due to the mass of water following the membrane being decelerated.

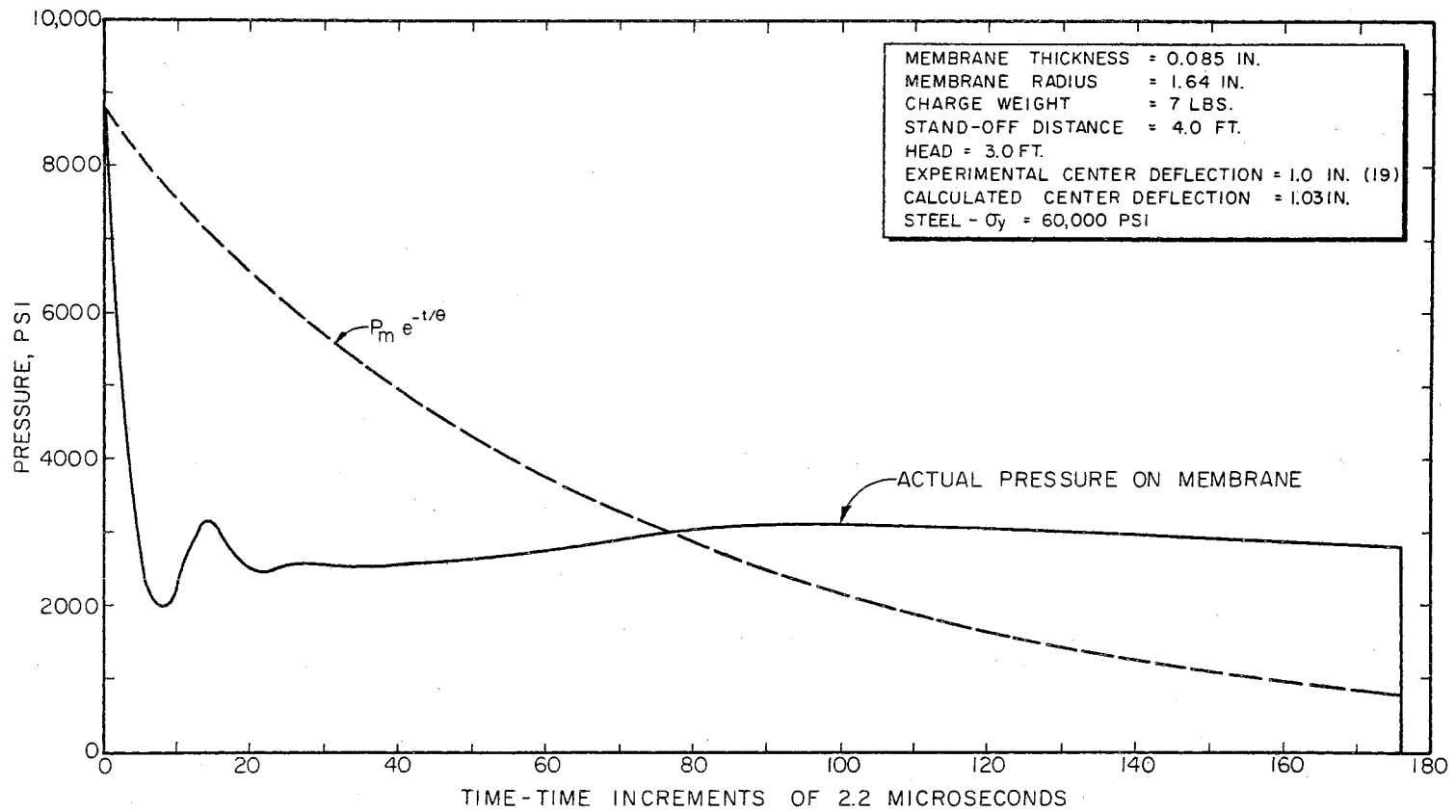


Figure 29. Pressure-Time History for a Charge Weight of 7.0 Pounds TNT

4.8 Summary of Results

The technique developed for finding the deformation of a membrane subjected to a nearby underwater explosion by the author in this dissertation is simple, yet a great many parametric studies are made. The author could not find a comparable method that would enable all of the parametric studies to be made and at the same time give information on the pressure, velocity, displacement, and other quantities at all times during the entire deformation process.

The results do not always compare favorably with the experimental work of Johnson (5). The most significant difference is the maximizing of the deformation at certain heads found by Johnson. Since investigators other than Johnson have not discovered this maximizing effect, this effect must occur only when a certain combination of conditions are met.

Another reason for some of the differences may be in the values of material properties used. The only information of the explosive given by Johnson (5) in his paper was the calorific value which was about 1.4 times that of TNT. To compare results, therefore, the author used the equations for TNT and multiplied the explosive power of TNT by 1.4. The yield strength of the metal membranes is obtained in the following manner. A power-law relation for the materials used was given by Johnson (4) in another paper. A yield stress for a perfectly plastic material was determined so that the areas under the stress-strain curves for the perfectly plastic condition and power-law representation are the same. It should be pointed out that under dynamic loading, the yield stress strength of a material changes with the intensity of the

dynamic loading, and in this study the yield strength was assumed constant. Since it is unlikely that the correct values for material properties were used in this study, the differences between this study and experimental findings are partially explained.

From the many parametric studies made, a number of observations have been made. Without the method for analyzing an underwater explosion developed in this study, these parametric studies would not have been possible. Of equal importance, the author was able to study the entire deformation process and gain much valuable insight into the phenomena. As a result several recommendations are made for future studies.

CHAPTER V

CONCLUSIONS AND RECOMMENDATIONS

5.1 General

The results obtained from this study show some interesting variations from earlier data, and lead to a number of significant conclusions and recommendations.

5.2 Conclusions From This Study

1. The numerical process, with the simplifying assumptions incorporated, provides a good tool for future quantitative and qualitative parametric studies. Any improvement to the mathematical model of any portion of the deformation process would, of course, yield improved results.

2. The "afterflow" theory of reloading by Schauer (11) adequately describes the phenomena when cavitation occurs; it gave good descriptive results when applied in this study.

3. The diffraction theory as applied in this study gives good results when cavitation does not occur. Further, before cavitation and after reloading, the diffraction theory can be applied successfully for smaller deformations.

4. The pressure-time information given by the study adequately describes the actual pressure felt by the membrane.

5. The velocity-displacement studies qualitatively describe the deformation process.

6. The parametric studies by the author involving stand-off distance and charge weight show the same trends that other investigators have found. Hence, this study demonstrates the influence of these parameters on the deformation process.

5.3 Recommendations for Future Studies

1. A better mathematical model of the membrane and an improved numerical process should be incorporated into the computer program. An improved model will permit the exact shape of the membrane to be found.

2. A method should be developed to predict the pressure at all points on the membrane so that the parabolic shape need not be assumed.

3. The method used to predict the time when reloading occurs and the intensity of the reloading should be improved.

4. Studies should be made on the membrane deformation of the influence of the water trailing the membrane.

5. Studies should be made on the influence of the free water surface on the damage to the membrane.

6. The mathematical stability of the numerical process should be investigated.

A SELECTED BIBLIOGRAPHY

- (1) Boyd, D. E., "Dynamic Deformation of Circular Membranes," ASCE, EMD, Vol. 92, June 1966.
- (2) Cole, R. H., Underwater Explosions. Princeton University Press, Princeton, New Jersey, 1948.
- (3) Hoffman, O. and Sachs, G., Introduction to the Theory of Plasticity for Engineers. McGraw Hill Book Company, New York, 1953.
- (4) Johnson, W., Duncan, J. L., Kormi, K., Sowerby, R., and Travis, F. W., "Some Contributions to High Rate Sheet Metal Forming," Proc. 4th International Conference on Machine Tool Design and Research, Manchester, Sept., 1963.
- (5) Johnson, W. and Sowerby, R., "Experiments on Circular Blanks Subject to an Underwater Explosive Charge," Proceedings of the Institution of Mechanical Engineers, Applied Mechanics Group, Vol. 179, pp 197-221, 1964-65.
- (6) Lamb, H., Hydrodynamics. Cambridge University Press, London, England, Fifth Edition, 1924.
- (7) Rayleigh, Lord, The Theory of Sound. V. I, MacMillan and Co., London, England, 1937.
- (8) Rayleigh, Lord, The Theory of Sound. V. II, MacMillan and Co., London, England, 1937.
- (9) Rinehart, J. S. and Pearson, J., Explosive Working of Metals. A Pergamon Press Book, The MacMillan Company, New York, New York, 1963.
- (10) Salvadori, M. G. and Baron, M. L., Numerical Methods in Engineering. Prentice-Hall, Inc., Englewood Cliffs, N. J., 1959.
- (11) Schauer, H. M., "The Afterflow Theory of the Reloading of Air-backed Plates at Underwater Explosions," Proceedings of the First U.S. National Congress of Applied Mechanics, Edited by Eli Sternberg et al., The American Society of Mechanical Engineers, Edwards Brothers Inc., Ann Arbor, Michigan, pp 887-892, 1952.
- (12) Schauer, H. M., "A Special Problem of Potential Flow," Underwater Explosions Research Division Report F-17-51.

- (13) Schauer, H. M., "The Influence of the Surface on the Afterflow Loading of Air-Backed Plates," Underwater Explosions Research Division Report 11-57, July, 1957.
- (14) Smythe, William R., Static and Dynamic Electricity. McGraw-Hill Book Company, Inc., New York, New York, Second Edition, 1950.
- (15) Timoshenko, S. and Young, D. H., Vibration Problems in Engineering. D Van Nostrand Company, Inc., Princeton, New Jersey, Third Edition, 1955.
- (16) Timoshenko, S. and Woinowsky-Krieger, S., Theory of Plates and Shells. McGraw-Hill Book Company, Inc., New York, New York, Second Edition, 1959.
- (17) "Underwater Explosion Research," A Compendium of British and American Reports, Volume I, The Shock Wave. Office of Naval Research, 1950.
- (18) "Underwater Explosion Research," A Compendium of British and American Reports, Volume II, The Gas Globe. Office of Naval Research, 1950.
- (19) "Underwater Explosions Research," A Compendium of British and American Reports, Volume III, The Damage Process. Office of Naval Research, 1950.
- (20) Whittaker, E. T. and Watson, G. N., A Course of Modern Analysis. Cambridge University Press, London, England, American Edition, 1946.

APPENDIX A

THE ACTUAL INCIDENT PRESSURE ON THE MEMBRANE FROM AN UNDERWATER EXPLOSION BASED ON DIFFRACTION THEORY

In this appendix a relationship between the actual incident pressure $p(\bar{r},t)$ on the membrane and the undisturbed pressure $p_i(\bar{r},t)$ of the shock wave is developed when the following assumptions are made (2):

- a) fluid is inviscid,
- b) fluid is incompressible,
- c) shock waves are of small amplitude, and
- d) cavitation does not occur.

The equation of motion of a fluid particle is

$$\frac{\partial \bar{v}}{\partial t} = - \frac{1}{\rho_0} \text{grad } p \quad (\text{A-1})$$

and the continuity equation is

$$\frac{\partial \rho}{\partial t} = - \rho_0 \text{div } \bar{v}, \quad (\text{A-2})$$

where

- \bar{v} = the fluid particle velocity,
- ρ = the density of the fluid,
- ρ_0 = the density of the fluid at zero pressure,
- p = pressure in the fluid medium, and
- t = time.

Since the fluid is assumed to be inviscid and there is no heat exchange

between fluid elements, the changes in the physical state of the element must take place at constant entropy. This situation may be expressed as follows (2):

$$\frac{ds}{dt} = 0, \quad (\text{A-3})$$

where s stands for entropy. From this, the conclusion is drawn that the pressure is a function of density only, that is,

$$p = p(\rho), \quad (\text{A-4})$$

where

p = pressure and

ρ = density of fluid.

It then follows that

$$\frac{\partial p}{\partial t} = \left(\frac{dp}{d\rho} \right)_{s_0} \frac{\partial \rho}{\partial t}, \quad (\text{A-5})$$

where the s_0 indicates the process is assumed to be taking place at constant entropy and in the undisturbed fluid.

The assumptions made at the beginning of this section permits the use of linearized acoustical theory. For this theory, a velocity potential ϕ is defined so that

$$\bar{v} = -\nabla\phi. \quad (\text{A-6})$$

Substituting this expression into the equation of motion gives

$$\frac{\partial}{\partial t} (-\nabla\phi) = -\frac{1}{\rho_0} \nabla p \quad (\text{A-7})$$

or

$$\nabla \left(\frac{\partial\phi}{\partial t} \right) = \frac{1}{\rho_0} \nabla p \quad (\text{A-8})$$

and finally

$$p = \rho_0 \frac{\partial\phi}{\partial t}. \quad (\text{A-9})$$

When the following equation

$$\frac{\partial p}{\partial t} = c_o^2 \frac{\partial \rho}{\partial t} \quad (\text{A-10})$$

is substituted into the continuity equation, it becomes

$$\frac{1}{c_o^2} \frac{\partial p}{\partial t} = - \rho_o \operatorname{div} \bar{v} , \quad (\text{A-11})$$

where c_o , the speed of sound in the fluid, is defined as follows:

$$c_o^2 = \frac{dp}{d\rho} . \quad (\text{A-12})$$

With

$$p = \rho_o \frac{\partial \phi}{\partial t}$$

and

$$\bar{v} = - \nabla \phi , \quad (\text{A-13})$$

the continuity equation becomes

$$\frac{1}{c_o^2} \frac{\partial^2 \phi}{\partial t^2} = \nabla^2 \phi \quad (\text{A-14})$$

or

$$\frac{1}{c_o^2} \frac{\partial^2 \phi}{\partial t^2} - \nabla^2 \phi = 0 .$$

This is the wave equation and any solution to it will give a velocity and pressure field, as defined earlier, which satisfies the equation of motion.

For spherical symmetry the wave equation has the following form:

$$\frac{1}{c_o^2} \frac{\partial^2 \phi}{\partial t^2} = \frac{1}{r^2} \frac{\partial}{\partial r} \left(r^2 \frac{\partial \phi}{\partial r} \right) . \quad (\text{A-15})$$

Lamb (10) has shown that the general solution to this equation can be expressed as the sum of retarded potentials due to distributions of

simple sources originating on the surface of the membrane and baffle surrounding the original plane membrane. The velocity potential ϕ vanishes at infinity and is valid at all points on and above the plane containing the baffle and membrane. The velocity potential has the following general form:

$$\phi = \frac{1}{r} f(t - r/c_0)$$

or more specifically (5)

$$\phi = \frac{1}{2\pi} \iint_A \frac{1}{|\bar{r}-\bar{r}'|} \bar{u}(\bar{r}', \tau) \cdot d\bar{A}' , \quad (\text{A-16})$$

where (see Figure 30 for amplification of the definitions)

\bar{r}' = the distance from a convenient origin to the point on the membrane where the disturbance originates,

\bar{r} = the distance from the above described origin to the membrane center,

$\bar{u}(\bar{r}', \tau)$ = the velocity of the fluid particle directed normal to $d\bar{A}'$ and away from the membrane, also at an earlier time τ ,

$d\bar{A}'$ = a vector element of area on and normal to the membrane or baffle at r , and

$\tau = t - \frac{|\bar{r}-\bar{r}'|}{c_0}$ = the time of origination of the disturbance which

arrives at the membrane center at time t .

From these definitions, it is obvious that the velocity \bar{u} depends on time and on the position \bar{r}' .

Let ϕ , p , and \bar{u} be the actual quantities in the water corresponding to the free field quantities ϕ_0 , p_1 and \bar{u}_0 that would exist if the diffracting surface were not present. Then apply the following equation to the perturbations $\phi-\phi_0$ and $\bar{u}-\bar{u}_0$ arising from the diffracting object.

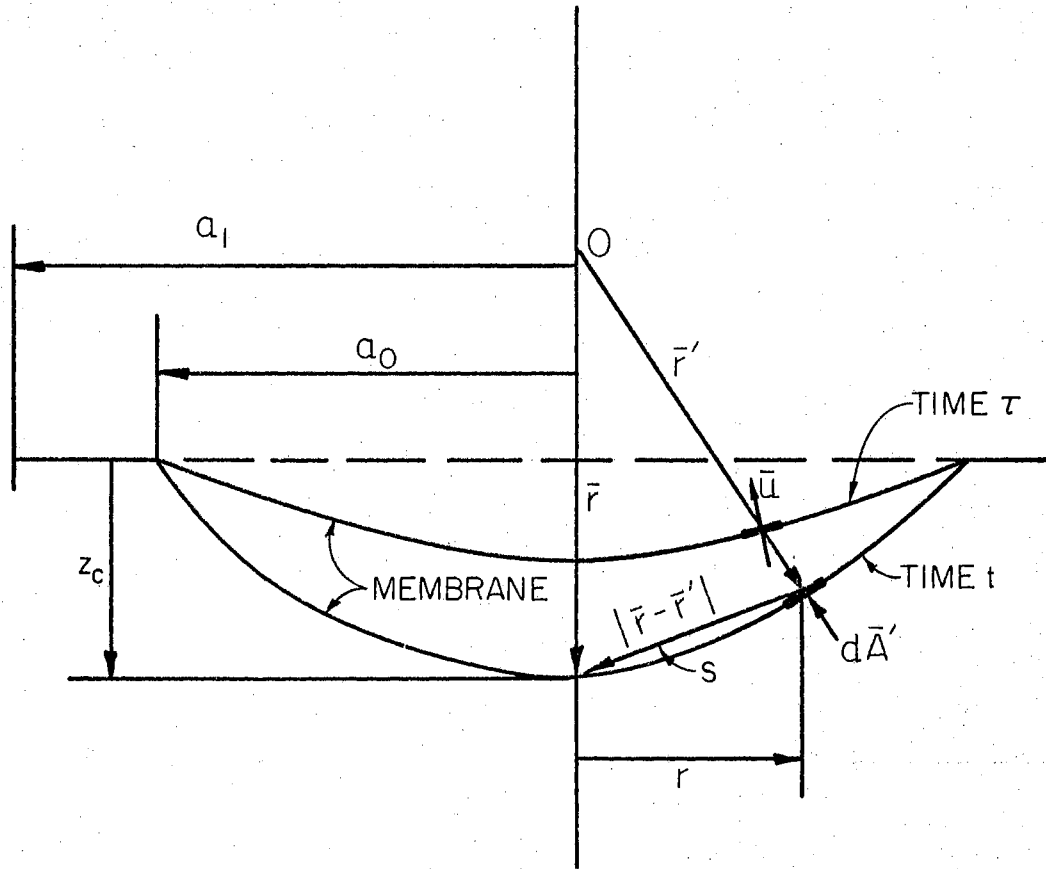


Figure 30. Membrane Geometry at Times t and τ

$$p = \rho_0 \frac{\partial \phi}{\partial t} .$$

Differentiation of $\phi - \phi_0$ and substitution yields

$$p(\bar{r}, t) = p_i(\bar{r}, t) + \frac{\rho_0}{2\pi} \iint_A \frac{1}{|\bar{r} - \bar{r}'|} \left[\frac{\partial \bar{u}(\bar{r}', \tau)}{\partial \tau} - \frac{\partial \bar{u}_0(\bar{r}', \tau)}{\partial \tau} \right] \cdot d\bar{A}' , \quad (\text{A-17})$$

where $p_i(\bar{r}, t)$ is the pressure in the shock wave.

In Figure 30, let A_0 be the area of the obstacle inside the radius a_0 ; let A_1 be the area of the baffle between the radii a_0 and a_1 ; and let A_2 be the area which lies outside the radius a_1 . Over the area $A_0 + A_1$, use the equation of motion as follows:

$$-\nabla p_i = \rho_0 \frac{\partial \bar{u}_0}{\partial t} . \quad (\text{A-18})$$

The equation (A-17) for the pressure becomes

$$\begin{aligned} p(\bar{r}, t) = p_i(\bar{r}, t) &+ \frac{1}{2\pi} \iint_{A_0 + A_1} \frac{1}{|\bar{r} - \bar{r}'|} \left[\nabla p_i(\bar{r}', \tau) \right] \cdot d\bar{A}' \\ &+ \frac{\rho_0}{2\pi} \iint_{A_0 + A_1} \left[\frac{1}{|\bar{r} - \bar{r}'|} \frac{\partial \bar{u}(\bar{r}', \tau)}{\partial \tau} \right] \cdot d\bar{A}' \quad (\text{A-19}) \\ &+ \frac{\rho_0}{2\pi} \iint_{A_2} \frac{1}{|\bar{r} - \bar{r}'|} \left[\frac{\partial \bar{u}(\bar{r}', \tau)}{\partial \tau} - \frac{\partial \bar{u}_0(\bar{r}', \tau)}{\partial \tau} \right] \cdot d\bar{A}' . \end{aligned}$$

If this development is restricted to the case of a plane wave impinging on a circular plane membrane of radius a_0 clamped in a rigid infinite baffle of radius a_1 , the first integral on the right hand side of equation (A-19) represents the reflected pressure on a plane. Setting

$$\frac{\partial u(\bar{r}', \tau)}{\partial \tau} = -\ddot{z}(\bar{r}', \tau) , \quad (\text{A-20})$$

equation (A-19) becomes

$$p(\bar{r}, t) = 2p_i(\bar{r}, t) - p_i(t - a_1/c_0) - \rho_0 \int_0^{a_0} \ddot{z}(\bar{r}', \tau) \frac{r}{s} dr, \quad (\text{A-21})$$

where

$$s = |\bar{r} - \bar{r}'|,$$

$$\bar{u}(\bar{r}', \tau) = 0 \text{ over the baffle, and}$$

$$\bar{u}(\bar{r}', \tau) = u_0(\bar{r}', \tau) \text{ outside the baffle.}$$

For use in this paper, two special forms of equation (A-21) are needed. The two cases are listed. First, for $a_1 \gg a_0$ (infinite baffle), the pressure at the membrane center is given as follows:

$$p(t) = 2p_i(t) - \rho_0 \int_0^{a_0} \ddot{z}(\bar{r}', \tau) \frac{r dr}{s}. \quad (\text{A-22})$$

Second, for a_1 approaching a_0 (a small baffle) and a_0 small, the pressure at the membrane center is

$$p(t) = p_i(t) - \rho_0 \int_0^{a_0} \ddot{z}(\bar{r}', \tau) \frac{r dr}{s}. \quad (\text{A-23})$$

The simple case of a circular plate of radius a_0 clamped in a large rigid baffle will be considered here, and the simplifying assumption used that the membrane deflection profile is always parabolic in shape. That is,

$$z(r, t) = z_c(t) \left(1 - r^2/a_0^2\right), \quad (\text{A-24})$$

where $z_c(t)$ is the center deflection of the membrane. Substituting equation (A-24) into equation (A-22) gives the pressure at the membrane center as

$$p(t) = 2p_i(t) - \rho_0 \int_0^{a_0} (\ddot{z}_c)_\tau \left(1 - \frac{r^2}{a_0^2}\right) \frac{r}{s} dr. \quad (\text{A-25})$$

With the assumption of a parabolic shape for the membrane at all times during the deformation process due to the nearby explosion and with $r=s$ (which is true for small deflections), the integral in equation (A-25) can be evaluated. The variable of integration is changed to $\tau = t-r/c_0$ and integration by parts gives Kirkwood's (19) equation for the pressure at the membrane center.

Consider the integral

$$\int_0^{a_0} (\ddot{z}_c)_\tau \left(1 - \frac{r^2}{a_0^2} \right) dr \quad (\text{A-26})$$

which can be separated as follows:

$$\int_0^{a_0} (\ddot{z}_c)_\tau dr - \frac{1}{2} \int_0^{a_0} (\ddot{z}_c)_\tau r^2 dr. \quad (\text{A-27})$$

Examine the first integral as follows:

$(\ddot{z}_c)_\tau$ is a function of r only, that is τ depends on only r at a particular time t . Also,

$$(\ddot{z}_c)_\tau = \frac{d\dot{z}_c}{d\tau}. \quad (\text{A-28})$$

From

$$\tau = t - r/c_0, \quad (\text{A-29})$$

the following result is obtained

$$d\tau = -\frac{dr}{c_0},$$

therefore

$$\frac{d\dot{z}_c}{d\tau} = -c_0 \frac{dz_c}{dr}, \quad (\text{A-30})$$

and upon substitution

$$\int_0^{a_0} (\ddot{z}_c)_\tau dr = - \int_0^{a_0} c_o \left(\frac{dz_c}{dr} \right)_\tau dr, \quad (\text{A-31})$$

which gives

$$\int_0^{a_0} (\ddot{z}_c)_\tau dr = -c_o \dot{z}_c \Big|_{\tau=t - \frac{a_0}{c_o}}^{\tau=t - \frac{0}{c_o} = t} \quad (\text{A-32})$$

or

$$\int_0^{a_0} (\ddot{z}_c)_\tau dr = c_o \dot{z}_c - c_o \dot{z}_c (t - a_0/c_o). \quad (\text{A-33})$$

This equation (A-33) could be applied to the center portion of the target where it is essentially flat, which gives the integral of equation (A-25) as follows:

$$- \rho_o c_o \dot{z}_c(t) + \rho_o c_o \dot{z}_c(t - r_1/c_o), \quad (\text{A-34})$$

where r_1 is the radius of the center flat portion of the membrane.

Examine now the second integral of equation (A-27), that is,

$$- \frac{1}{2} \int_0^{a_0} (\ddot{z}_c)_\tau r^2 dr. \quad (\text{A-35})$$

Since

$$\tau = t - r/c_o,$$

$$\left(\frac{dz_c}{dt} \right)_\tau = \frac{dz_c}{d\tau}, \quad \text{and}$$

$$d\tau = -dr/c_o,$$

which when substituted into equation (A-35) gives

$$-\frac{1}{2} \int_0^{a_0} -c_o \left(\frac{dz_c}{dr} \right)_\tau r^2 dr. \quad (\text{A-36})$$

This integrates to give

$$\frac{c_o}{2} \left(\left[(z_c)_\tau r^2 \right]_0^{a_0} - 2 \int_0^{a_0} (z_c)_\tau r dr \right), \quad (\text{A-37})$$

which is

$$-\frac{2c_o}{2} \int_0^{a_0} -c_o \left(\frac{dz_c}{dr} \right)_\tau r dr + c_o \dot{z}_c (t - a_0/c_o). \quad (\text{A-38})$$

or

$$\frac{2c_o^2}{2} \int_0^{a_0} (dz_c)_\tau r + c_o \dot{z}_c (t - a_0/c_o). \quad (\text{A-39})$$

This integral gives

$$\frac{2c_o^2}{2} \left(\left[(z_c)_\tau r \right]_0^{a_0} - \int_0^{a_0} (z_c)_\tau dr \right). \quad (\text{A-40})$$

The integral in equation (A-35) is now

$$\frac{2c_o^2}{2} \left[(z_c)_\tau a_0 + \int_t^{t-a_0/c_o} c_o z_c(\tau) d\tau \right] + c_o \dot{z}_c (t - a_0/c_o) \quad (\text{A-41})$$

or

$$\frac{2c_o}{\theta_d} z_c(t - \theta_d) - \frac{2c_o}{\theta_d^2} \int_{t-\theta_d}^t z_c(\tau) d\tau + c_o \dot{z}_c (t - a_0/c_o), \quad (\text{A-42})$$

which when combined with equation (A-33) gives the integrated form of the integral in equation (A-25), that is,

$$\begin{aligned}
& - \rho_o \int_0^{a_0} (\ddot{z}_c)_\tau \left(1 - \frac{r^2}{a_0^2} \right) \frac{r}{s} dr \\
& = - \rho_o \left[c_o \dot{z}_c - c_o \dot{z}_c (t - a_0/c_o) + \frac{2c_o}{\theta_d} z_c (t - \theta_d) \right. \\
& \quad \left. - \frac{2c_o}{\theta_d} \int_{t-\theta_d}^t z_c(\tau) d\tau + c_o \dot{z}_c (t - a_0/c_o) \right].
\end{aligned} \tag{A-43}$$

Equation (A-43) reduces to

$$\begin{aligned}
& - \rho_o \int_0^{a_0} (\ddot{z}_c)_\tau \left(1 - \frac{r^2}{a_0^2} \right) \frac{r}{s} dr \\
& = - \rho_o c_o \dot{z}_c - \frac{2\rho_o c_o}{\theta_d} z_c (t - \theta_d) + \frac{2\rho_o c_o}{\theta_d} \int_{t-\theta_d}^t z_c(\tau) d\tau,
\end{aligned} \tag{A-44}$$

where θ_d is equal to a_0/c_o .

When this result is substituted into equation (A-25), the expression for the pressure at the center of the plate in an infinite rigid baffle is (2,19).

$$p(t) = 2p_i(t) - \rho_o c_o \left[\frac{dz_c}{dt} + \frac{2}{\theta_d} z_c (t - \theta_d) - \frac{2}{\theta_d} \int_{t-\theta_d}^t z_c(\tau) d\tau \right]. \tag{A-45}$$

For $t < \theta_d$, the pressure is

$$p(t) = 2p_i(t) - \rho_o c_o \frac{dz_c}{dt}. \tag{A-46}$$

During the latter stages of the membrane deformation process, when the acceleration is changing slowly, equation (A-25) becomes

$$p(t) = 2p_1(t) - \frac{2}{3} \rho_o a_o \frac{d^2 z_c}{dt^2}, \quad (\text{A-47})$$

which is the equation needed for the last phase of the membrane deformation.

APPENDIX B

THE RELOADING VELOCITY FOR A MEMBRANE SUBJECTED TO AN UNDERWATER EXPLOSION

The following development is paraphrased from reference 12. This development is the determination of the potential flow resulting from a source of strength $4\pi Q$. The source is located a distance D from a circular hole of radius a in an infinite rigid baffle. In addition, the source is located on the normal through the center of the hole so that axial symmetry results. For cylindrical coordinates (x, z, ϕ) with the z -axis through the center of the hole and normal to the infinite baffle (see Figure 8), the coordinates of the source are $z = D$, $x = 0$ and the edge of the membrane is at $x = a$, $z = 0$. The introduction of spheroidal coordinates (ξ, ζ, ϕ) of the oblate type (see Figure 8) is necessary to find the potential function V . The coordinate transformation follows:

$$z = a\zeta\xi, \quad (\text{B-1})$$

$$x = a\sqrt{(1+\zeta^2)(1-\xi^2)}, \quad \text{and} \quad (\text{B-2})$$

$$\psi = \psi. \quad (\text{B-3})$$

Laplace's equation can be written using these coordinates as follows:

$$\frac{\partial}{\partial \xi} \left[(1-\xi^2) \frac{\partial V}{\partial \xi} \right] + \frac{\partial}{\partial \zeta} \left[(1+\zeta^2) \frac{\partial V}{\partial \zeta} \right] + \frac{\xi^2 + \zeta^2}{(1+\xi^2)(1-\xi^2)} \frac{\partial^2 V}{\partial \psi^2} = 0 \quad (\text{B-4})$$

where V is the velocity potential. The general solution of equation (B-4) for axial symmetry is

$$V = \sum_n [a_n P_n(\xi) + b_n Q_n(\xi)] [a'_n P_n(i\zeta) + b'_n Q_n(i\zeta)] . \quad (B-5)$$

The necessary boundary conditions are

$$V = 0 \text{ for } \zeta = 0 \text{ (in the hole}^1\text{) and} \quad (B-6)$$

$$\frac{\partial V}{\partial \xi} = 0 \text{ for } \xi = 0 \text{ (on the baffle) .} \quad (B-7)$$

For the spheroidal coordinates, the source is located at $\xi = 1$, $\zeta = \zeta_0 = D/a$. Reference 14 shows that the special form of equation (B-5), which represents a source of strength $4\pi Q$ at $\xi = 1$, $\zeta = \zeta_0$ is

$$V_1 = \sum_{n=0}^{\infty} iQ \frac{(2n+1)}{a} Q_n(i\zeta_0) P_n(i\zeta) P_n(\xi) . \quad (B-8)$$

for $\zeta < \zeta_0$.

In order to satisfy the boundary conditions, a source is necessary at $\zeta = \zeta_0$, $\xi = -1$. A potential function, which is a special form of equation (B-5) and represents the source just described, is

$$V_2 = \sum_{n=0}^{\infty} (-1)^n iQ \frac{(2n+1)}{a} Q_n(i\zeta_0) P_n(i\zeta) P_n(\xi) \quad (B-9)$$

for $\zeta < \zeta_0$.

In addition, a third form of equation (B-5) is needed and is given as follows:

$$V_3 = \sum_{n=0}^{\infty} 4Q \cdot \left(\frac{4n+1}{\pi a} \right) \cdot Q_{2n}(i\zeta_0) Q_{2n}(i\zeta) P_{2n}(\xi) \quad (B-10)$$

for all values of ζ except $\zeta = \zeta_0 = 0$.

The sum $V_1 + V_2 + V_3$ is the desired potential function, i.e.,

¹The hole itself is considered a free surface.

$$V = V_1 + V_2 + V_3$$

or

$$V = \sum_{n=0}^{\infty} \left[2iQ \cdot \left(\frac{4n+1}{a} \right) \cdot Q_{2n}(i\zeta_0) P_{2n}(\xi) \right] \left[P_{2n}(i\zeta) + \frac{2}{i\pi} Q_{2n}(i\xi) \right] \quad (B-11)$$

This potential function (V) is a solution of Laplace's equation because it is a form of equation (B-5).

The boundary condition $V = 0$ at $\zeta = \zeta_0$, $\xi = 1$ is met since

$$\frac{P_{2n}(i0)}{Q_{2n}(i0)} = -\frac{2}{i\pi}$$

The other boundary condition $\partial V / \partial \xi = 0$ for $\xi = 0$ is met because

$$\frac{\partial}{\partial \xi} \left[P_{2n}(\xi) \right]_{\xi=0} = \left(\xi \frac{\partial}{\partial \xi} \left[P_{2n-1}(\xi) \right] + \left[2n P_{2n-1}(\xi) \right] \right) \Big|_{\xi=0} = 0$$

for $n \geq 1$, and also

$$\frac{\partial}{\partial \xi} P_0(\xi) = 0$$

Thus, V is the required velocity potential.

The normal velocity v in the hole is found as follows:

$$v = \frac{i}{a\xi} \frac{\partial V}{\partial (i\zeta)} \Big|_{\xi=0} \quad (B-12)$$

Differentiation and substitution gives

$$v = \sum_{n=0}^{\infty} (-1)^n 4iQ \frac{(4n+1)}{\pi a^2} \frac{2^{2n} (n!)^2}{(2n)!} \frac{P_{2n}(\xi)}{\xi} Q_{2n}(i\zeta_0) \quad (B-13)$$

For large values of ζ_0 , equation (B-13) becomes

$$v = \sum_{n=0}^{\infty} \frac{4Q}{\pi a^2} \frac{2^{4n} (2n)! (n!)^2}{(4n)!} \frac{P_{2n}(\xi)}{\xi} \frac{1}{\zeta_0^{2n+1}} \quad (B-14)$$

and since only the first term need be considered, the velocity at the hole is

$$v = \frac{4Q}{\pi a^2} \frac{1}{\xi} \frac{1}{\zeta_0} .$$

The velocity (v_0) at the center ($\xi=1, \zeta=0$) of the hole is

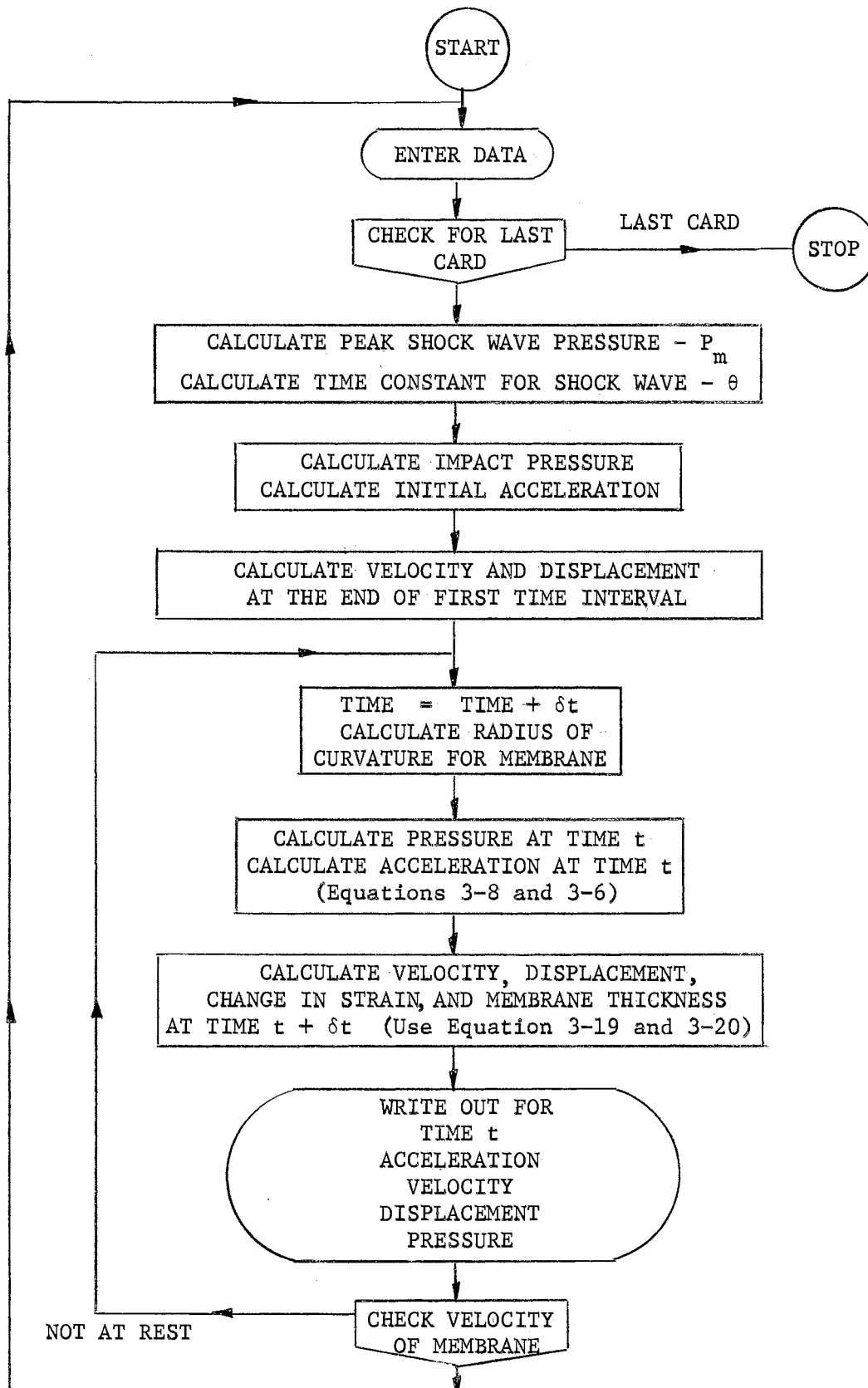
$$v_0 = \frac{4Q}{\pi a D} = \frac{1.27Q}{aD}$$

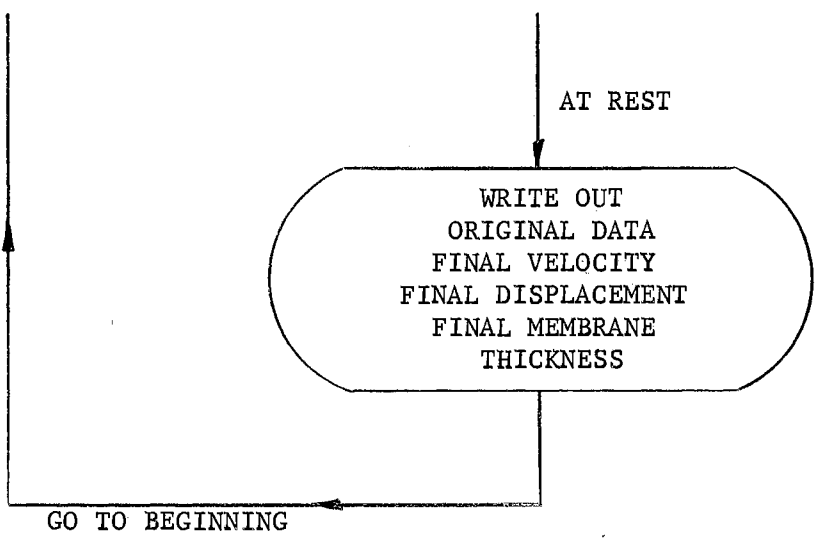
which is the reloading velocity.

APPENDIX C

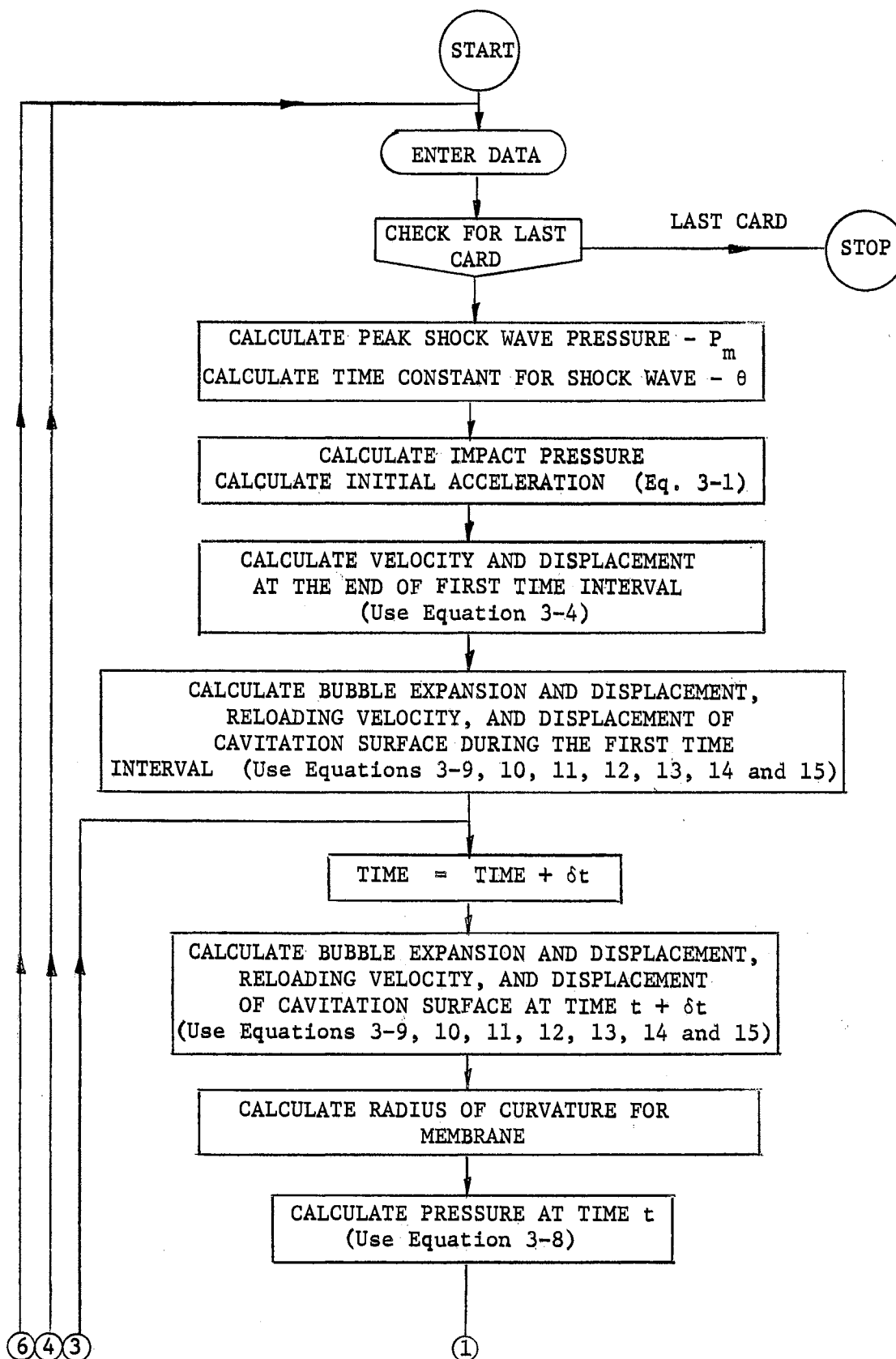
FLOW CHARTS

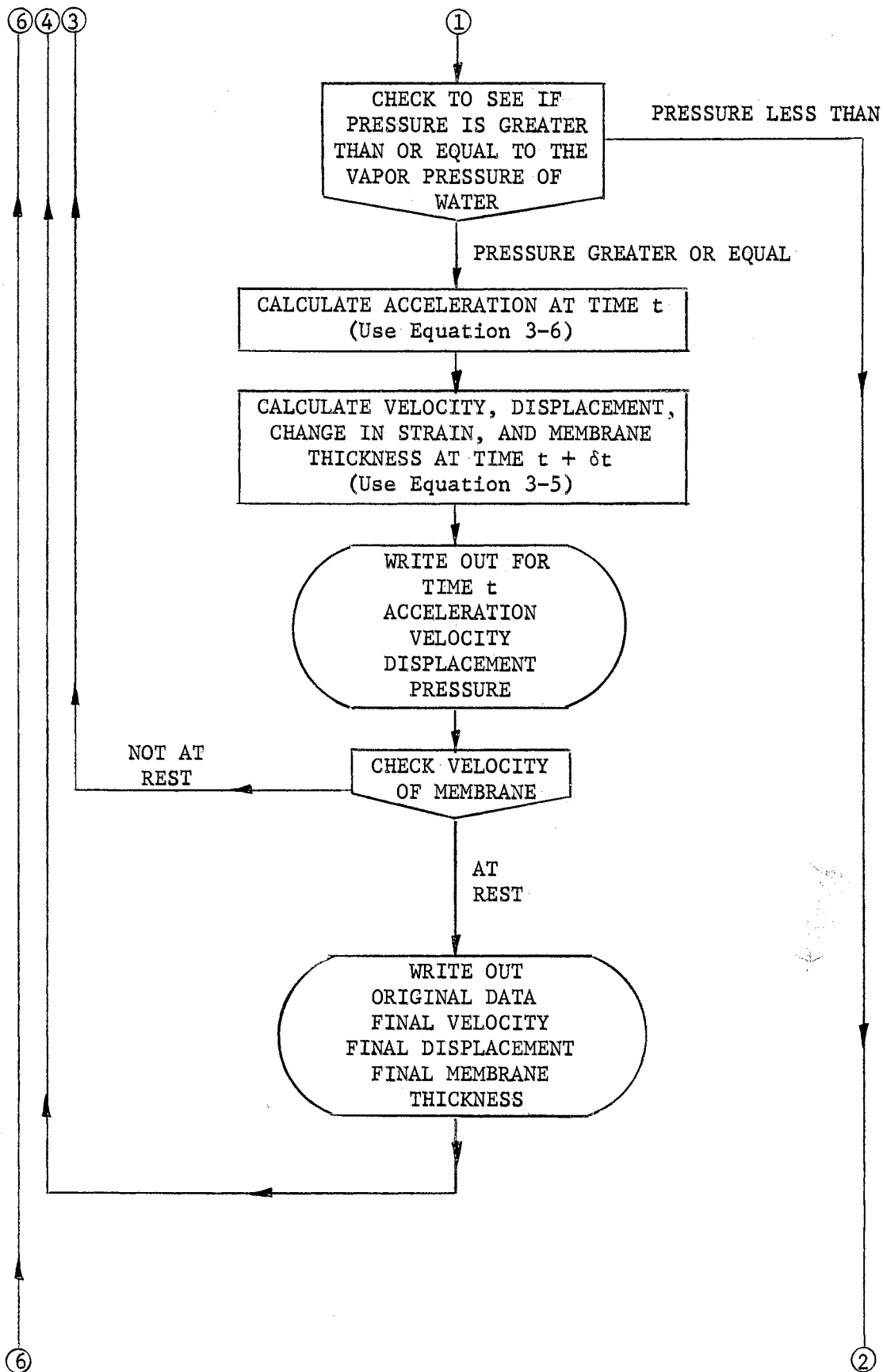
Flow Chart - No Cavitation

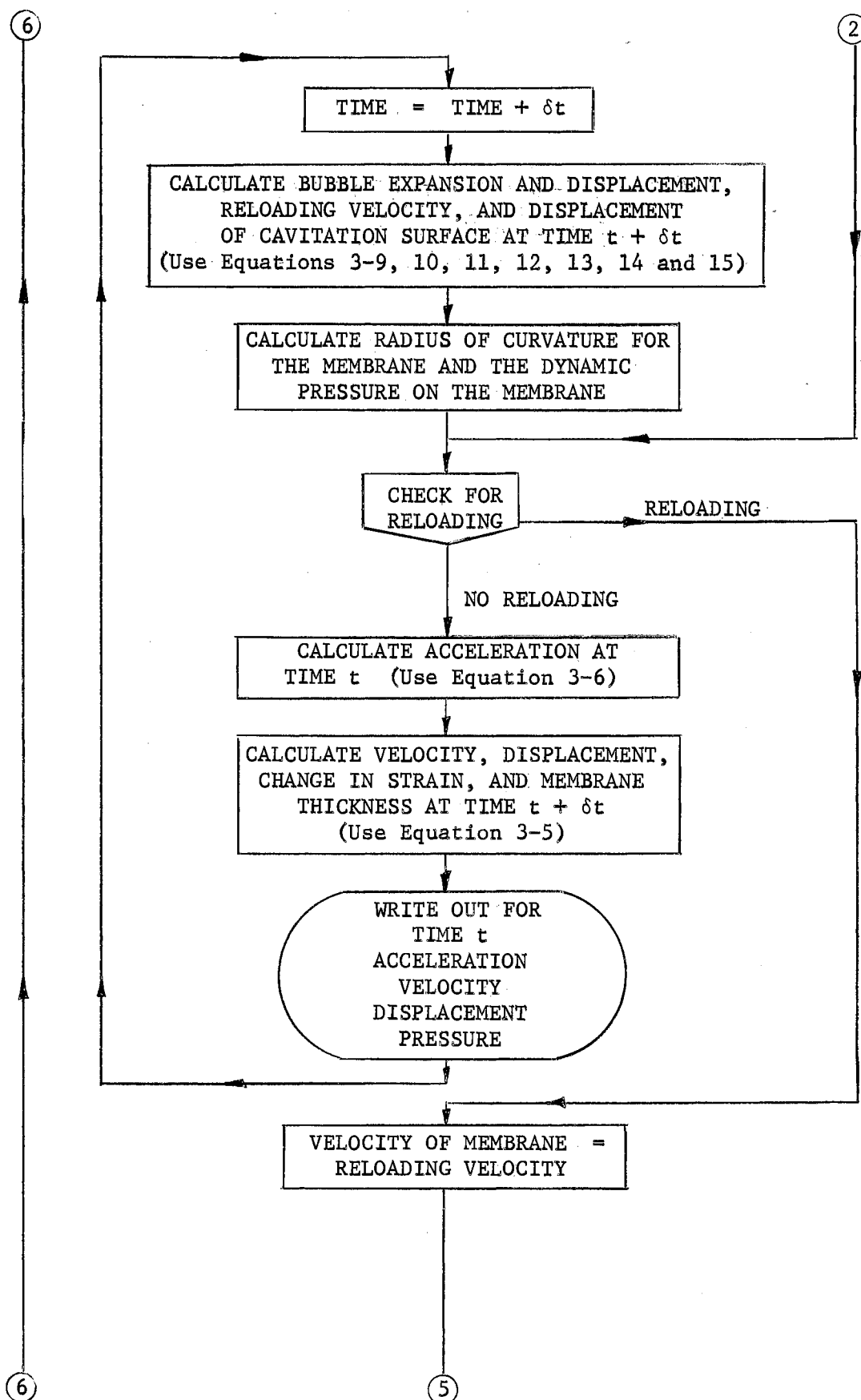


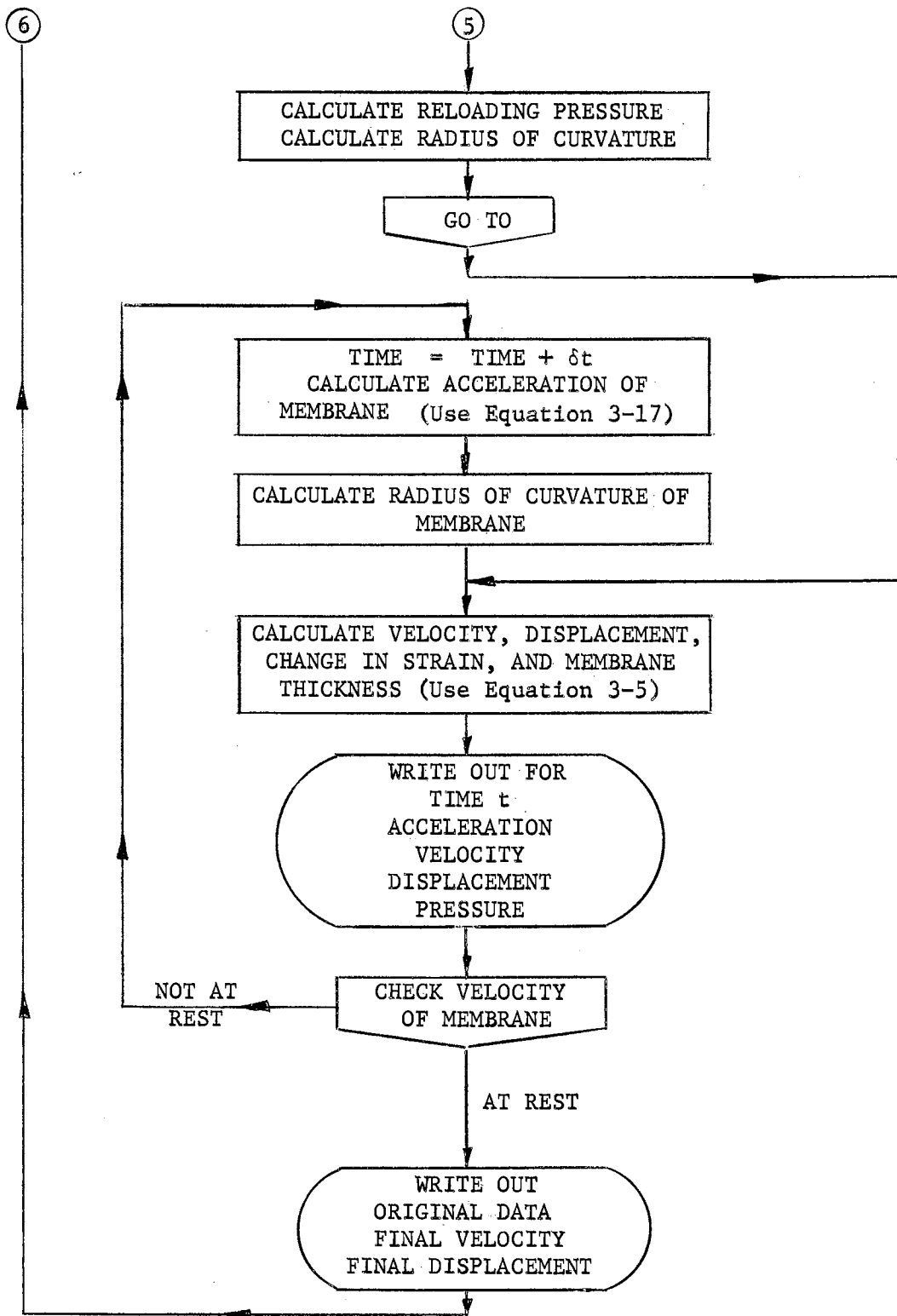


Flow Chart - With Cavitation









VITA

3

Lawrence Edward Ehlers

Candidate for the Degree of
Doctor of Philosophy

Thesis: ANALYSIS OF MEMBRANES SUBJECTED TO AN UNDERWATER EXPLOSION

Major Field: Engineering

Biographical:

Personal Data: Born October 4, 1933, in Junction City, Kansas, the son of Alvin and Florence Ehlers.

Education: Attended elementary school at Spring Valley rural school near Junction City, Kansas; graduated from Junction City High School, Junction City, Kansas in May, 1952. Received the Bachelor of Science degree in Architectural Engineering and the Master of Science degree in Applied Mechanics from Kansas State University in February, 1957, and June, 1960, respectively. Completed the requirements for the Doctor of Philosophy degree in August, 1969, from Oklahoma State University.

Professional Experience: Employed by Kansas State University, Manhattan, Kansas, from February, 1957 to June, 1962 as an Instructor. Employed as a part-time Instructor at Oklahoma State University, Stillwater, Oklahoma, from September, 1962 to February, 1965 and as an Instructor from February, 1965 to September, 1965. Employed by the University of Omaha, Omaha, Nebraska, as an Associate Professor from September, 1965 to September, 1967. Again employed as an Instructor at Oklahoma State University from September, 1967 to February, 1969. Also on leave of absence from the University of Omaha from September, 1967 to February, 1969. Employed as an Associate Professor at the University of Nebraska at Omaha (formerly the University of Omaha) from February, 1969 to present.

Professional Organization: Member of the American Society for Engineering Education, the National Society of Professional Engineers, the Professional Engineers of Nebraska, the Creative Education Foundation, and Sigma Tau.